IPPJ-AM-34

DEPENDENCE OF THE BACKSCATTERING COEFFICIENTS OF LIGHT IONS UPON ANGLE OF INCIDENCE

T. TABATA, R. ITO, Y. ITIKAWA
N. ITOH, K. MORITA AND H. TAWARA

INSTITUTE OF PLASMA PHYSICS
NAGOYA UNIVERSITY

NAGOYA, JAPAN

IPPJ-AM-34

DEPENDENCE OF THE BACKSCATTERING COEFFICIENTS OF LIGHT IONS UPON ANGLE OF INCIDENCE

Tatsuo TABATA[1], Rinsuke ITO[1], Yukikazu ITIKAWA[2]
Noriaki ITOH[3], Kenji MORITA[3] and Hiroyuki TAWARA

Institute of Plasma Physics, Nagoya University
Chikusa-ku, Nagoya 464, Japan

February 1984

Permanent address:

1) Radiation Center of Osaka Prefecture, Shinke-cho, Sakai, Osaka 593, Japan
2) The Institute of Space and Astronautical Science, Meguro-ku, Tokyo 153, Japan
3) Department of Crystalline Materials Science, Faculty of Engineering, Nagoya University, Chikusa-ku, Nagoya 464, Japan

ABSTRACT

The data on the dependence of the number-backscattering coefficient R_N and the energy-backscattering coefficient R_E of H, D, ^3He and ^4He ions upon the angle of incidence θ are compiled into tables. The compilation includes the data generated by computer simulation as well as those obtained experimentally. The references up to the middle of 1983 have been covered. Incident energies of the existing data range from 0.01 to 46 keV. Analytic formulas to express R_N and R_E as a function of θ are briefly reviewed. The data compiled are also shown in graphs together with the curves of new analytic formulas developed by the present authors.

CONTENTS

I. INTRODUCTION

To evaluate the effect of recycling of plasma particles in a fusion reactor, data on various aspects of the backscattering of light ions from solids are necessary. We have published a compilation of the experimental data on the number-backscattering coefficient R_N and the energy-backscattering coefficient R_E of H, D and ^4He ions normally incident on elemental solids,[1] and have proposed empirical formulas for these coefficients.[2] In the present report, the data on the dependence of R_N and R_E of H, D, ^3He and ^4He ions upon the angle of incidence θ are compiled. A brief review is given of analytic formulas to express this dependence, and new formulas are proposed. Since only a few sets of such data have been obtained experimentally, the data generated by computer simulation are included; reliability of computer simulation has been found to be moderate[3-7] for energies above 50 eV by comparing the results of R_N and R_E for normal incidence with experimental data.

II. COMPILATION OF DATA

The data on $R_N(\theta)$ and $R_E(\theta)$ reported before the middle of 1983 have been compiled and stored in the computer of the Institute of Plasma Physics, Nagoya University. The available combinations of the incident ion, the target element and the incident energy are listed at the beginning of the sections MAIN TABLES and MAIN FIGURES. Numerical values of the data are given in MAIN TABLES, and the data are compared with the new analytic formulas in MAIN FIGURES. Sources of the data are shown in the tables and the figures by the use of abbreviations, and the corresponding references are listed in the alphabetical order at the end of this report. The abbreviations are followed by the letters CS or EXP; the former means computer simulation, and the latter, experiment.

III. ANALYTIC FORMULAS

A. Previous Formulas

To denote either $R_N(\theta)$ or $R_E(\theta)$, the symbol $R(\theta)$ is used here. Most of the data show that $R(\theta)$ increases with increasing θ.

Sørensen[8] compared their experimental data on $R_E(\theta)$ with the following expression, which was originally used by Sigmund[9] to approximate the dependence of sputtering yield on θ:

$$R(\theta)=R(0°)+[1/2-R(0°)](1-\cos\theta)^2 . \qquad (1)$$

Clarke and Sigmar[10] have given a simple expression for $R(\theta)$:

$$R(\theta)=1-[1-R(0°)]\cos\theta . \qquad (2)$$

Akkerman[11] has proposed an empirical formula of the form

$$R(\theta)=R(0°)+b(1-\cos\theta)^{\beta} ,\qquad (3)$$

where b and β are parameters depending on the combination of the projectile and target material, and ε is the Thomas-Fermi reduced energy. The reduced energy ε is given by[12)]

$$\varepsilon=32.5E_0M_2/[(Z_1^{2/3}+Z_2^{2/3})^{1/2}(M_1+M_2)Z_1Z_2] \quad (E_0 \text{ in keV}), \qquad (4)$$

where E_0 is the incident kinetic energy of the projectile, and Z_i and M_i (i=1,2) are the atomic number and the mass, respectively, of the projectile (i=1) and the target atom (i=2). Akkerman's formula is valid for $\theta<75°$ and $0.1\leq\varepsilon\leq2$. Sone and Murakami[13)] have used eq. (3) with b=1 and $\beta=2$ in a model calculation on hydrogen recycling in a fusion device. Chen et al.[14)] have found that their experimental data on $R_N(\theta)$ of ^{3}He ions incident on Ni are expressed by eq. (3) with $R(0°)=0.30-0.18\cdot\ln E_0$ (E_0 in keV), b =0.58 and $\beta=1.40$.

Koborov et al.[15)] have given an analytic expression for $R_E(\theta)$:

$$R_E(\theta)=0.66\exp(-2.3\varepsilon^{1/2}\cos\theta) ,\qquad (5)$$

which is valid in the range: $0.1<\varepsilon^{1/2}\cos\theta<1.0$.

Yamamura[16)] has discussed that $R_N(\theta)$ for small θ is approximately given by

$$R_N(\theta)=R_N(0°)/\cos^f\theta ,\qquad (6)$$

where f is nearly equal to 2 when M_2/M_1 is large.

We have tried to develop formulas which fit better to the data and are valid in wider regions of E_0 and θ than the previous formulas.

B. Present Formulas

When $R(\theta)$ is plotted on linear scales, the curve rises rapidly at large values of θ. To relax this rapid increase, we consider the following transformation of the independent variable:

$$t=\ln(\tan^2\theta) \quad . \tag{7}$$

Then, R(t) is a function of t defined for all real values of t, and is approximately expressed by a logistic curve:

$$R(t)=A_0+(1-A_0)/(1+A_1 e^{-A_2 t}) \quad , \tag{8}$$

where the symbols A_i (i=0, 1, 2) denote constants for a given combination of the projectile, incident energy and target material. Transforming back to the variable θ, we obtain

$$R(\theta)=A_0+(1-A_0)/(1+A_1 \cot^{2A_2}\theta) \quad . \tag{9}$$

Values of A_i have been determined by fitting eq. (9) to each data set compiled in this report. The fit has been made under the constraint: $A_2 \leq 0.5$, because $dR(\theta)/d\theta$ becomes infinite at $\theta=0°$ for $A_2<0.5$. The results obtained are given in Tables 1 and 2 together with the values of relative rms deviation δ of the data from the formula; δ is defined by

$$\delta=((1/n)\sum_{i=1}^{n}\{[R_i-R(\theta_i)]/R(\theta_i)\}^2)^{1/2} , \qquad (10)$$

where n is the number of data in the data set, R_i is the i-th data at the angle θ_i. The average value of δ is 4.1% for $R_N(\theta)$ and 5.8% for $R_E(\theta)$, showing good fit of eq. (9).

The values of A_i (i=1, 2) are plotted as a function of ε in Figs. 1-4. From these figures it can be seen that the dependence of each A_i on ε is roughly expressed by a straight line on logarithmic scales independently of the projectile and target material. Therefore, we express A_i by

$$A_i=B_{i1}\varepsilon^{B_{i2}} \quad (i=1, 2) , \qquad (11)$$

where the symbols B_{ij} (j=1, 2) denote constants independent of the projectile, incident energy and target material. Values of B_{ij} have been determined by fitting eq. (11) to the values of A_i. The results are shown in Table 3.

A generalized analytic formula for $R(\theta)$ valid for each of H, D and ^{4}He ions in a wide region of projectile energy can be obtained by putting eq. (11) into eq. (9) and replacing A_0 by the empirical formulas for R(0°) given by Tabata et al.[2] (see Appendix). The values of relative rms deviation δ_G of the data from the generalized formulas are shown in the last columns of

Tables 1 and 2. The average value of δ_G is 22% for $R_N(\theta)$ and 27% for $R_E(\theta)$, indicating deterioration of the generalized formulas from the formula fitted to each data set. This deterioration is in considerable part due to deviations of the formulas for $R(0°)$ from the data. A study to improve the formulas for $R(0°)$ is in progress.

APPENDIX

In this appendix the empirical formulas of Tabata et al.[2) for $R_N(0°)$ and $R_E(0°)$ are presented. The formula for $R_N(0°)$ is written as

$$R_N(0°)=[S_a/(S_n+S_e)]a_1/[\varepsilon^{a_2}(1+a_3\varepsilon+a_4\varepsilon^2)] \quad , \tag{A1}$$

where S_a is an approximate expression for the electronic stopping power in which the Z_2 oscillation is neglected and the mass M_2 of the target atom is assumed to be much greater than the mass M_1 of the projectile, S_n is the nuclear stopping power, and S_e is an accurate expression for the electronic stopping power including the Z_2 oscillation. The coefficients a_i (i=1, 2, 3, 4) are constants for a given projectile and are given in Table A1. The expression for the reduced energy ε is given by eq. (4). For S_a, the expression given by the theory of Lindhard, Scharff and Schiøtt[12) is used:

$$S_a=0.0793Z_1^{2/3}M_1^{-1/2}(M_2/M_1)\varepsilon^{1/2} \quad . \tag{A2}$$

For S_n, the formula proposed by Kalbitzer et al.[17) with the coefficients determined by Ziegler[18) is used:

$$S_n=1.593\varepsilon^{1/2} \qquad \text{for } \varepsilon<0.01 \quad , \tag{A3}$$

$$=1.7\varepsilon^{1/2}\ln(\varepsilon+e)/(1+6.8\varepsilon+3.4\varepsilon^{3/2}) \qquad \text{for } 0.01\leq\varepsilon\leq10 \quad , \tag{A4}$$

$$=\ln(0.47\varepsilon)/2\varepsilon \qquad \text{for } \varepsilon>10 , \qquad \text{(A5)}$$

where e is the base of the natural logarithm. For S_e, the semiempirical formulas given by Andersen and Ziegler[19] (H and D ions) and by Ziegler[18] (He ion) are used.*

For H and D ions, S_e is given by

$$S_e=c_1KE^{1/2} \qquad \text{for } 1\leq E<10 \text{ keV/amu} , \qquad \text{(A6)}$$

$$1/S_e=1/S_{L1}+1/S_{H1} \qquad \text{for } 10\leq E<1000 \text{ keV/amu} , \qquad \text{(A7)}$$

where

$$S_{L1}=c_2KE^{0.45} , \qquad \text{(A8)}$$

$$S_{H1}=(c_3K/E)\ln(1+c_4/E+c_5E) , \qquad \text{(A9)}$$

$$K=0.118(M_1+M_2)(Z_1{}^{2/3}+Z_2{}^{2/3})^{1/2}/Z_1Z_2M_1 , \qquad \text{(A10)}$$

E is the incident energy per projectile mass expressed in units of keV/amu, and the symbols c_i (i=1, 2, ..., 5) denote coefficients whose values are given for each element in ref. 19.

---

* We use the formulas for S_e also at energies below the regions of validity stated. Since these formulas are utilized so as to account only for the relative importance of the Z_2 oscillations of the electronic stopping power, the resulting error in R(0°) due to the uncertainty in S_e is considered to be small.

The values for three elements of technological interest are quoted in Table A2.

For He ion, S_e is given by

$$1/S_e = 1/S_{L2} + 1/S_{H2} \quad \text{for } 1 \le E < 1000 \text{ keV} , \tag{A11}$$

where

$$S_{L2} = d_1 K E^{d_2} , \tag{A12}$$

$$S_{H2} = (d_3 K/E') \ln(1 + d_4/E' + d_5 E') , \tag{A13}$$

$$E' = E/1000 , \tag{A14}$$

E is the incident energy in keV, and the symbols d_i (i=1, 2, ..., 5) denote coefficients whose values are given in ref. 18. Some examples are shown in Table A2.

The formula for $R_E(0°)$ is given by

$$R_E(0°) = [1 - b_1/(1 + b_2 \varepsilon^{-b_3})] R_N(0°) , \tag{A15}$$

where b_1 is a constant independent of the projectile and the target material, and b_2 and b_3 are constants for a given projectile. Values of these constants are shown in Table A1.

REFERENCES

1) T. Tabata, R. Ito, Y. Itikawa, N. Itoh and K. Morita: Data on the Backscattering Coefficients of Light Ions from Solids, Inst. Plasma Phys., Nagoya Univ. Rep. IPPJ-AM-18 (1981); At. Data & Nucl. Data Tables 28 (1983) 493.
2) T. Tabata, R. Ito, K. Morita and Y. Itikawa: Jpn. J. Appl. Phys. 20 (1981) 1929.
3) W. Eckstein and H. Verbeek: Data on Light Ion Reflection, Max-Planck Inst. Plasma Phys. Rep. IPP 9/32 (1979).
4) O. S. Oen and M. T. Robinson: Nucl. Instrum. & Methods 132 (1976) 647.
5) J. E. Robinson, K. K. Kwok and D. A. Thompson: Nucl. Instrum. & Methods 132 (1976) 667.
6) G. Staudenmaier, J. Roth, R. Behrisch, J. Bohdansky, W. Eckstein, P. Staib, S. Matteson and S. K. Erents: J. Nucl. Mater. 84 (1979) 149.
7) M. W. Schleehauf and C. N. Manikopoulos: Radiat. Eff. 54 (1981) 149.
8) H. Sørensen: Appl. Phys. Lett. 29 (1976) 148.
9) P. Sigmund: Phys. Rev. 184 (1969) 383.
10) J. F. Clarke and D. J. Sigmar: Proc. 7th European Conf. Plsmas and Controlled Fusion, Lausanne, 1975, p. 134.
11) A. F. Akkerman: Phys. Status Solidi a 48 (1978) K47.
12) J. Lindhard, M. Scharff and H. E. Schiøtt: Kgl. Danske Videnskab. Selskab., Mat.-Fys. Medd. 33 (1963) No. 14.
13) K. Sone and Y. Murakami: Symp. Energy Removal and Particle Control in Troidal Fusion Devices, 26-29 July, 1983,

Princeton.

14) C. K. Chen, W. Eckstein and B. M. U. Scherzer: Appl. Phys. A 31 (1983) 37.

15) N. N. Koborov, V. A. Kurnaev. V. G. Telkovsky and G. I. Zhabrev: Radiat. Eff. 69 (1983) 135.

16) Y. Yamamura: to be published.

17) S. Kalbitzer, H. Oetzmann, H. Grahmann and A. Freuerstein: Z. Phys. A 278 (1976) 223.

18) J. F. Ziegler: Helium Stopping Powers and Ranges in All Elements (Pergamon, Elmsford, N. Y., 1978).

19) H. H. Andersen and J. F. Ziegler: Hydrogen Stopping Powers and Ranges in All Elements (Pergamon, Elmsford, N. Y., 1977).

Table 1. Values of A_i (i=0, 1, 2), δ and δ_G for R_N. Sources of the data are shown by the use of abbreviations; the corresponding references are given at the end of this report. CS means computer simulation, EXP experiment.

Incident Ion and Target Material	Data Source	Incident Energy (keV)	A_0	A_1	A_2	δ	δ_G
H on Cu	OE76 CS	0.1	0.570	2.50	1.20	2.1	26
H on Cu	OE76 CS	1	0.360	5.77	0.879	3.9	13
H on Cu	OE76 CS	5	0.159	4.93	0.674	4.2	15
H on Nb	RO74 CS	4.6	0.190	6.36	0.618	0	45
H on Nb	RO74 CS	9.1	0.120	7.80	0.693	0	42
H on Nb	RO74 CS	23	0.045	13.7	0.811	0	21
H on Nb	RO74 CS	46	0.014	26.4	0.957	0	22
D on C	EC79 CS	0.01	0.466	2.19	1.60	1.5	70
D on C	EC79 CS	0.03	0.300	1.95	1.18	4.4	50
D on C	EC79 CS	0.05	0.247	2.83	1.18	4.2	33
D on C	EC79 CS	0.07	0.226	3.84	1.20	4.5	24
D on C	EC79 CS	0.09	0.208	4.28	1.13	5.0	18
D on C	EC79 CS	0.15	0.176	5.62	1.09	4.5	8
D on C	EC79 CS	0.25	0.150	6.58	1.01	5.7	8
D on C	EC79 CS	0.35	0.129	6.87	0.950	5.3	11
D on C	EC79 CS	0.45	0.116	7.11	0.923	4.3	13
D on C	BR82 EXP	0.5	0.110	23.4	0.500	22	38
D on C	EC79 CS	0.55	0.108	7.71	0.977	2.9	15
D on C	EC79 CS	0.65	0.094	7.72	0.879	2.9	16
D on C	EC79 CS	0.75	0.086	7.99	0.858	2.7	17
D on C	EC79 CS	0.85	0.076	7.95	0.839	3.0	19
D on C	EC79 CS	0.95	0.072	8.45	0.851	3.6	19
D on C	EC79 CS	1.5	0.048	9.71	0.820	3.7	23
D on Au	EC79 CS	0.5	0.486	5.25	1.019	1.1	8
D on Au	EC79 CS	5	0.282	5.53	0.717	2.8	12
^{3}He on Ni	CH83 EXP	1	0.294	2.93	0.91	5.6	-
^{3}He on Ni	CH83 EXP	3	0.212	6.46	0.667	0.4	-
^{3}He on Ni	CH83 EXP	8	0.128	5.68	0.607	6.7	-
^{3}He on Ni	CH83 EXP	25	0.049	19.7	0.97	12	-
^{4}He on Cu	OE76 CS	0.1	0.510	1.34	1.15	1.6	8
^{4}He on Cu	OE76 CS	1	0.302	3.70	0.780	5.3	15
^{4}He on Cu	OE76 CS	5	0.191	4.12	0.619	4.2	15
Average						4.1	22

Table 2. Values of A_i (i=0, 1, 2), δ and δ_G for R_E. Sources of the data are shown by the use of abbreviations; the corresponding references are given at the end of this report. CS means computer simulation, EXP experiment.

Incident Ion and Target Material	Data Source	Incident Energy (keV)	A_0	A_1	A_2	δ	δ_G
H on Cu	OE76 CS	0.1	0.381	3.28	1.16	3.3	30
H on Cu	OE76 CS	1	0.185	9.79	0.908	6.5	33
H on Cu	OE76 CS	5	0.058	14.2	0.763	8.3	32
H on Nb	RO74 CS	4.6	0.070	10.6	0.597	0	65
H on Nb	RO74 CS	9.1	0.037	17.9	0.723	0	54
H on Nb	RO74 CS	23	0.0077	86.8	1.08	0	25
H on Nb	RO74 CS	46	0.0018	138	1.11	0	44
H on Au	SO76 EXP	1.5	0.13	4.05	0.500	34	32
H on Au	AK78 CS	2	0.159	20.0	0.78	3.1	20
H on Au	SO76 EXP	2	0.147	19.4	0.500	8.3	27
H on Au	SO76 EXP	3	0.118	16.7	0.500	9.2	25
H on Au	AK78 CS	5	0.098	13.1	0.537	4.9	16
H on Au	SO76 EXP	5	0.095	16.6	0.500	6.5	22
H on Au	SO76 EXP	7	0.076	15.8	0.500	4.0	19
H on Au	AK78 CS	10	0.057	13.2	0.543	8.5	17
H on Au	SO76 EXP	10	0.060	16.8	0.504	4.2	20
D on C	EC79 CS	0.03	0.114	4.15	1.02	9.1	26
D on C	EC79 CS	0.05	0.099	6.24	1.20	6.8	25
D on C	EC79 CS	0.07	0.088	7.96	1.19	7.4	24
D on C	EC79 CS	0.09	0.078	8.20	1.11	6.9	23
D on C	EC79 CS	0.15	0.066	11.8	1.13	6.4	23
D on C	EC79 CS	0.25	0.054	14.3	1.08	7.4	26
D on C	EC79 CS	0.35	0.044	15.3	1.01	7.4	29
D on C	EC79 CS	0.45	0.039	16.8	0.914	11	28
D on C	EC79 CS	0.55	0.035	17.9	1.04	4.5	33
D on C	EC79 CS	0.65	0.030	18.7	0.950	4.1	30
D on C	EC79 CS	0.75	0.027	19.9	0.937	3.3	31
D on C	EC79 CS	0.85	0.023	20.0	0.910	3.2	30
D on C	EC79 CS	0.95	0.021	21.0	0.902	2.3	30
D on C	EC79 CS	1.5	0.013	27.1	0.887	3.8	34
D on Au	EC79 CS	0.5	0.287	7.84	1.00	2.0	7
D on Au	KO83 EXP	2.5	0.205	7.85	0.576	3.2	29
D on Au	EC79 CS	5	0.130	10.9	0.749	4.2	15
D on Au	KO83 EXP	5	0.157	8.46	0.595	3.7	40
D on Au	KO83 EXP	8.3	0.089	10.4	0.592	10	24
^{4}He on Ti	KO83 EXP	5	0.030	21.6	0.635	1.6	22
^{4}He on Cu	OE76 CS	0.1	0.317	1.95	1.04	1.9	12
^{4}He on Cu	OE76 CS	1	0.152	7.02	0.831	8.7	18
^{4}He on Cu	KO83 EXP	4	0.091	9.77	0.611	4.6	23
^{4}He on Cu	OE76 CS	5	0.081	8.94	0.686	6.0	23
^{4}He on Au	KO83 EXP	5	0.137	6.3	0.556	5.7	10
Average						5.8	27

Table 3. Values of the constants in the generalized analytic formulas. Errors attached are those of least-squares fit.

Constant	R_N	R_E
B_{11}	7.38 ±0.048	17.9 ±1.3
B_{12}	0.359±0.038	0.453±0.049
B_{21}	0.836±0.034	0.771±0.042
B_{22}	-0.087±0.023	-0.014±0.036

Table A1. Values for projectile-dependent coefficients used in eqs. (A1) and A(15).

Constant	H ion	D ion	He ion
a_1	0.375	0.300	0.197
a_2	0.107	0.316	0.416
a_3	0.64	0.282	0.148
a_4	0.0338	0.0121	0
b_1	0.872	0.872	0.872
b_2	0.306	0.465	0.470
b_3	0.50	0.273	0.262

Table A2. Selected values for target-dependent coefficients used in eqs. (A6) through (A13).

Coefficient	$_{26}Fe$	$_{42}Mo$	$_{74}W$
c_1	3.519E 00	6.425E 00	4.574E 00
c_2	3.963E 00	7.248E 00	5.144E 00
c_3	6.065E 03	9.545E 03	1.593E 04
c_4	1.243E 03	4.802E 02	4.424E 02
c_5	7.782E-03	5.367E-03	3.144E-03
d_1	5.013E 00	9.276E 00	6.335E 00
d_2	4.707E-01	4.18 E-01	4.825E-01
d_3	8.558E 01	1.571E 02	2.551E 02
d_4	1.655E 01	8.038E 00	2.834E 00
d_5	3.211E 00	1.29 E 00	8.228E-01

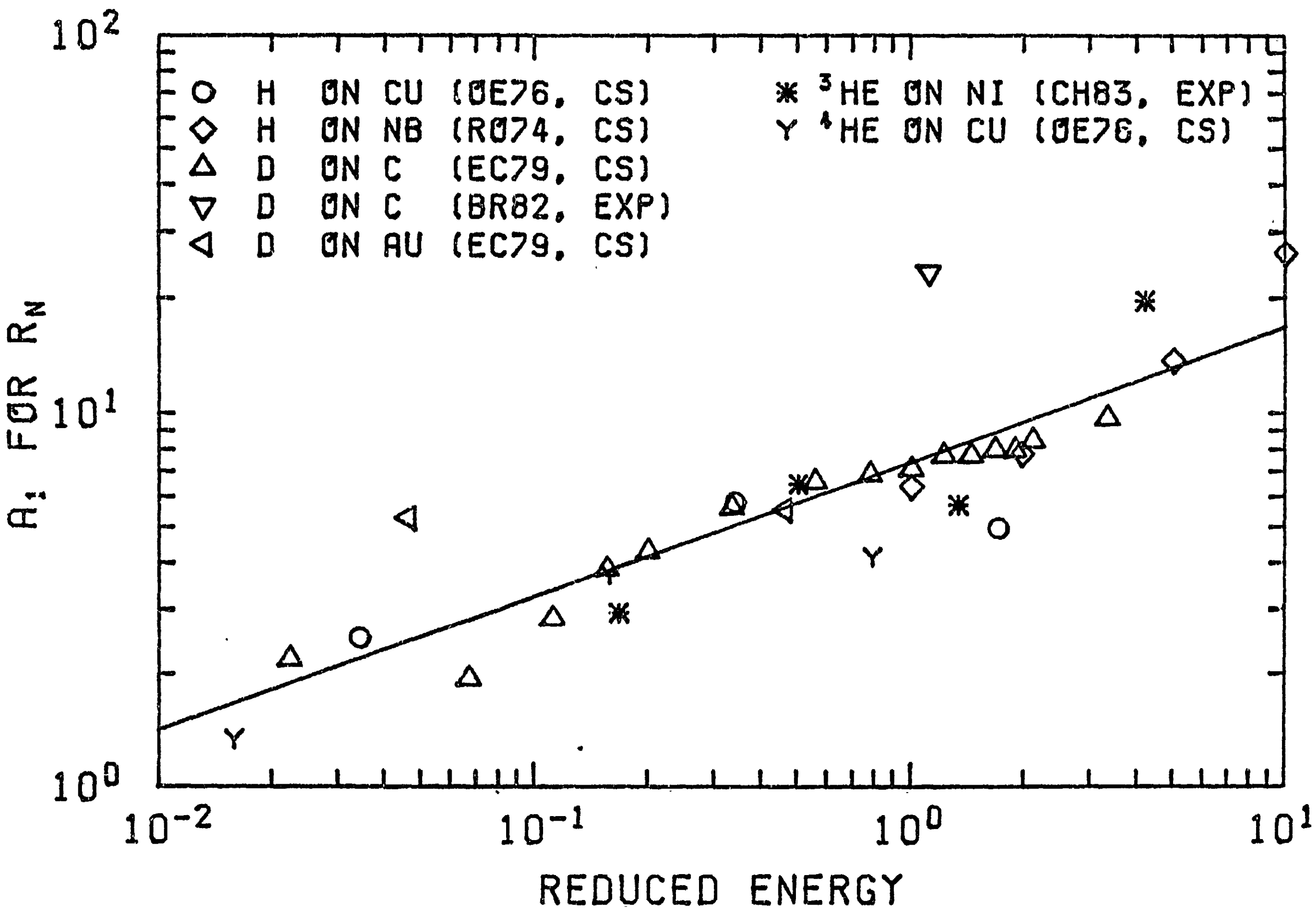

Fig. 1. The parameter A_1 in the analytic formula for the number-backscattering coefficient R_N is plotted as a function of the reduced energy ε. Points represent the values of A_1 determined by fitting eq. (9) to data, and the straight line represents the fit to the points with eq. (11).

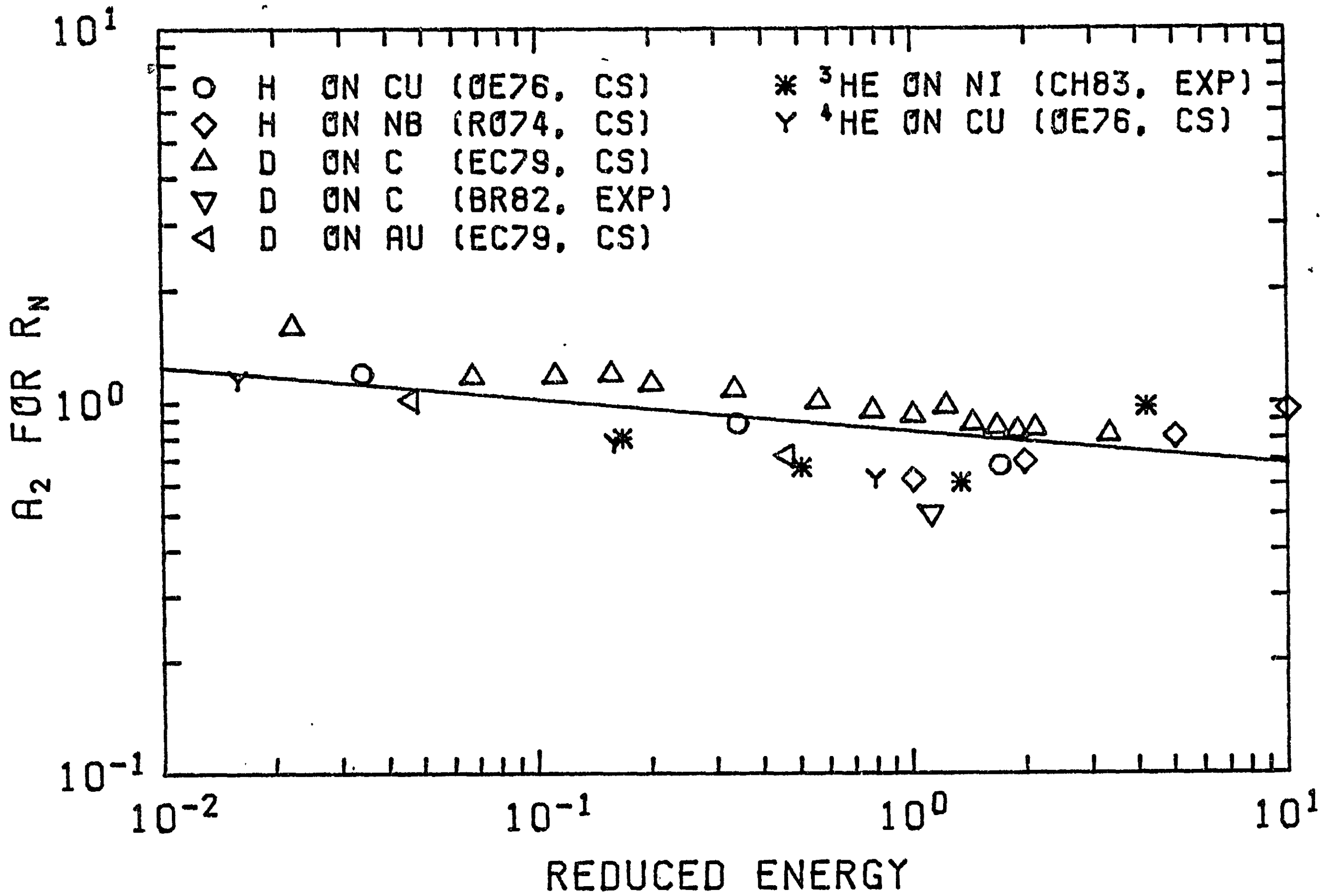

Fig. 2. The parameter A_2 in the analytic formula for the number-backscattering coefficient R_N is plotted as a function of the reduced energy ε. Points represent the values of A_2 determined by fitting eq. (9) to data, and the straight line represents the fit to the points with eq. (11).

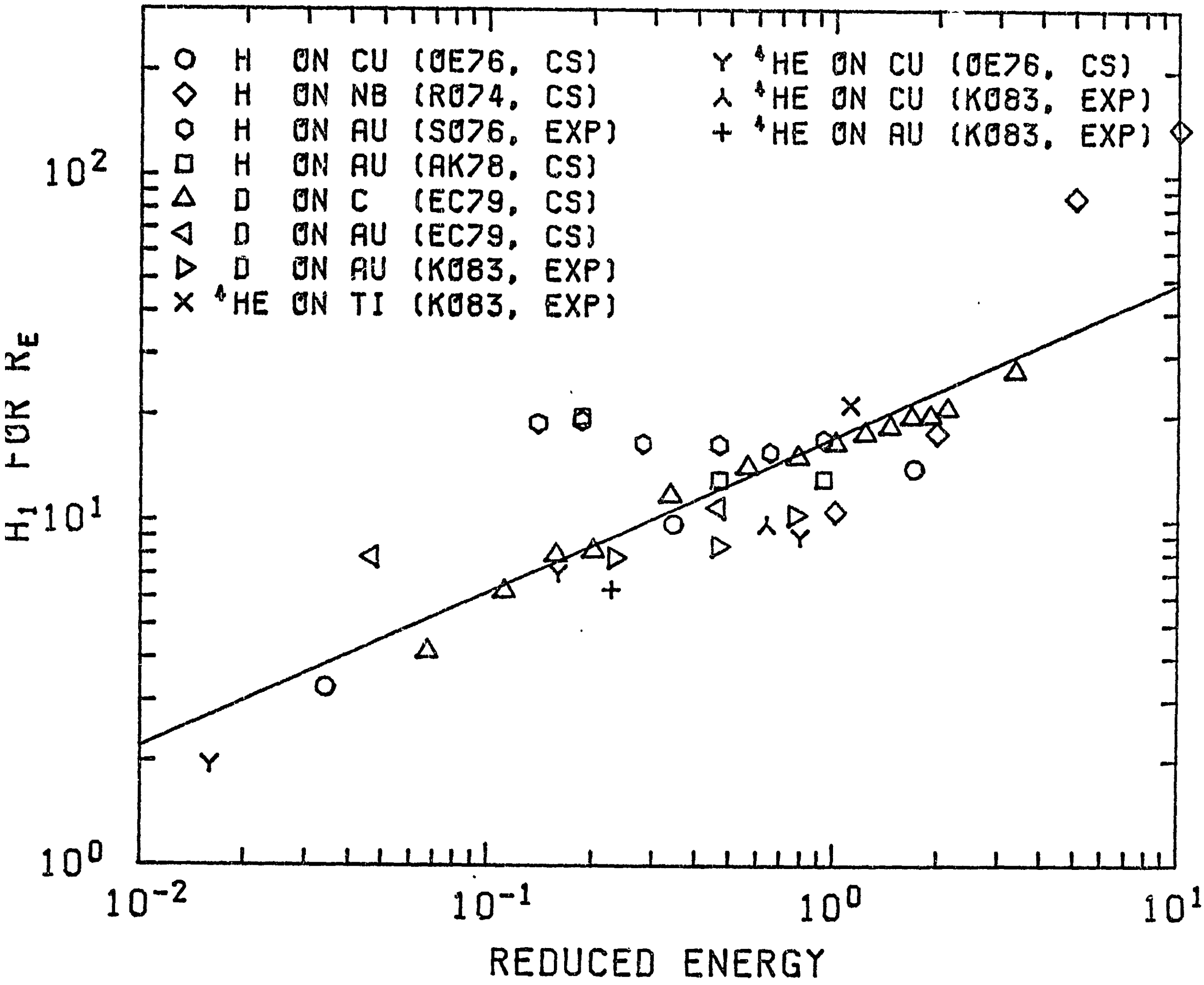

Fig. 3. The parameter A_1 in the analytic formula for the energy-backscattering coefficient R_E is plotted as a function of the reduced energy ε. Points represent the values of A_1 determined by fitting eq. (9) to data, and the straight line represents the fit to the points with eq. (11).

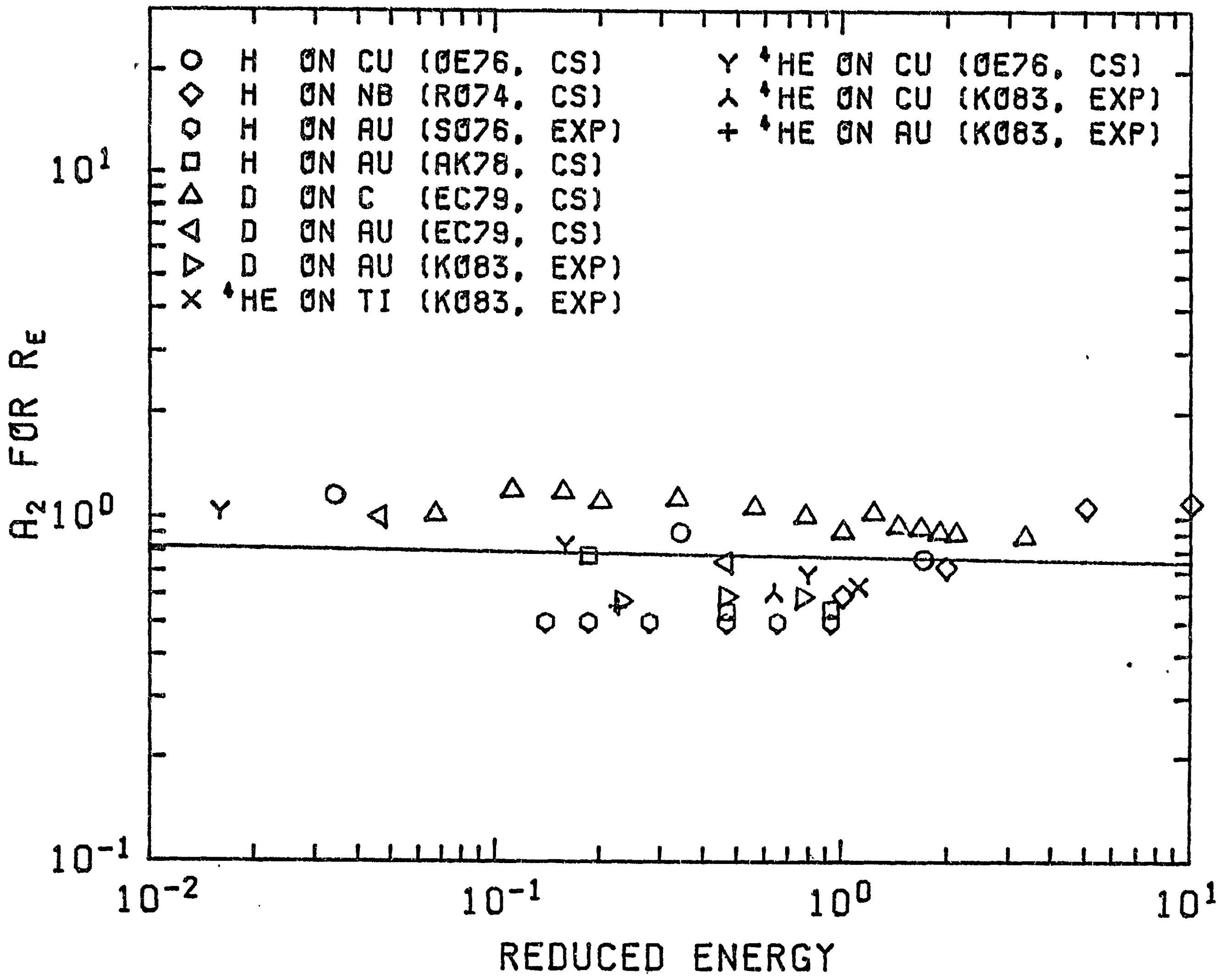

Fig. 4. The parameter A_2 in the analytic formula for the energy-backscattering coefficient R_E is plotted as a function of the reduced energy ε. Points represent the values of A_2 determined by fitting eq. (9) to data, and the straight line represents the fit to the points with eq. (11).

MAIN TABLES

Data on the number-backscattering coefficient R_N and the energy-backscattering coefficient R_E as a function of the angle of incidence θ.

The order in which each combination of the incident ions, the target materials and the incident energies appears is given in the following list. Sources of the data are shown by the use of abbreviations, and the corresponding references are given in the alphabetical order at the end of this report. The abbreviations are followed by the letters CS or EXP. The former means computer simulation, and the latter, experiment.

Notes

1) Data from AK78, KO83, OE76 and RO74 have been read off from the graphs. Some data of OE76 at the largest angles have been omitted, leaving enough number of points to feature the curve.

2) Numerical data of BR82 have been provided by courtesy of Dr. Braun.

3) As for SO76, smoothed data compiled in the following publication have been adopted:

   E. W. Thomas, S. W. Hawthorne, F. W. Meyer and B. J. Farmer: Atomic Data for Controlled Fusion Research, ORNL-5207/R1 (1979).

LIST OF MAIN TABLES

LIST OF MAIN TABLES (Continued)

Table 1. H on Cu, E_0=0.1 keV (OE76 CS).

θ (deg)	R_N	R_E
0	0.55	0.36
9	0.57	0.38
18	0.59	0.41
27	0.63	0.44
36	0.64	0.47
45	0.68	0.51
54	0.76	0.61
63	0.85	0.73
72	0.95	0.90
75	0.98	0.95
77.5	0.99	0.97
80	1.00	0.99

Table 2. H on Cu, E_0=1 keV (OE76 CS).

θ (deg)	R_N	R_E
0	0.35	0.18
9	0.35	0.17
18	0.38	0.21
27	0.41	0.22
36	0.44	0.25
45	0.47	0.27
54	0.50	0.31
63	0.56	0.37
72	0.60	0.51
80	0.87	0.77
83	0.97	0.94
84	0.98	0.955
85	1.00	0.97

Table 3. H on Cu, E_0=5 keV (OE76 CS).

θ (deg)	R_N	R_E
0	0.16	0.06
30	0.23	0.08
60	0.42	0.21
80	0.72	0.51
85	0.81	0.68
86.3	0.96	0.92
87.5	1.00	0.98

Table 4. H on Nb, E_0=4.6 keV (RO74 CS).

θ (deg)	R_N	R_E
0	0.19	0.070
45	0.30	0.15
75	0.55	0.36

Table 5. H on Nb, E_0=9.1 keV (RO74 CS).

θ (deg)	R_N	R_E
0	0.12	0.037
45	0.22	0.088
75	0.51	0.30

Table 6. H on Nb, E_0=23 keV (RO74 CS).

θ (deg)	R_N	R_E
0	0.045	0.0077
45	0.11	0.019
75	0.41	0.17

Table 7. H on Nb, E_0=46 keV (RO74 CS).

θ (deg)	R_N	R_E
0	0.014	0.0018
45	0.050	0.0090
75	0.33	0.12

Table 8. H on Au, E_0=1.5 keV (SO76 EXP).

θ (deg)	R_N	R_E
0		0.15
45		0.22
60		0.26
75		0.27

Table 9a. H on Au, E_0=2 keV (AK79 CS).

θ (deg)	R_N	R_E
0		0.16
22.5		0.17
45		0.19
60		0.26
75		0.39

Table 9b. H on Au, E_0=2 keV (SO76 EXP).

θ (deg)	R_N	R_E
0		0.14
22.5		0.16
45		0.21
60		0.24
75		0.26

Table 10. H on Au, E_0=3 keV (SO76 EXP).

θ (deg)	R_N	R_E
0		0.11
22.5		0.14
45		0.19
60		0.22
75		0.25

Table 11a. H on Au, E_0=5 keV (AK78 CS).

θ (deg)	R_N	R_E
0		0.097
22.5		0.13
45		0.15
60		0.22
75		0.31

Table 11b. H on Au, E_0=5 keV (SO76 EXP).

θ (deg)	R_N	R_E
0		0.09
22.5		0.12
45		0.16
60		0.19
75		0.24

Table 12. H on Au, E_0=7 keV (SO76 EXP).

θ (deg)	R_N	R_E
0		0.074
22.5		0.10
45		0.14
60		0.17
75		0.24

Table 13a. H on Au, E_0=10 keV (AK78 CS).

θ (deg)	R_N	R_E
0		0.056
22.5		0.096
45		0.11
60		0.18
75		0.29

Table 13b. H on Au, E_0=10 keV (SO76 EXP).

θ (deg)	R_N	R_E
0		0.06
45		0.12
60		0.14
75		0.23

Table 14. D on C, E_0=0.01 keV (EC79 CS).

θ (deg)	R_N	R_E
10	0.457	
20	0.484	
30	0.514	
40	0.567	
50	0.708	
60	0.847	
70	0.979	
80	0.994	
87.5	1.000	

Table 15. D on C, E_0=0.03 keV (EC79 CS).

θ (deg)	R_N	R_E
10	0.302	0.12
20	0.333	0.14
30	0.385	0.18
40	0.515	0.26
50	0.556	0.30
60	0.769	0.54
70	0.950	0.76
80	0.989	0.82
87.5	1.000	0.83

Table 16. D on C, E_0=0.05 keV (EC79 CS).

θ (deg)	R_N	R_E
10	0.247	0.10
20	0.269	0.11
30	0.322	0.14
40	0.413	0.20
50	0.472	0.25
60	0.668	0.44
70	0.909	0.75
80	0.981	0.86
87.5	0.997	0.90

Table 17. D on C, E_0= 0.07 keV (EC79 CS).

θ (deg)	R_N	R_E
10	0.221	0.085
20	0.245	0.10
30	0.290	0.13
40	0.357	0.17
50	0.416	0.21
60	0.594	0.37
70	0.865	0.69
80	0.985	0.90
87.5	0.996	0.92

Table 18. D on C, E_0=0.09 keV (EC79 CS).

θ (deg)	R_N	R_E
10	0.202	0.076
20	0.231	0.092
30	0.268	0.12
40	0.337	0.16
50	0.384	0.20
60	0.541	0.33
70	0.814	0.63
80	0.983	0.91
87.5	0.997	0.94

Table 19. D on C, E_0=0.15 keV (EC79 CS).

θ (deg)	R_N	R_E
0	0.178	0.066
10	0.172	0.064
20	0.189	0.073
30	0.228	0.093
40	0.283	0.13
50	0.331	0.16
60	0.461	0.26
70	0.696	0.51
80	0.986	0.91
87.5	0.995	0.96

Table 20. D on C, E_0=0.25 keV (EC79 CS).

θ (deg)	R_N	R_E
0	0.152	0.054
10	0.150	0.053
20	0.161	0.059
30	0.197	0.078
40	0.255	0.109
50	0.291	0.134
60	0.401	0.218
70	0.595	0.402
80	0.970	0.881
87.5	0.996	0.964

Table 21. D on C, E_0=0.35 keV (EC79 CS).

θ (deg)	R_N	R_E
0	0.132	0.044
10	0.128	0.044
20	0.145	0.051
30	0.176	0.068
40	0.225	0.093
50	0.272	0.122
60	0.373	0.195
70	0.537	0.344
80	0.933	0.834
87.5	0.996	0.956

Table 22. D on C, E_0=0.45 keV (EC79 CS).

θ (deg)	R_N	R_E
0	0.118	0.039
10	0.117	0.040
20	0.135	0.047
30	0.159	0.059
40	0.207	0.084
50	0.261	0.115
60	0.356	0.180
70	0.509	0.257
80	0.887	0.773
87.5	0.997	0.957

Table 23. D on C, E_0=0.5 keV (BR82 EXP).

θ (deg)	R_N	R_E
0	0.100	
15	0.108	
30	0.130	
45	0.178	
55	0.222	
65	0.245	
80	0.228	

Table 24. D on C, E_0=0.55 keV (EC79 CS).

θ (deg)	R_N	R_E
0	0.108	0.034
10	0.109	0.035
20	0.124	0.043
30	0.148	0.054
40	0.191	0.074
50	0.243	0.104
60	0.333	0.164
70	0.559	0.359
80	0.836	0.708
87.5	0.997	0.959

Table 25. D on C, E_0=0.65 keV (EC79 CS).

θ (deg)	R_N	R_E
0	0.095	0.029
10	0.101	0.033
20	0.109	0.036
30	0.139	0.049
40	0.178	0.068
50	0.232	0.097
60	0.324	0.159
70	0.465	0.273
80	0.795	0.656
87.5	0.998	0.957

Table 26. D on C, E_0=0.75 keV (EC79 CS).

θ (deg)	R_N	R_E
0	0.088	0.027
10	0.091	0.029
20	0.103	0.034
30	0.127	0.043
40	0.169	0.064
50	0.223	0.092
60	0.309	0.147
70	0.444	0.255
80	0.758	0.612
87.5	0.998	0.958

Table 27. D on C, E_0=0.85 keV (EC79 CS).

θ (deg)	R_N	R_E
0	0.080	0.024
10	0.078	0.024
20	0.096	0.031
30	0.121	0.041
40	0.158	0.060
50	0.211	0.085
60	0.302	0.140
70	0.435	0.245
80	0.729	0.576
87.5	0.998	0.957

Table 28. D on C, E_0=0.95 keV (EC79 CS).

θ (deg)	R_N	R_E
0	0.077	
10	0.075	0.023
20	0.087	0.028
30	0.114	0.038
40	0.152	0.055
50	0.202	0.080
60	0.295	0.135
70	0.424	0.233
80	0.711	0.546
87.5	0.998	0.956

Table 29. D on C, E_0=1.5 keV (EC79 CS).

θ (deg)	R_N	R_E
0	0.051	0.014
10	0.052	0.014
20	0.065	0.019
30	0.085	0.026
40	0.117	0.040
50	0.167	0.061
60	0.250	0.104
70	0.382	0.192
80	0.616	0.432
87.5	0.998	0.954

Table 30. D on Au, E_0=0.5 keV (EC79 CS).

θ (deg)	R_N	R_E
0	0.487	0.287
10	0.484	0.287
20	0.497	0.301
30	0.518	0.317
40	0.555	0.352
50	0.598	0.393
60	0.669	0.482
70	0.785	0.633
75	0.863	0.746
80	0.959	0.894
85	0.988	0.935
87.5	0.989	0.947

Table 31. D on Au, E_0=2.5 keV (KO83 EXP).

θ (deg)	R_N	R_E
0		0.21
12		0.22
24		0.23
36		0.27
48		0.32
60		0.36
66		0.41
72		0.44

Table 32a. D on Au, E_0=5 keV (EC79 CS).

θ (deg)	R_N	R_E
0	0.290	0.134
10	0.286	0.131
20	0.304	0.142
30	0.340	0.167
40	0.369	0.187
50	0.426	0.228
60	0.500	0.290
70	0.593	0.384
75	0.651	0.455
80	0.749	0.581
82.5	0.830	0.700
85	0.950	0.891
87.5	0.997	0.963

Table 32b. D on Au, E_0=5 keV (KO83 EXP).

θ (deg)	R_N	R_E
0		0.16
12		0.17
24		0.19
36		0.22
48		0.25
60		0.34
66		0.36
72		0.40

Table 33. D on Au, E_0=8.3 keV (KO83 EXP).

θ (deg)	R_N	R_E
0		0.08
0		0.11
12		0.10
24		0.11
24		0.14
36		0.13
36		0.15
48		0.18
60		0.24
60		0.26
72		0.31
72		0.35
78		0.41

Table 34. ^3He on Ni, E_0=1 keV (CH83 EXP).

θ (deg)	R_N	R_E
0	0.291	
40	0.465	
60	0.561	
70	0.780	
80	0.933	

Table 35. ^3He on Ni, E_0=3 keV (CH83 EXP).

θ (deg)	R_N	R_E
0	0.212	
40	0.300	
60	0.402	
70	0.505	
80	0.696	

Table 36. ^3He on Ni, E_0=8 keV (CH83 EXP).

θ (deg)	R_N	R_E
0	0.134	
25	0.175	
40	0.221	
60	0.378	
65	0.439	
70	0.478	
75	0.518	
80	0.627	
85	0.723	

Table 37. ^{3}He on Ni, E_0=25 keV (CH83 EXP).

θ (deg)	R_N	R_E
0	0.052	
40	0.072	
60	0.190	
70	0.348	
80	0.536	

Table 38. ^{4}He on Ti, E_0=5 keV (KO83 EXP).

θ (deg)	R_N	R_E
0		0.03
36		0.06
60		0.11
72		0.19

Table 39. ^{4}He on Cu, E_0=0.1 keV (OE76 CS).

θ (deg)	R_N	R_E
0	0.50	0.31
15	0.54	0.35
30	0.60	0.41
45	0.71	0.55
60	0.86	0.72
67.5	0.94	0.85
75	0.987	0.94
77.5	0.994	0.96

Table 40. ^{4}He on Cu; E_0=1 keV (OE76 CS).

θ (deg)	R_N	R_E
0	0.29	0.14
15	0.33	0.17
30	0.41	0.23
45	0.44	0.26
60	0.57	0.36
67.5	0.62	0.43
75	0.77	0.62
80	0.93	0.86
84	0.98	0.95
85	1.00	0.99

Table 41. ^{4}He on Cu, E_0=4 keV (KO83 EXP).

θ (deg)	R_N	R_E
0		0.09
12		0.11
24		0.12
36		0.15
48		0.19
60		0.22
60		0.26
66		0.30
72		0.36
78		0.45

Table 42. ^4He on Cu, E_0=5 keV (OE76 CS).

θ (deg)	R_N	R_E
0	0.19	0.08
30	0.28	0.13
60	0.47	0.27
75	0.61	0.42
80	0.71	0.56
85	0.87	0.81
86.3	0.96	0.92
87.5	1.00	0.98

Table 43. ^4He on Au, E_0=5 keV (KO83 EXP).

θ (deg)	R_N	R_E
0		0.14
24		0.18
48		0.27
60		0.37
72		0.42
72		0.44

MAIN FIGURES

Dependence on angle of incidence θ of the number-backscattering coefficient R_N and the energy-backscattering coefficient R_E. Points: data; dashed lines: the analytic formula fitted to each data set; solid lines: the generalized analytic formula for R_N (upper) and that for R_E (lower).

The order in which each combination of the incident ions, the target materials and the incident energies appears is given in the following list. Sources of the data are shown by the use of abbreviations, and the corresponding references are given in the alphabetical order at the end of this report. The abbreviations are followed by the letters CS or EXP. The former means computer simulation, and the latter, experiment.

LIST OF MAIN FIGURES

No. of Figure	Incident Ion and Target Material	Incident Energy (keV)
1	H on Cu	0.1
2	H on Cu	1
3	H on Cu	5
4	H on Nb	4.6
5	H on Nb	9.1
6	H on Nb	23
7	H on Nb	46
8	H on Au	1.5
9	H on Au	2
10	H on Au	3
11	H on Au	5
12	H on Au	7
13	H on Au	10
14	D on C	0.01
15	D on C	0.03
16	D on C	0.05
17	D on C	0.07
18	D on C	0.09
19	D on C	0.15
20	D on C	0.25
21	D on C	0.35
22	D on C	0.45
23	D on C	0.5
24	D on C	0.55
25	D on C	0.65
26	D on C	0.75
27	D on C	0.85
28	D on C	0.95
29	D on C	1.5
30	D on Au	0.5
31	D on Au	2.5
32	D on Au	5
33	D on Au	8.3
34	^{3}He on Ni	1
35	^{3}He on Ni	3
36	^{3}He on Ni	8
37	^{3}He on Ni	25

LIST OF MAIN FIGURES (Continued)

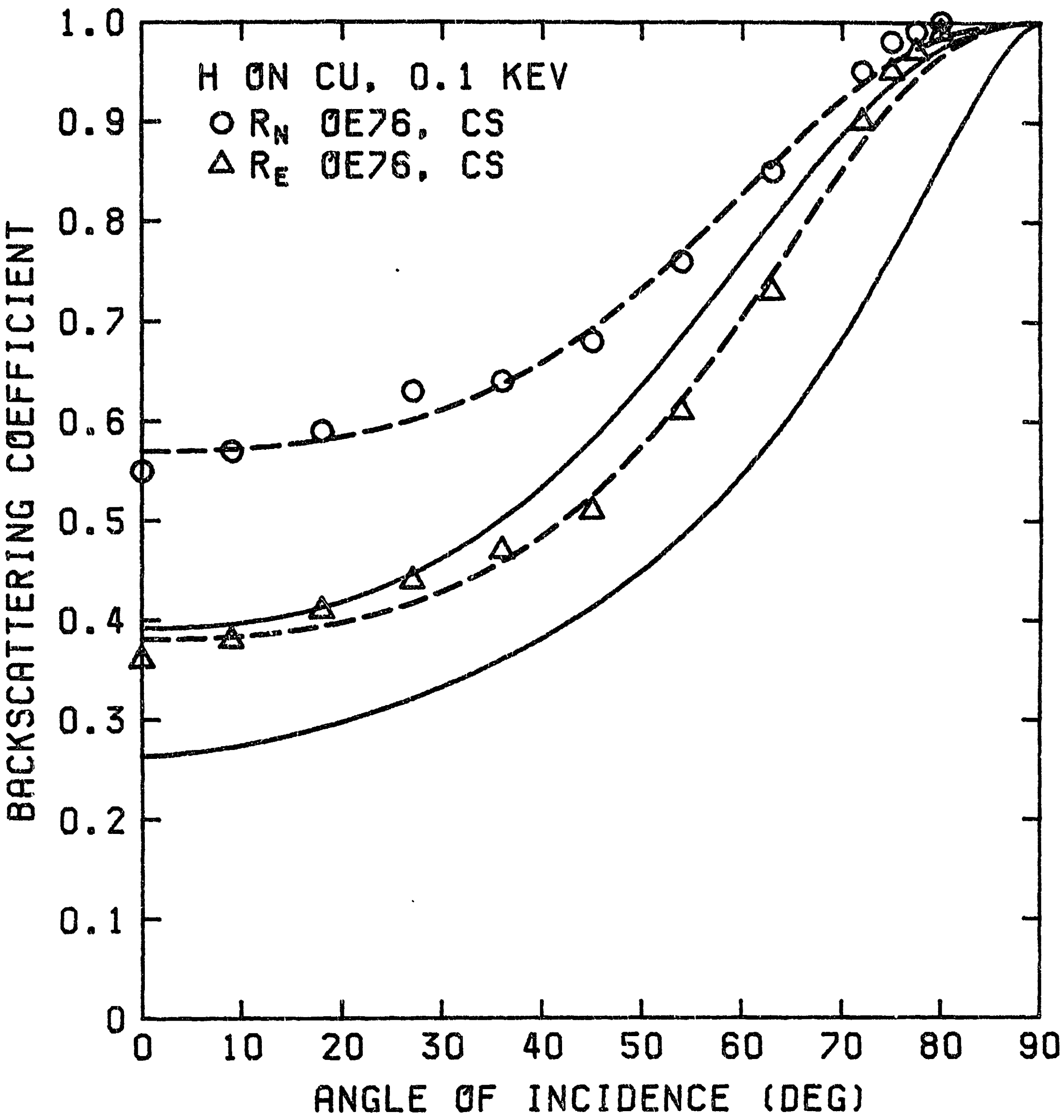
H ØN CU, 0.1 KEV
O R_N ØE76, CS
Δ R_E ØE76, CS
BACKSCATTERING CØEFFICIENT
ANGLE ØF INCIDENCE (DEG)
1.0
0.9
0.8
0.7
0.6
0.5
0.4
0.3
0.2
0.1
0
0 10 20 30 40 50 60 70 80 90

FIG.1

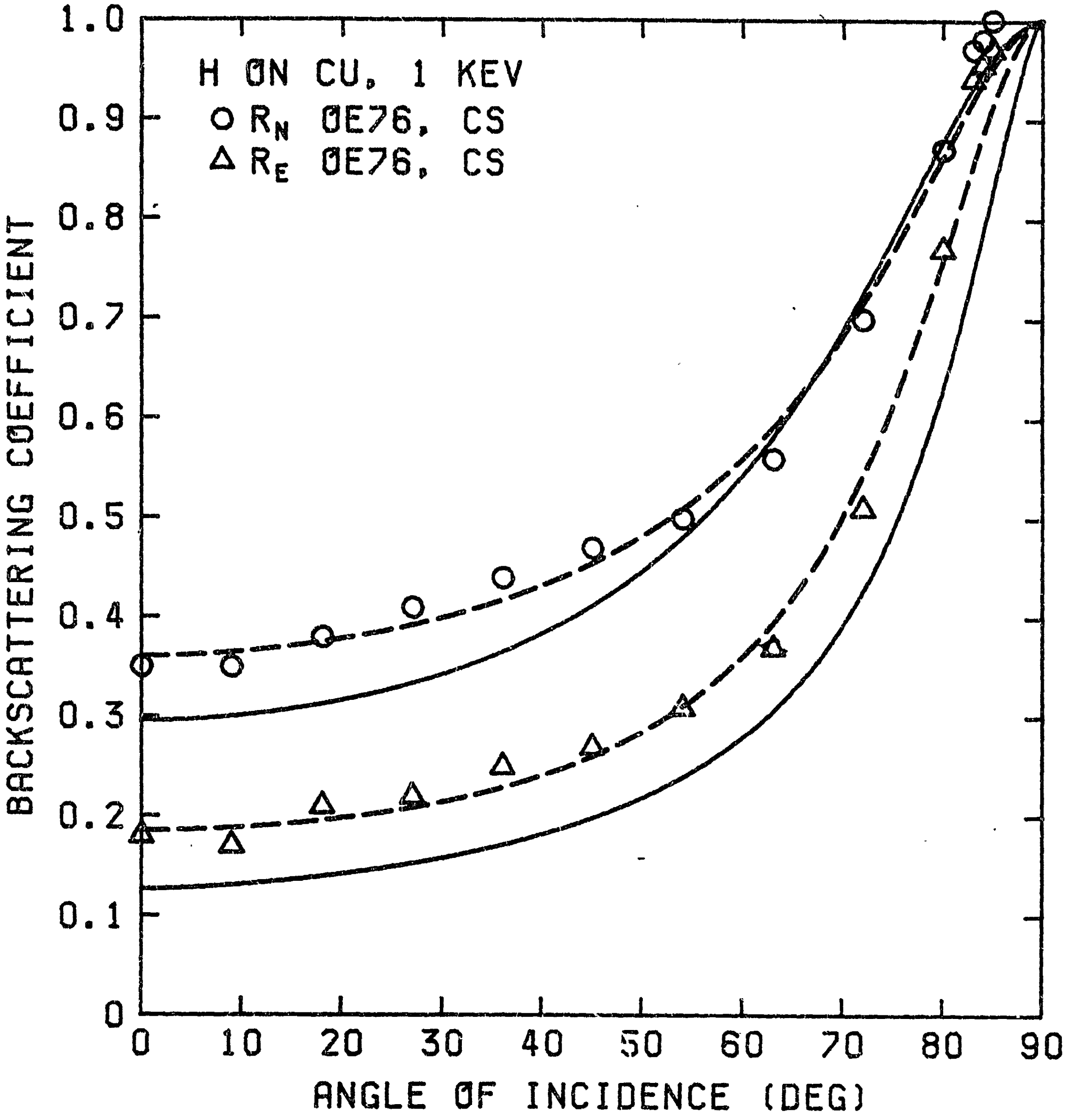
H ON CU, 1 KEV
○ R_N OE76, CS
△ R_E OE76, CS
BACKSCATTERING COEFFICIENT
ANGLE OF INCIDENCE (DEG)
1.0
0.9
0.8
0.7
0.6
0.5
0.4
0.3
0.2
0.1
0
0
10
20
30
40
50
60
70
80
90

FIG.2

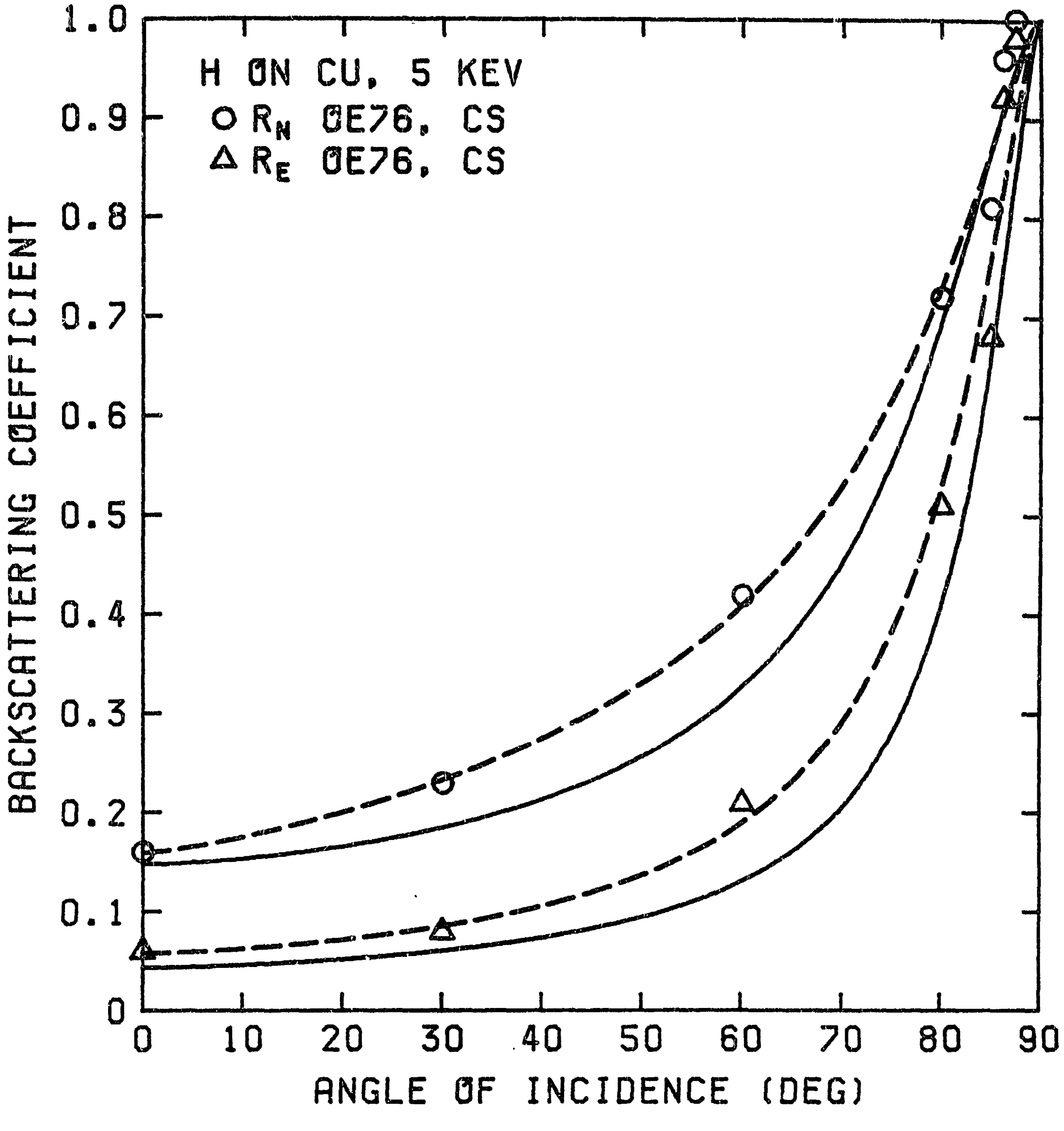

H ØN CU, 5 KEV
O R_N ØE76, CS
Δ R_E ØE76, CS
BACKSCATTERING CØEFFICIENT
ANGLE ØF INCIDENCE (DEG)
1.0
0.9
0.8
0.7
0.6
0.5
0.4
0.3
0.2
0.1
0
0
10
20
30
40
50
60
70
80
90

FIG.3

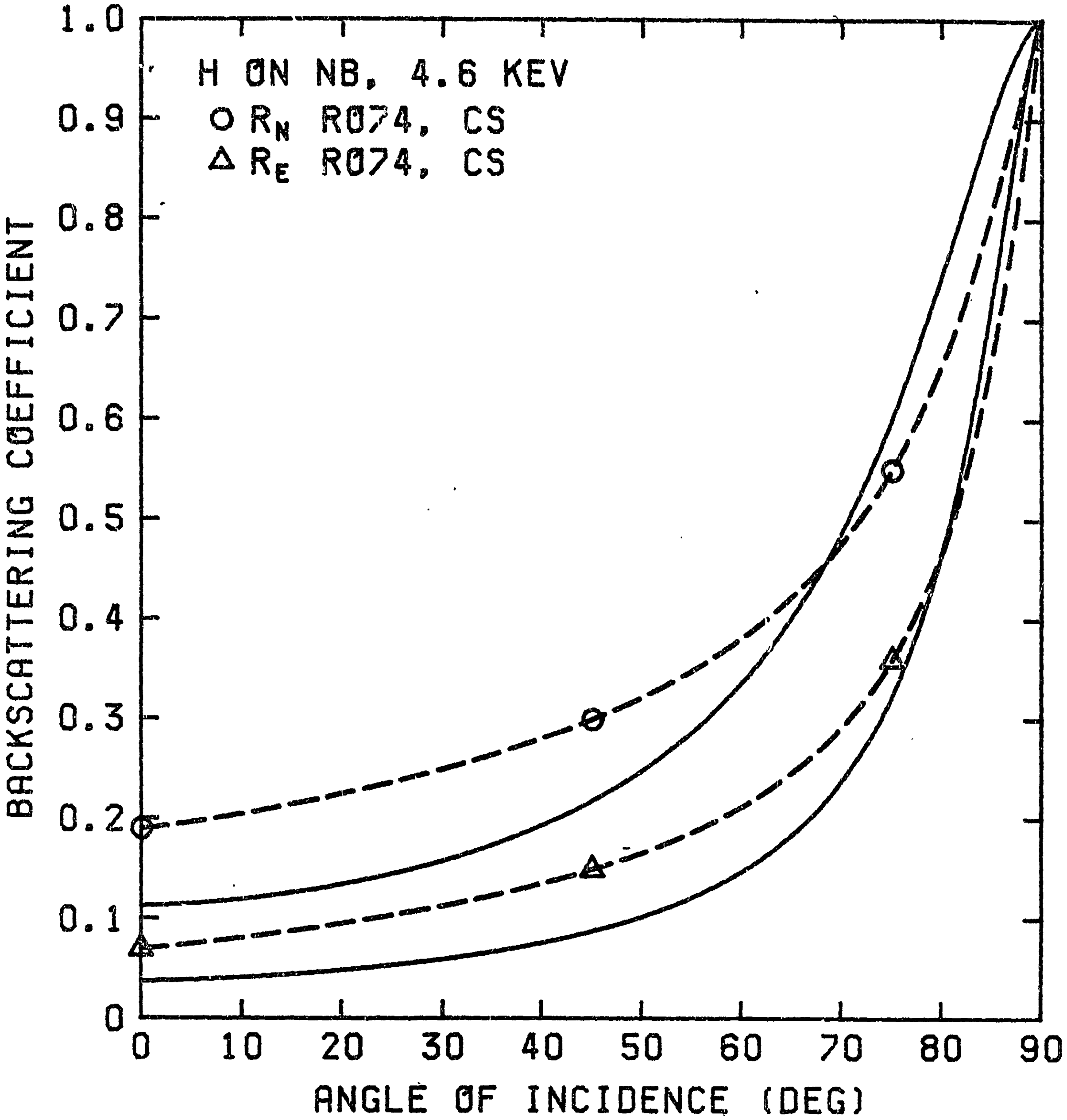
H ON NB, 4.6 KEV
○ R_N R074, CS
△ R_E R074, CS
BACKSCATTERING COEFFICIENT
ANGLE OF INCIDENCE (DEG)
1.0
0.9
0.8
0.7
0.6
0.5
0.4
0.3
0.2
0.1
0
0 10 20 30 40 50 60 70 80 90

FIG.4

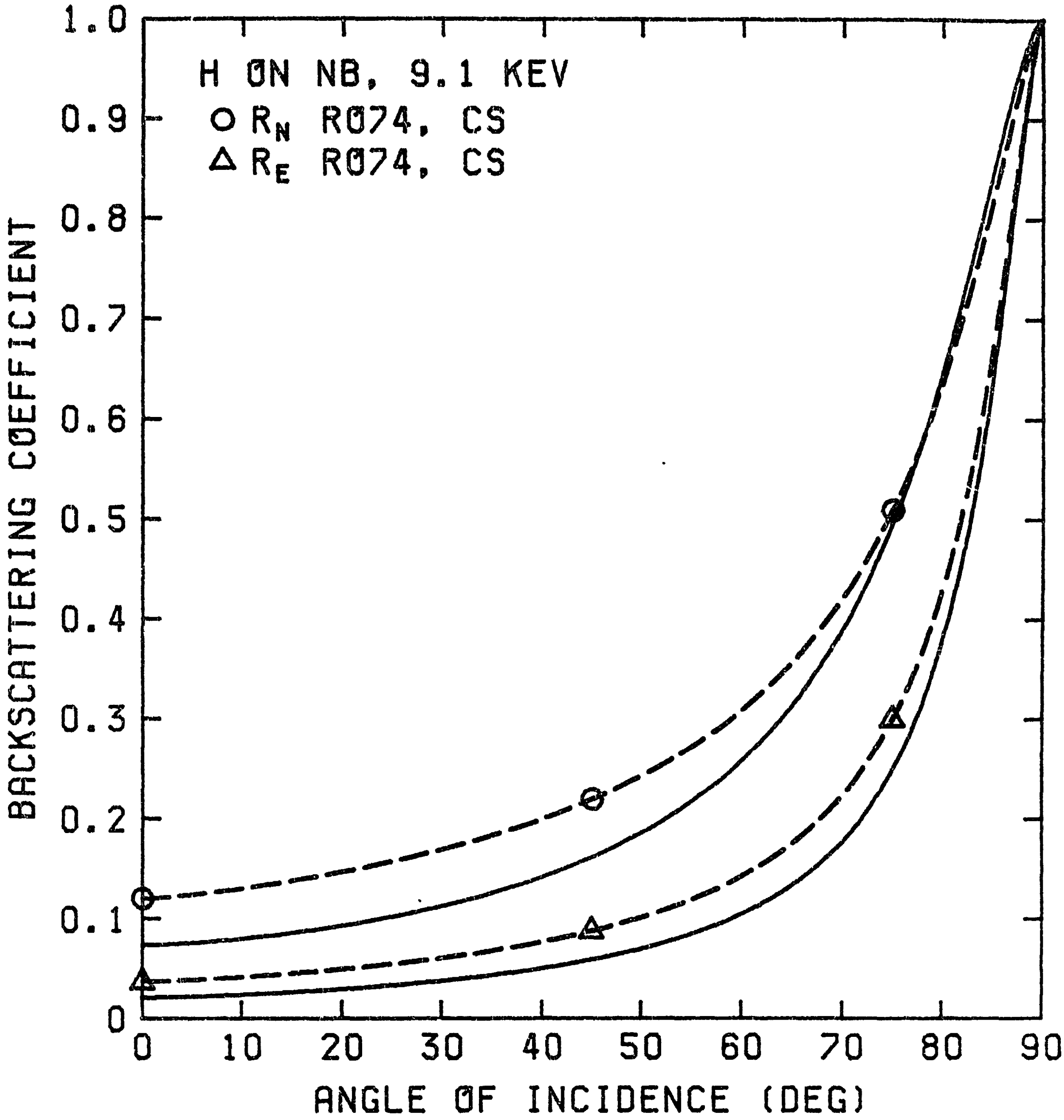

H ØN NB, 9.1 KEV
○ R_N RØ74, CS
△ R_E RØ74, CS
BACKSCATTERING CØEFFICIENT
1.0
0.9
0.8
0.7
0.6
0.5
0.4
0.3
0.2
0.1
0
0
10
20
30
40
50
60
70
80
90
ANGLE ØF INCIDENCE (DEG)

FIG.5

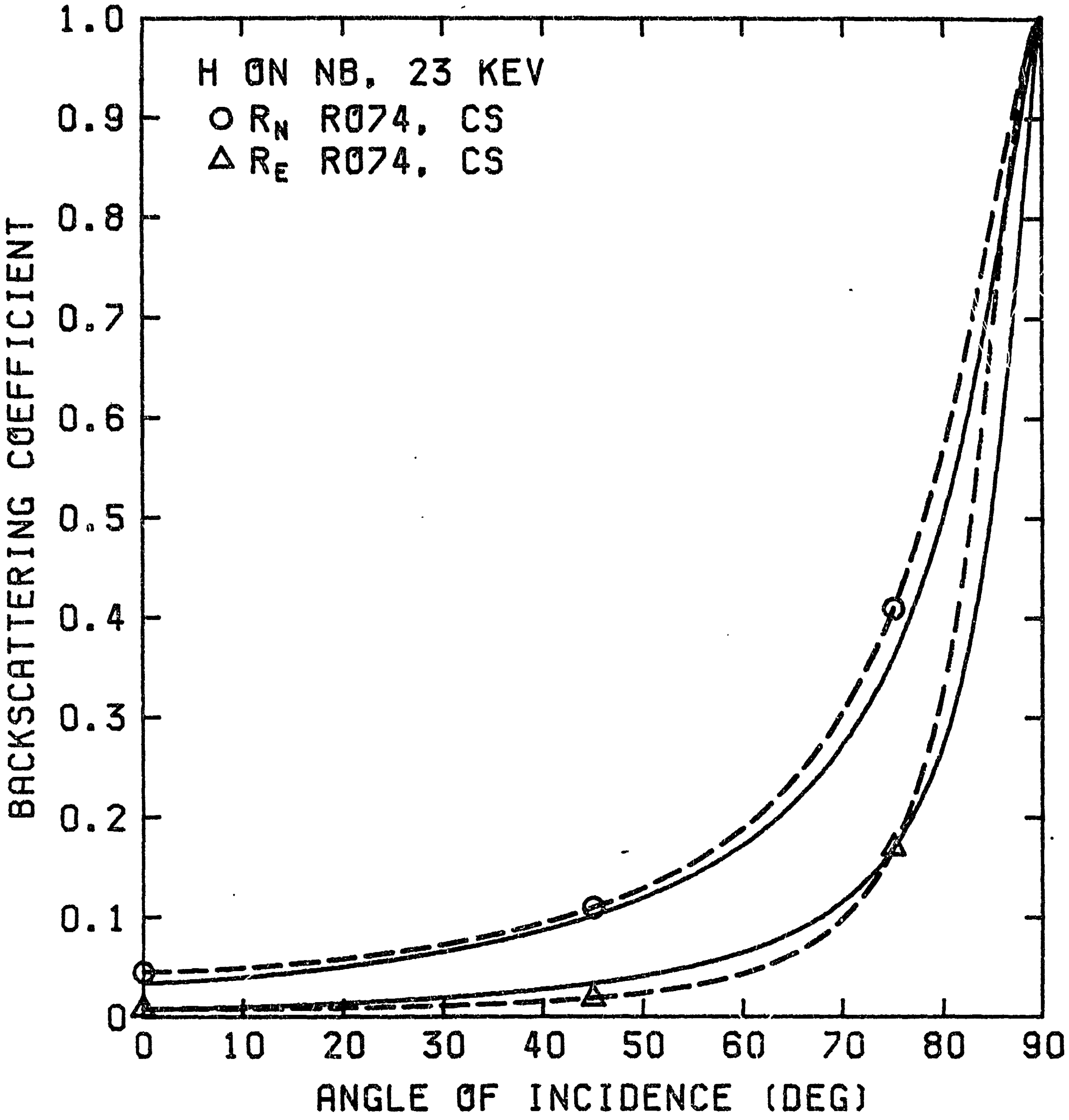
H ØN NB, 23 KEV
○ R_N RØ74, CS
△ R_E RØ74, CS
BACKSCATTERING CØEFFICIENT
1.0
0.9
0.8
0.7
0.6
0.5
0.4
0.3
0.2
0.1
0
0
10
20
30
40
50
60
70
80
90
ANGLE ØF INCIDENCE (DEG)

FIG.6

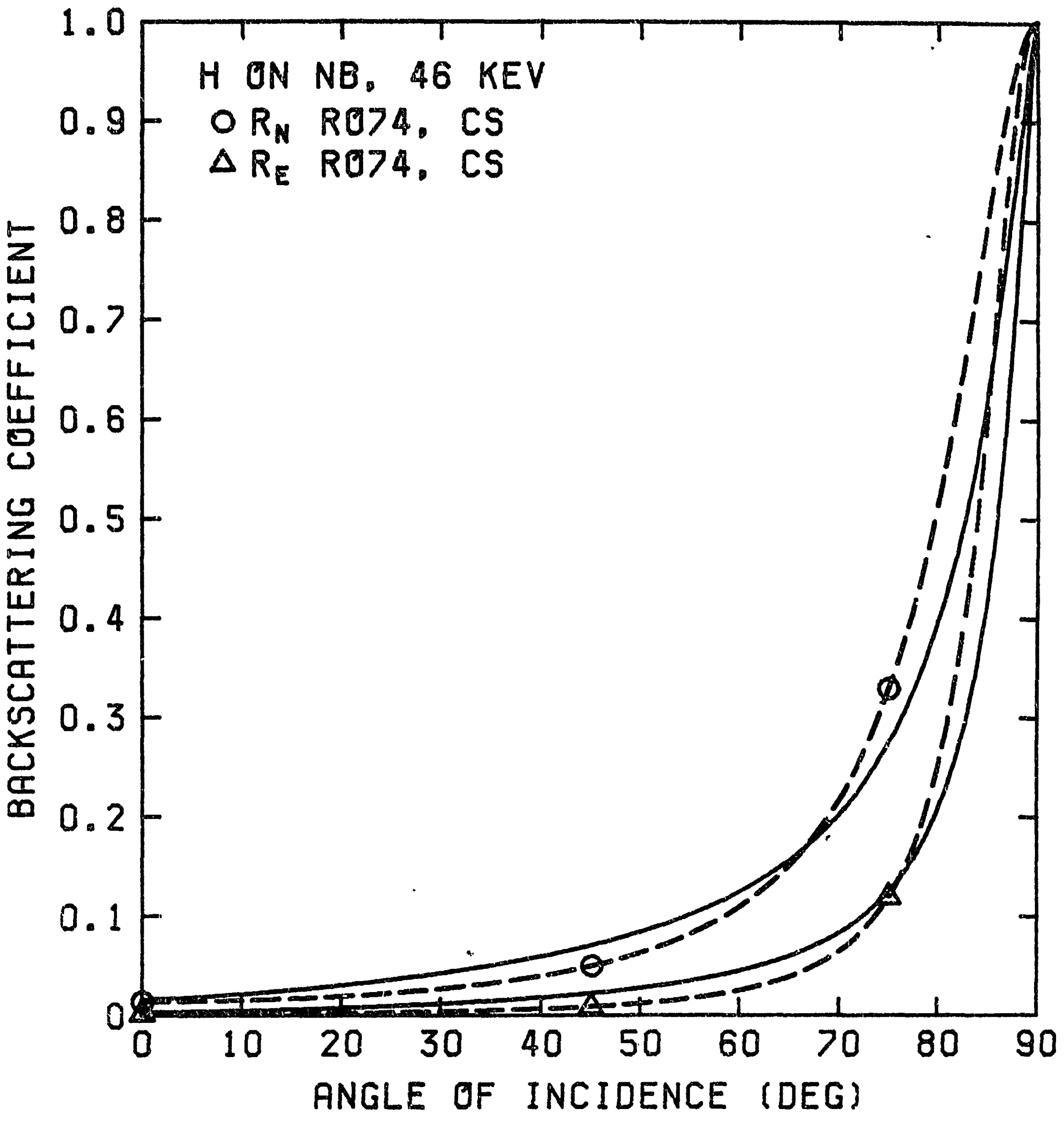
H ON NB, 46 KEV
○ R_N R074, CS
△ R_E R074, CS
BACKSCATTERING COEFFICIENT
1.0
0.9
0.8
0.7
0.6
0.5
0.4
0.3
0.2
0.1
0
0
10
20
30
40
50
60
70
80
90
ANGLE OF INCIDENCE (DEG)

FIG.7

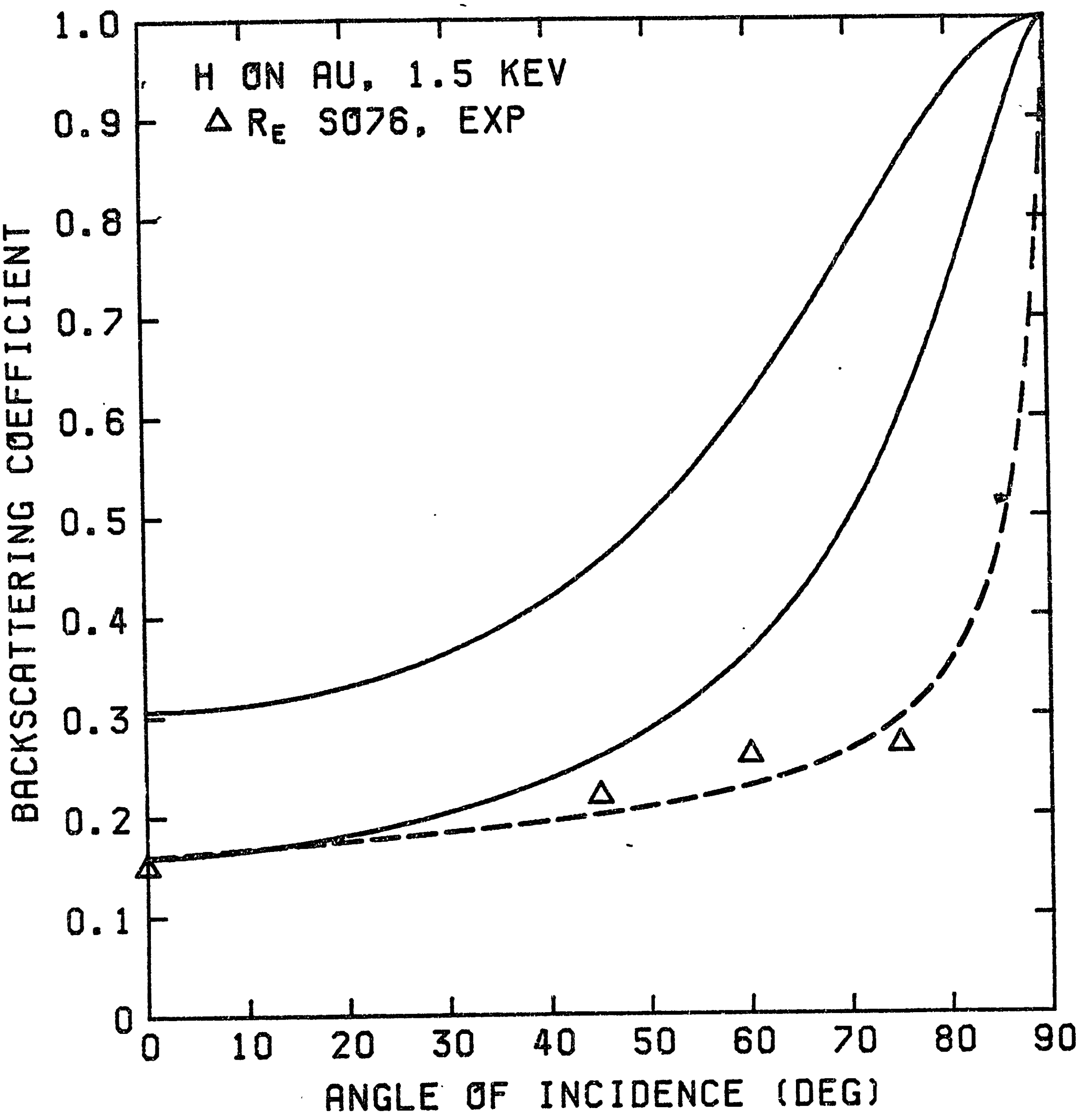
H ØN AU, 1.5 KEV
△ R_E SØ76, EXP
BACKSCATTERING CØEFFICIENT
ANGLE ØF INCIDENCE (DEG)
1.0
0.9
0.8
0.7
0.6
0.5
0.4
0.3
0.2
0.1
0
0
10
20
30
40
50
60
70
80
90

FIG.8

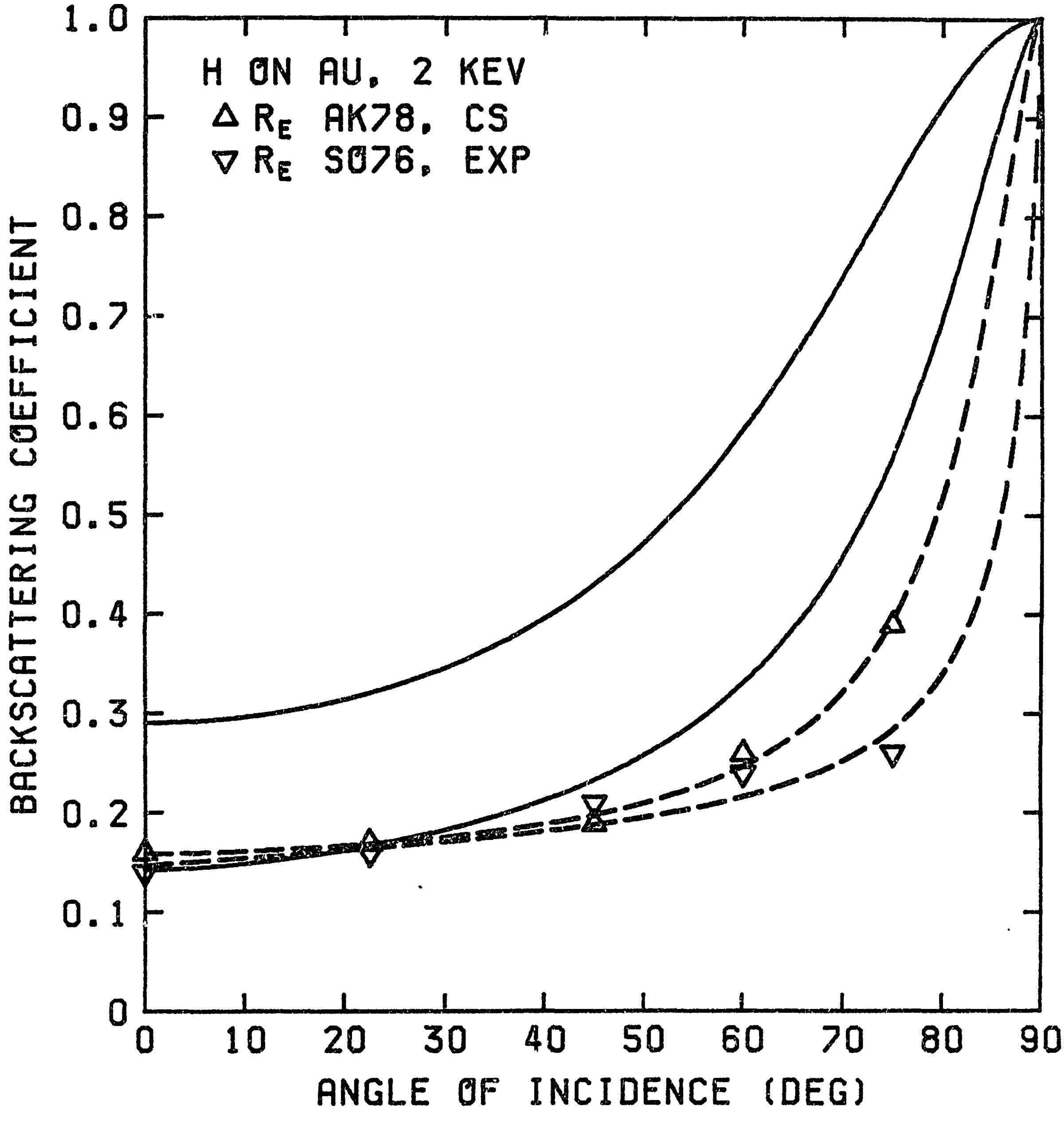
H ØN AU, 2 KEV
△ R_E AK78, CS
▽ R_E SØ76, EXP
BACKSCATTERING CØEFFICIENT
ANGLE ØF INCIDENCE (DEG)
1.0
0.9
0.8
0.7
0.6
0.5
0.4
0.3
0.2
0.1
0
0 10 20 30 40 50 60 70 80 90

FIG.9

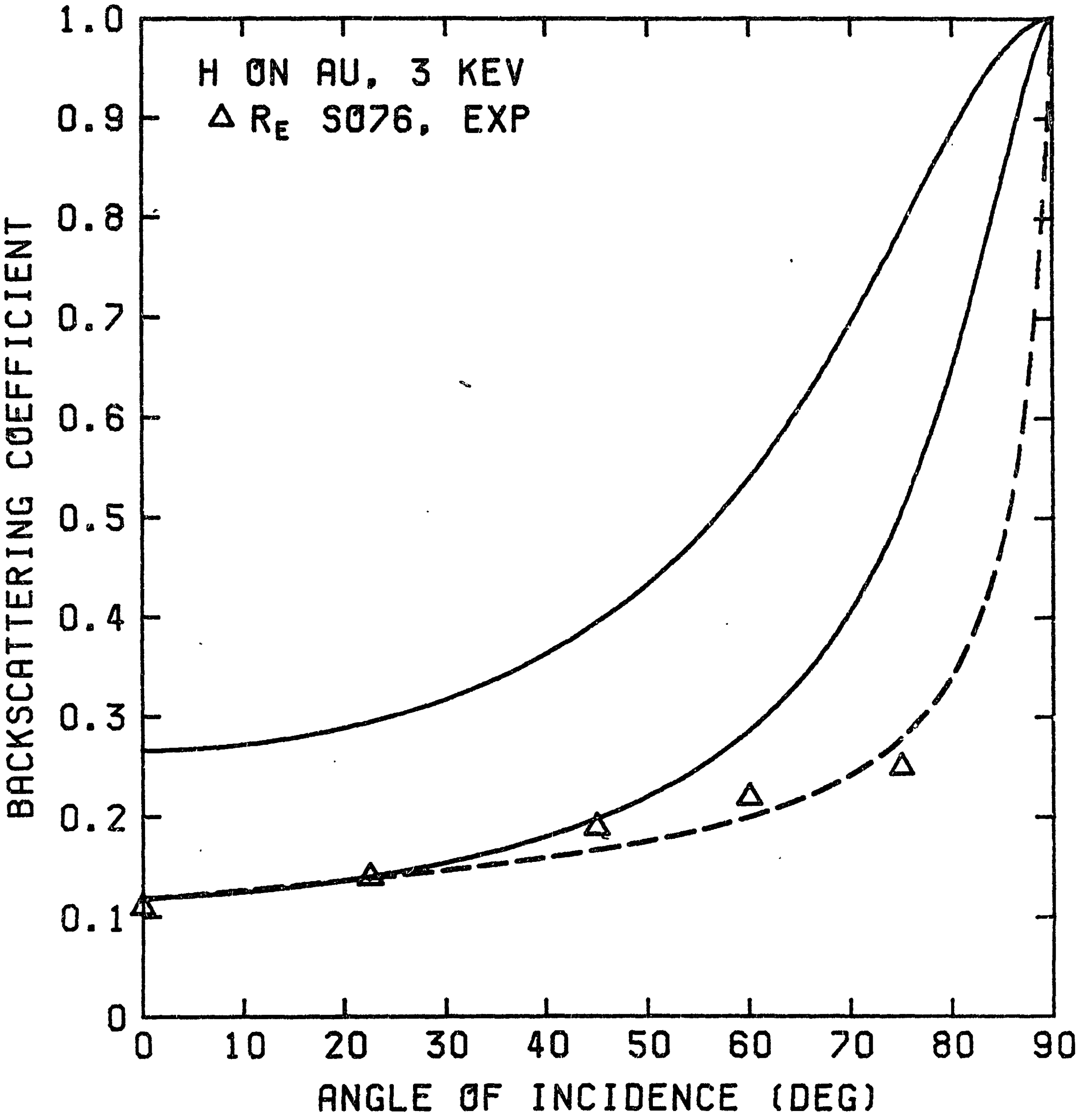
1.0
0.9
0.8
0.7
0.6
0.5
0.4
0.3
0.2
0.1
0
BACKSCATTERING COEFFICIENT
H ØN AU, 3 KEV
Δ R_E SØ76, EXP
0 10 20 30 40 50 60 70 80 90
ANGLE ØF INCIDENCE (DEG)

FIG.10

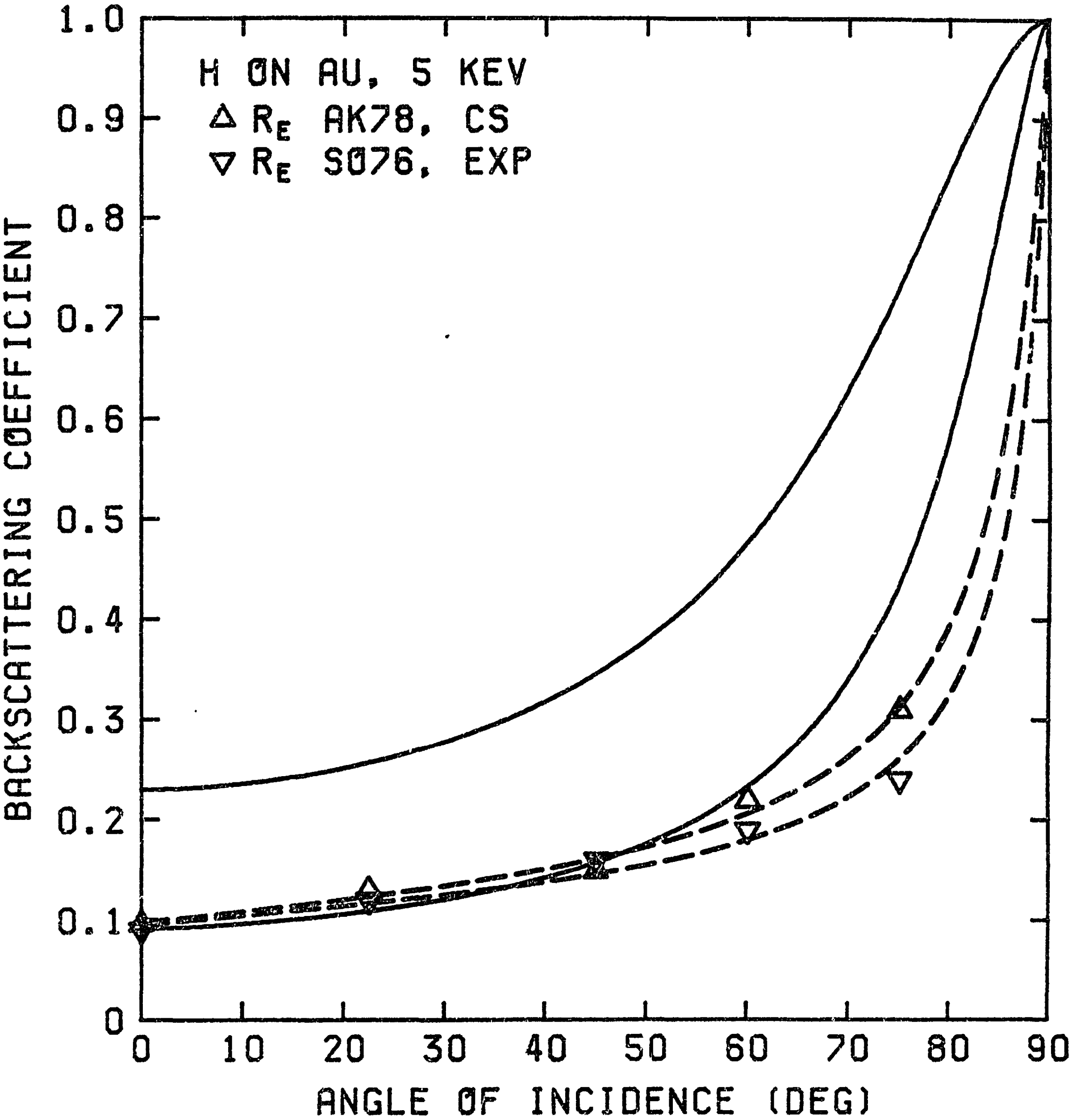
H ØN AU, 5 KEV
△ R_E AK78, CS
▽ R_E SØ76, EXP
BACKSCATTERING CØEFFICIENT
ANGLE ØF INCIDENCE (DEG)
1.0
0.9
0.8
0.7
0.6
0.5
0.4
0.3
0.2
0.1
0
0
10
20
30
40
50
60
70
80
90

FIG.11

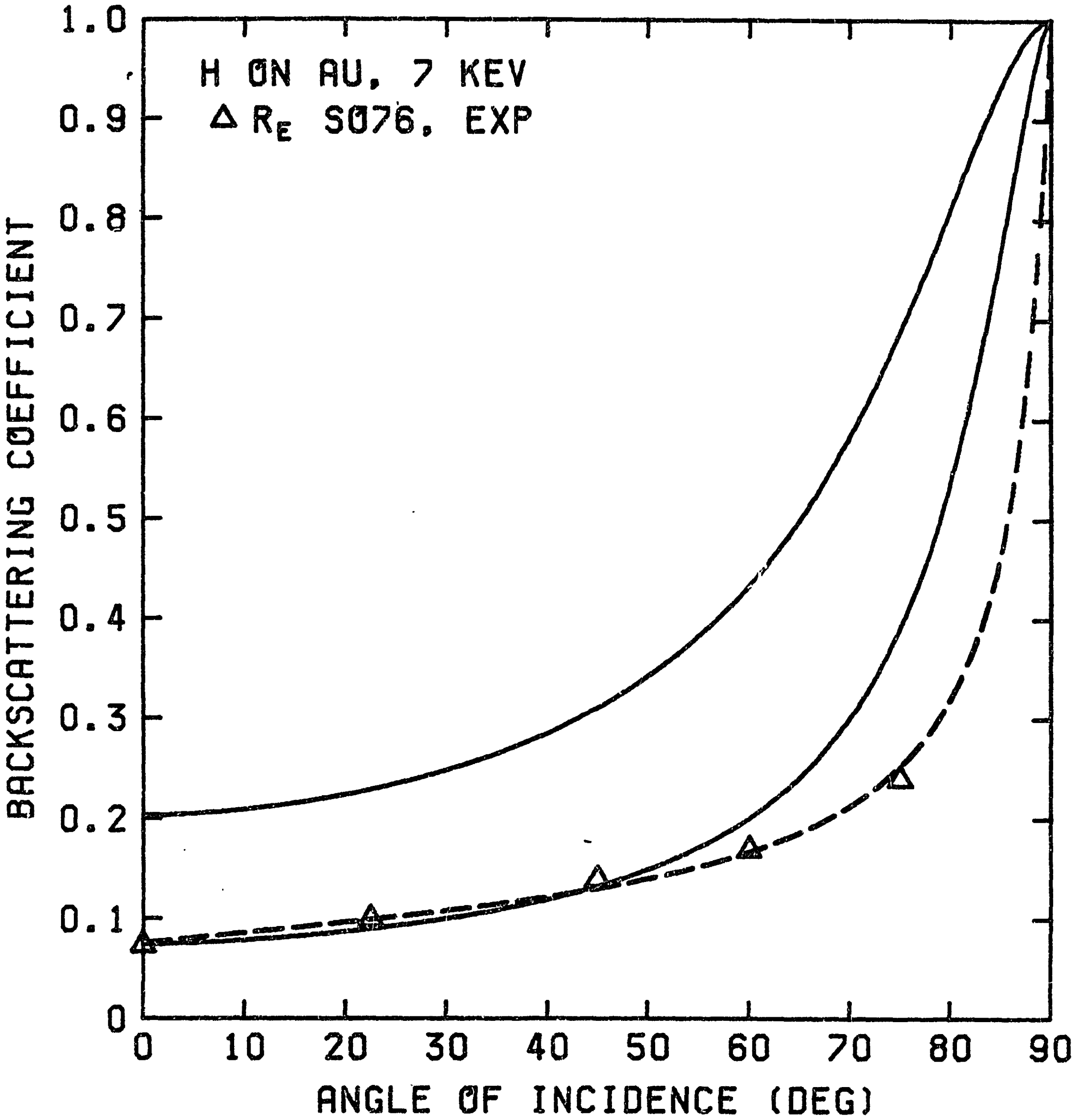
H ON AU, 7 KEV
Δ R_E S076, EXP
BACKSCATTERING COEFFICIENT
1.0
0.9
0.8
0.7
0.6
0.5
0.4
0.3
0.2
0.1
0
0
10
20
30
40
50
60
70
80
90
ANGLE OF INCIDENCE (DEG)

FIG.12

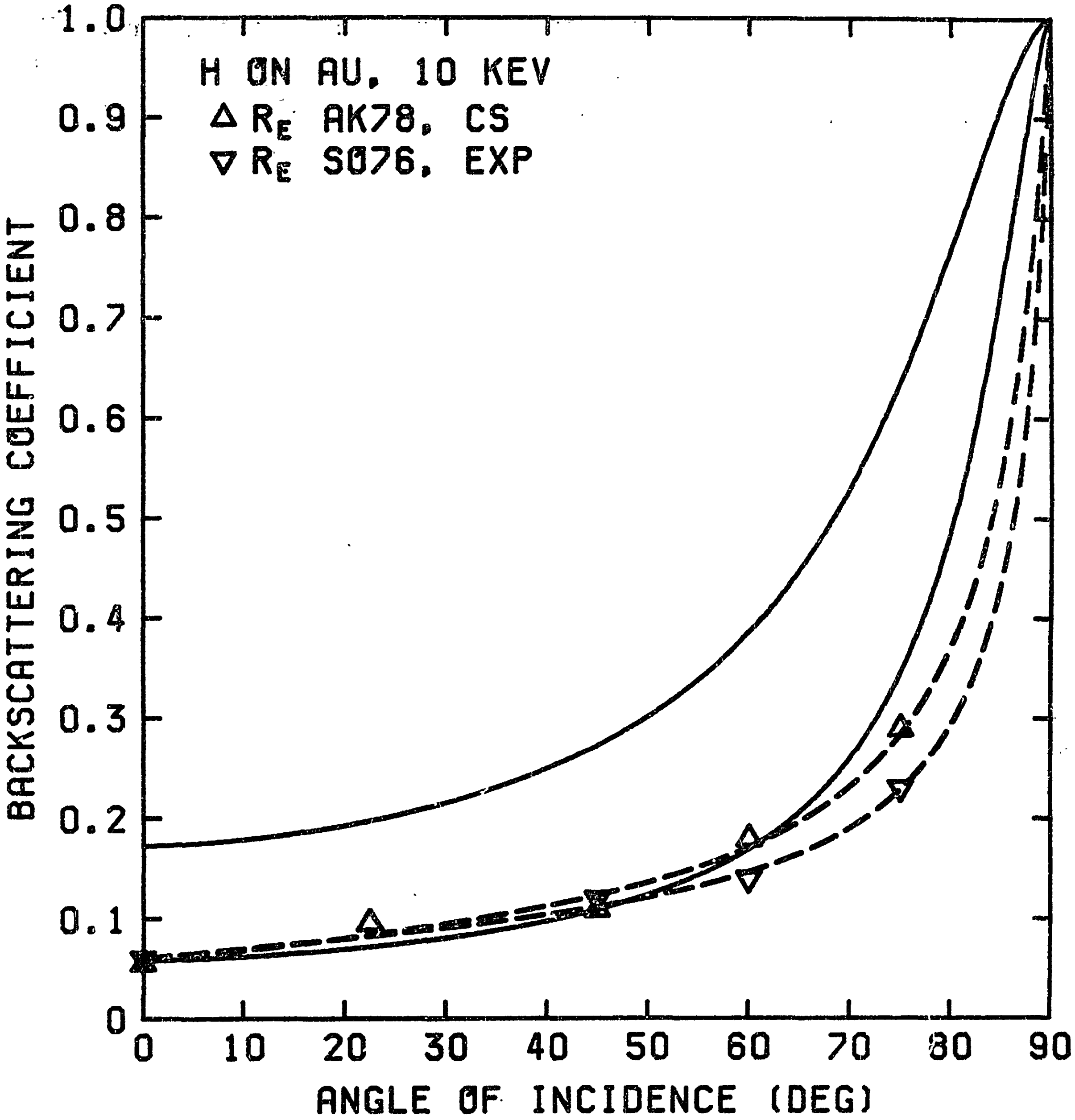
H ØN AU, 10 KEV
△ R_E AK78, CS
▽ R_E SØ76, EXP
BACKSCATTERING COEFFICIENT
ANGLE ØF INCIDENCE (DEG)
1.0
0.9
0.8
0.7
0.6
0.5
0.4
0.3
0.2
0.1
0
0
10
20
30
40
50
60
70
80
90

FIG.13

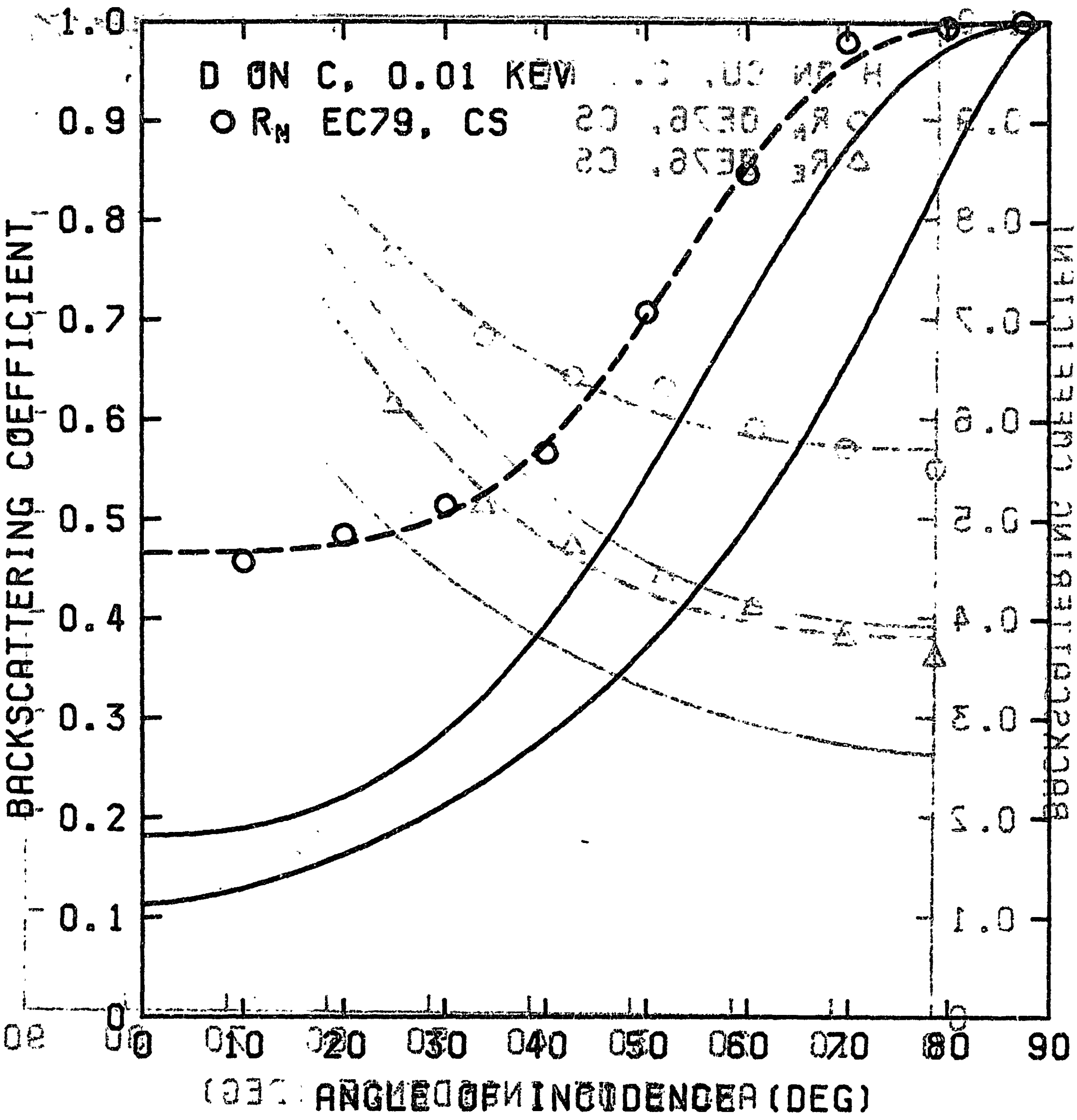
D ON C, 0.01 KEV
O R_N EC79, CS
BACKSCATTERING COEFFICIENT
1.0
0.9
0.8
0.7
0.6
0.5
0.4
0.3
0.2
0.1
0
10
20
30
40
50
60
70
80
90
ANGLE OF INCIDENCE (DEG)

FIG. 14

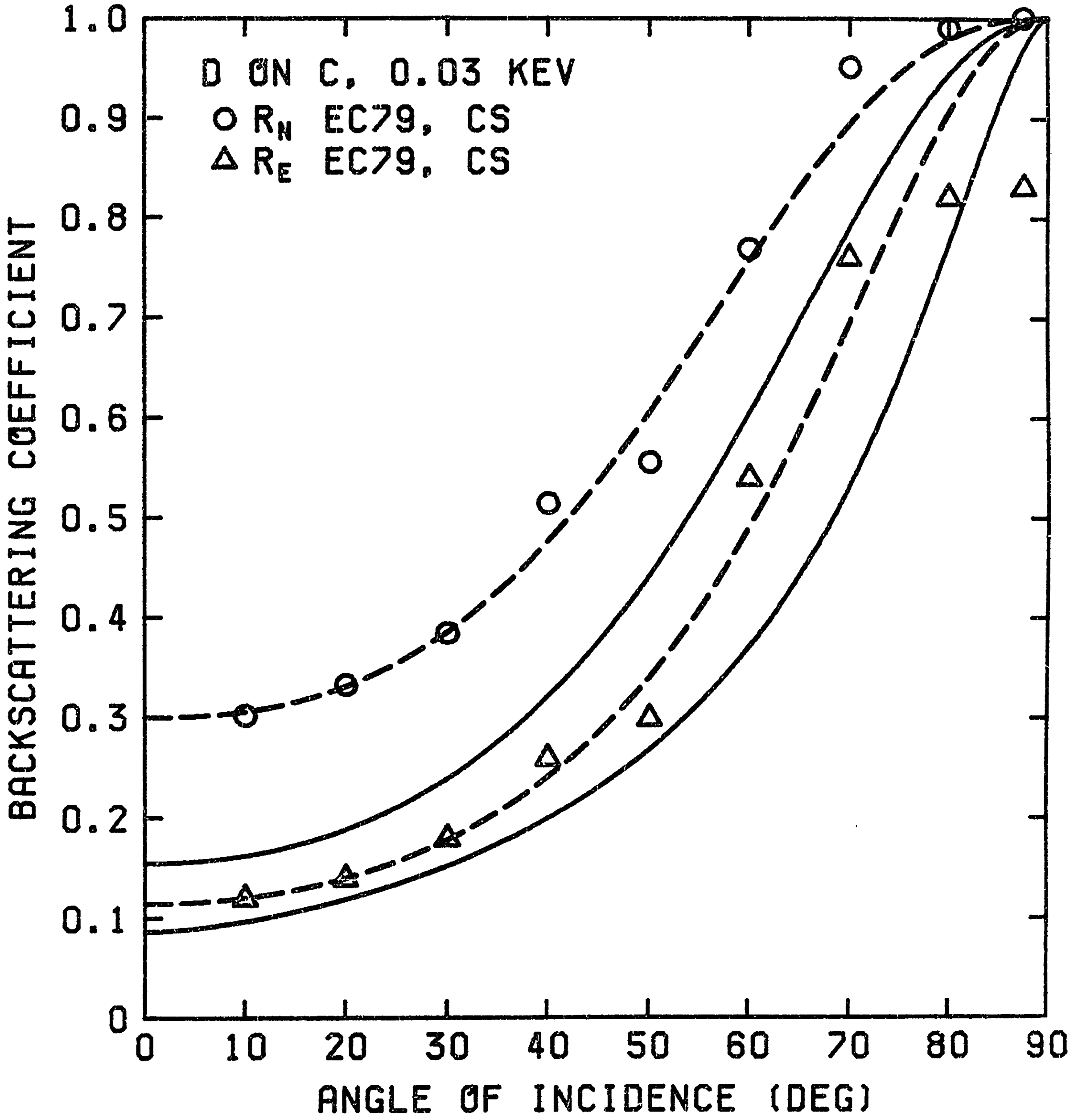

D ØN C, 0.03 KEV
○ R_N EC79, CS
△ R_E EC79, CS
BACKSCATTERING CØEFFICIENT
1.0
0.9
0.8
0.7
0.6
0.5
0.4
0.3
0.2
0.1
0
0
10
20
30
40
50
60
70
80
90
ANGLE ØF INCIDENCE (DEG)

FIG. 15

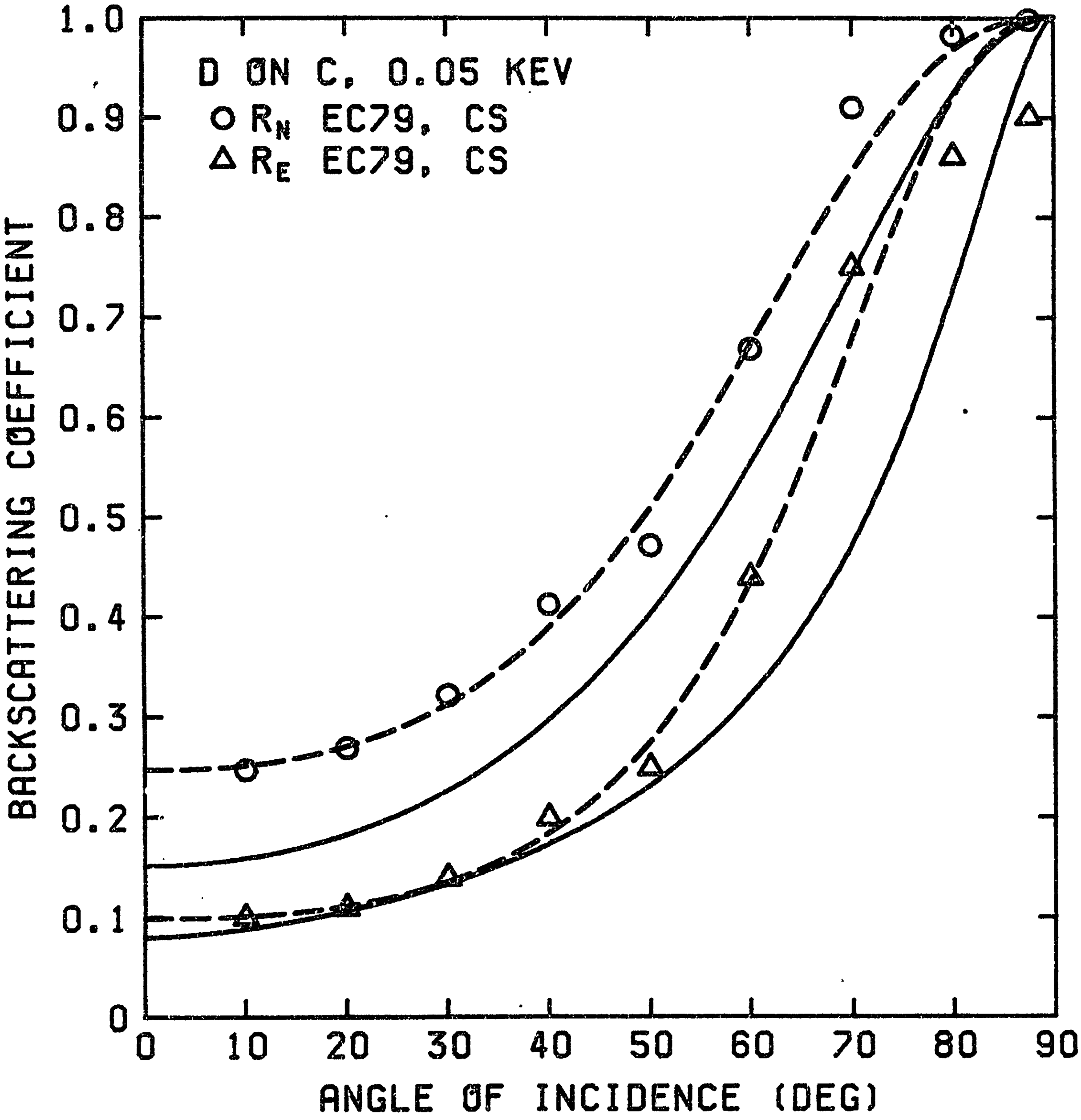

D ØN C, 0.05 KEV
O R_N EC79, CS
Δ R_E EC79, CS
BACKSCATTERING CØEFFICIENT
ANGLE ØF INCIDENCE (DEG)
1.0
0.9
0.8
0.7
0.6
0.5
0.4
0.3
0.2
0.1
0
0 10 20 30 40 50 60 70 80 90

FIG. 16

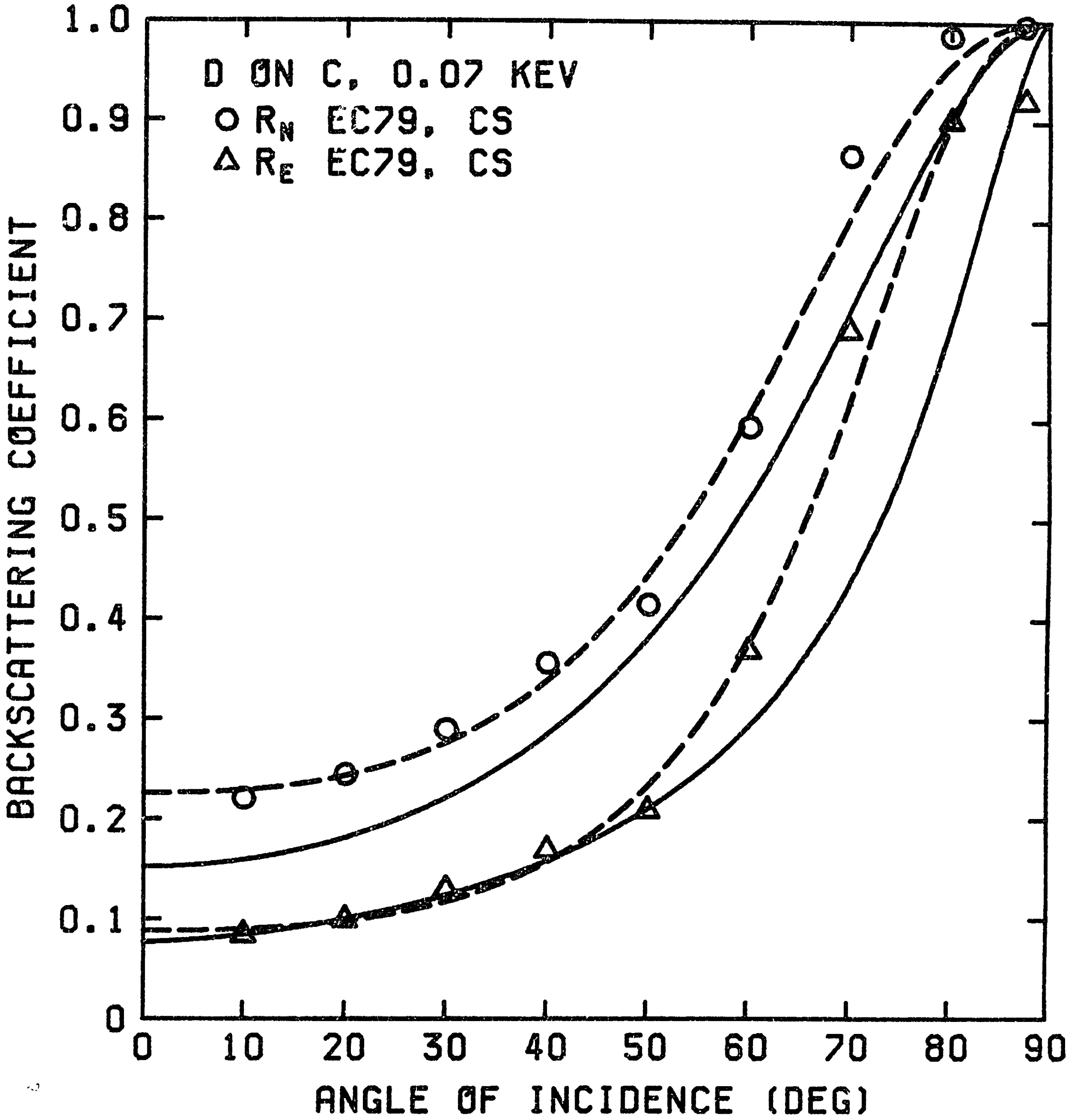
D ØN C, 0.07 KEV
O R_N EC79, CS
Δ R_E EC79, CS
BACKSCATTERING CØEFFICIENT
ANGLE ØF INCIDENCE (DEG)
0
0.1
0.2
0.3
0.4
0.5
0.6
0.7
0.8
0.9
1.0
0
10
20
30
40
50
60
70
80
90

FIG.17

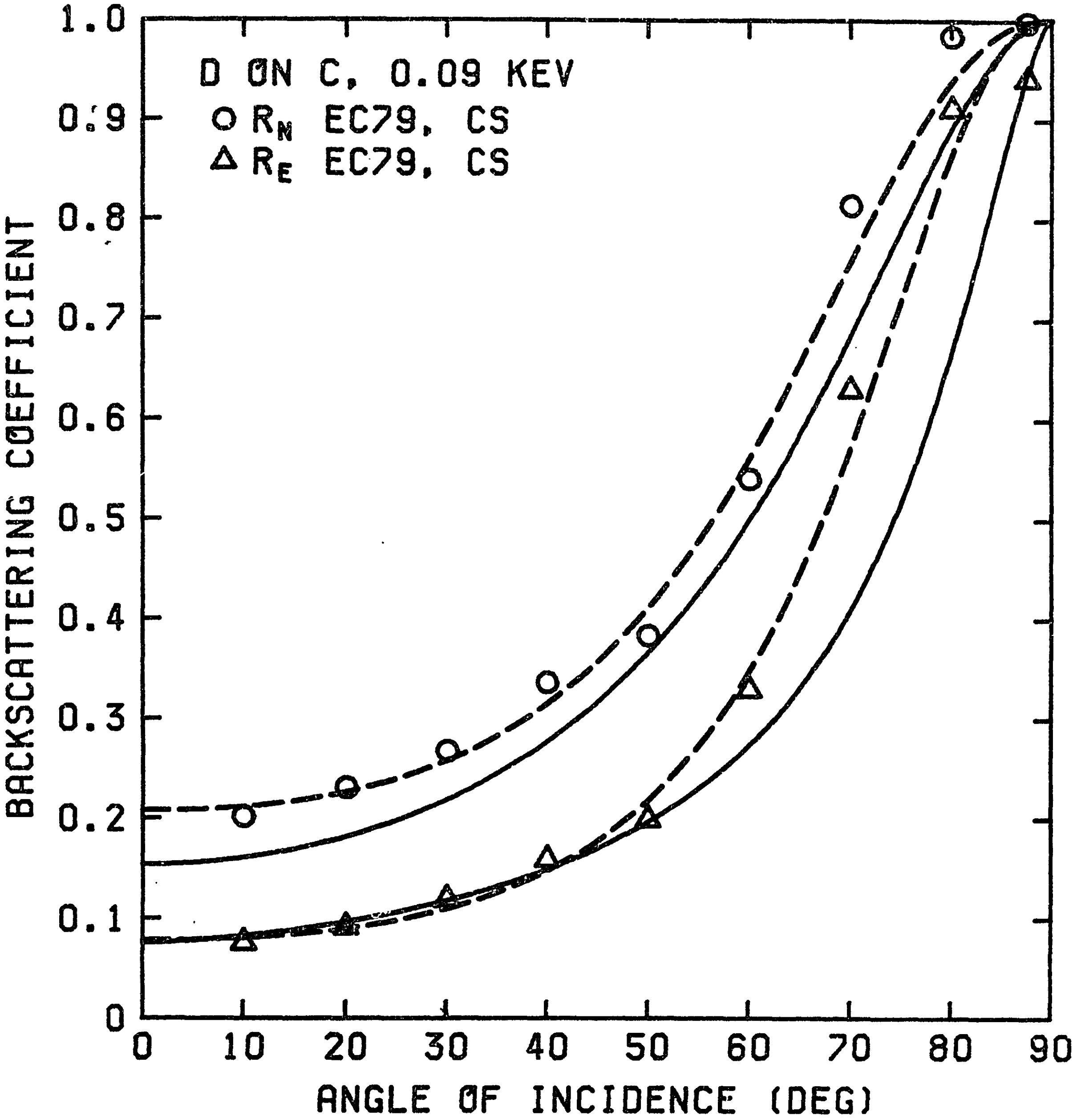
D ON C, 0.09 KEV
RN EC79, CS
RE EC79, CS
BACKSCATTERING COEFFICIENT
ANGLE OF INCIDENCE (DEG)
0
0.1
0.2
0.3
0.4
0.5
0.6
0.7
0.8
0.9
1.0
0
10
20
30
40
50
60
70
80
90

FIG. 18

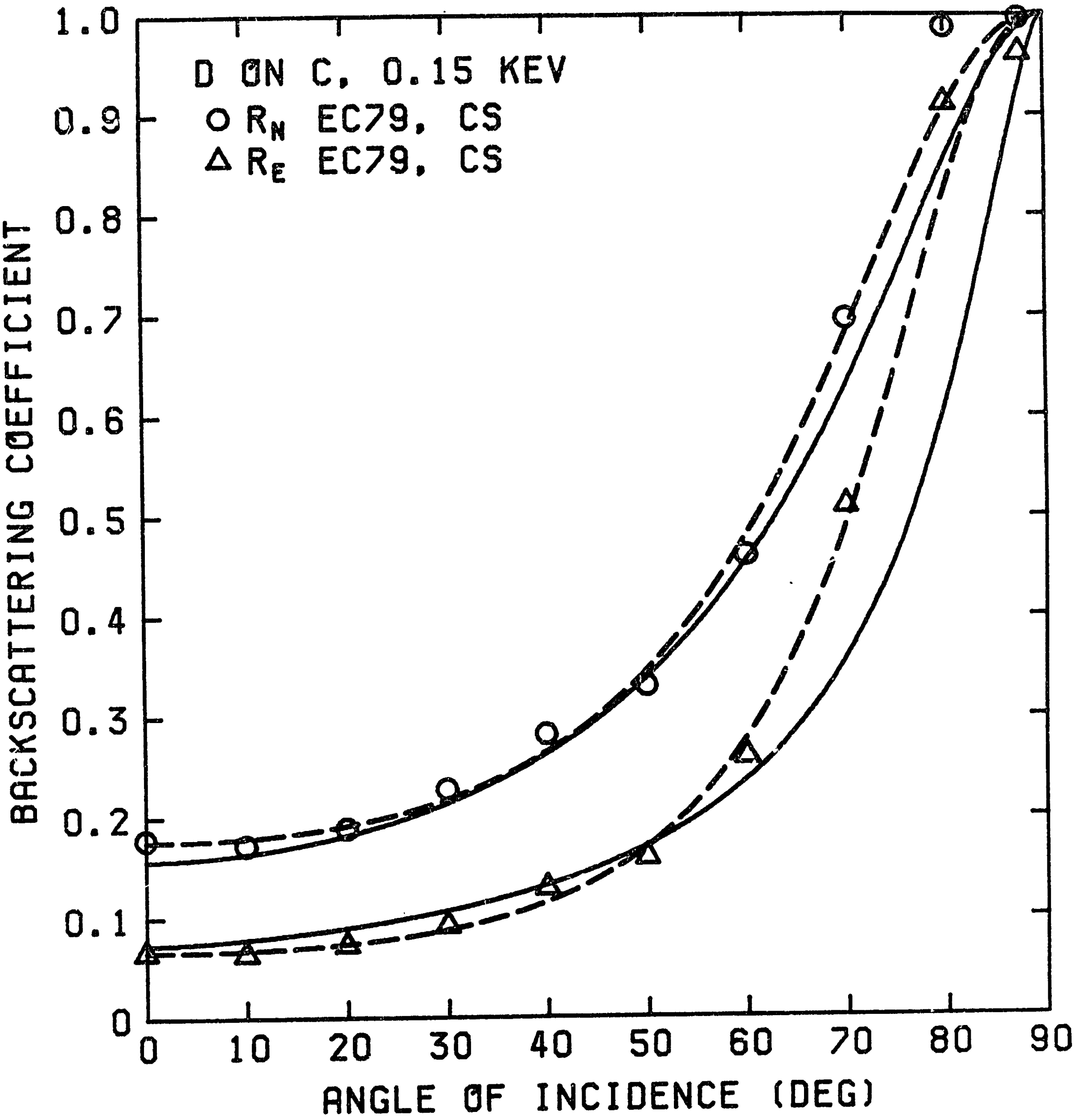
D ØN C, 0.15 KEV
○ R_N EC79, CS
△ R_E EC79, CS
1.0
0.9
0.8
0.7
0.6
0.5
0.4
0.3
0.2
0.1
0
BACKSCATTERING CØEFFICIENT
0
10
20
30
40
50
60
70
80
90
ANGLE ØF INCIDENCE (DEG)

FIG.19

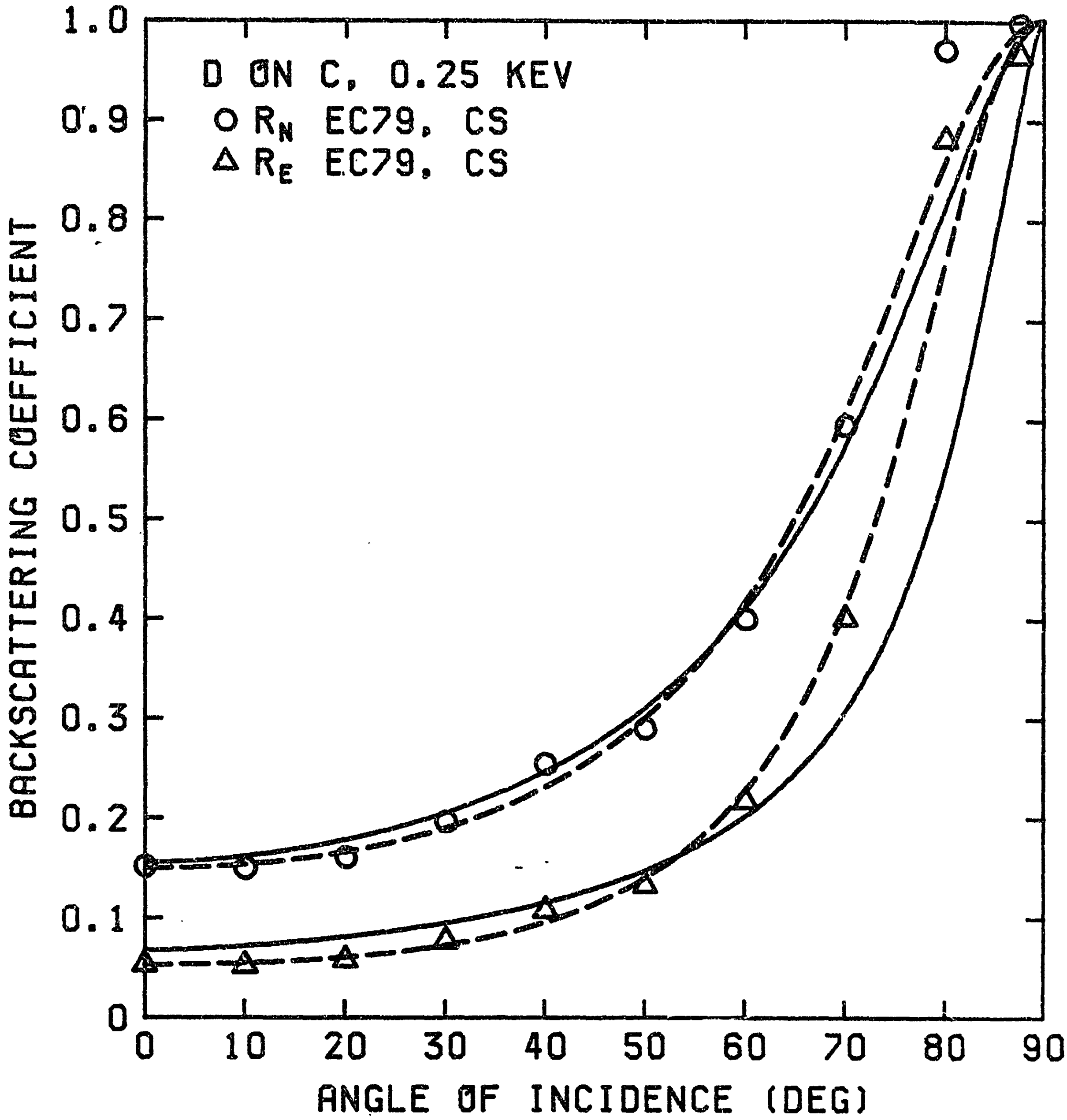
D ON C, 0.25 KEV
○ R_N EC79, CS
△ R_E EC79, CS
BACKSCATTERING COEFFICIENT
ANGLE OF INCIDENCE (DEG)
0
0.1
0.2
0.3
0.4
0.5
0.6
0.7
0.8
0.9
1.0
0
10
20
30
40
50
60
70
80
90

FIG.20

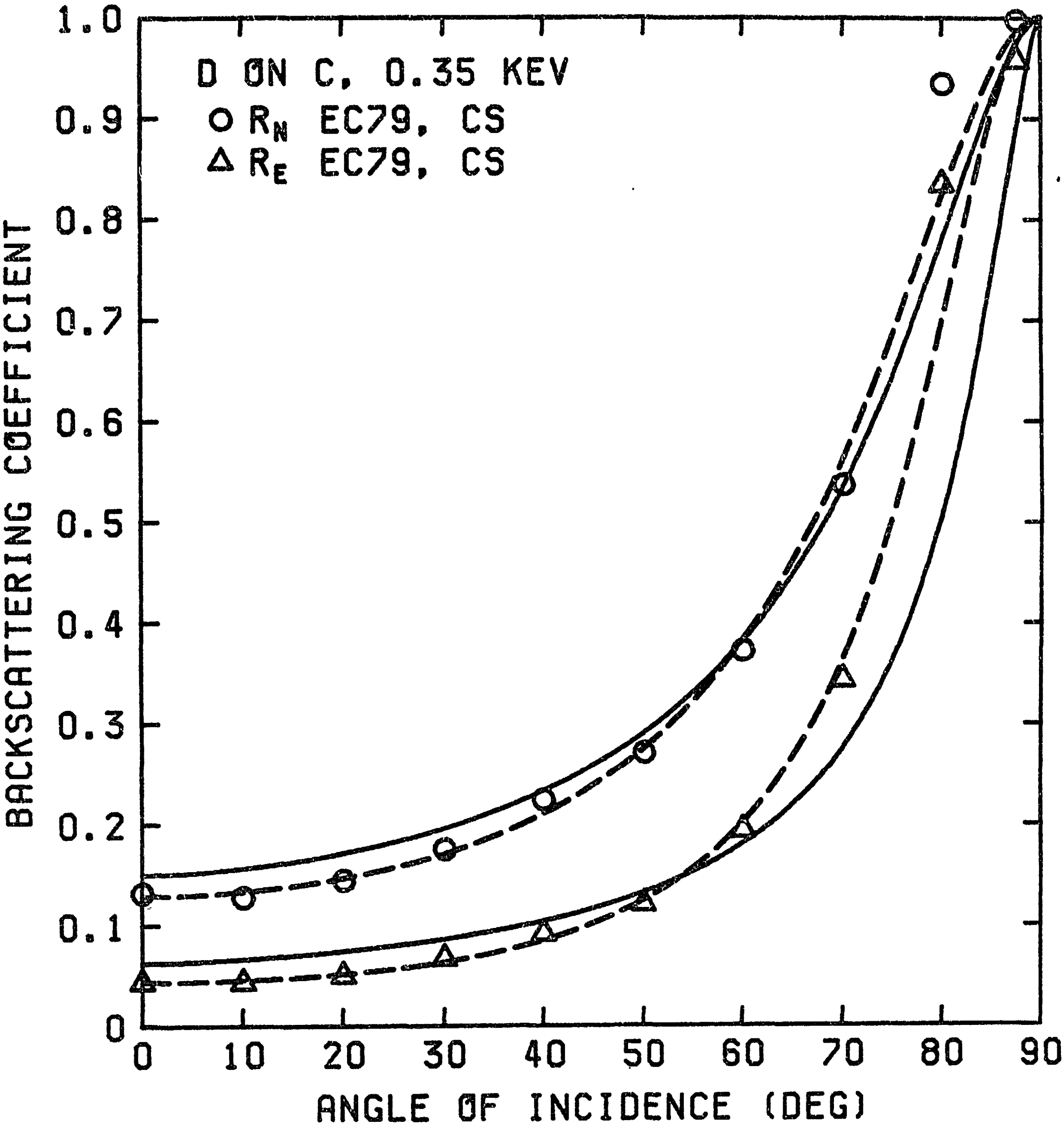
D ØN C, 0.35 KEV
○ R_N EC79, CS
△ R_E EC79, CS
BACKSCATTERING CØEFFICIENT
ANGLE ØF INCIDENCE (DEG)
1.0
0.9
0.8
0.7
0.6
0.5
0.4
0.3
0.2
0.1
0
0 10 20 30 40 50 60 70 80 90

FIG. 21

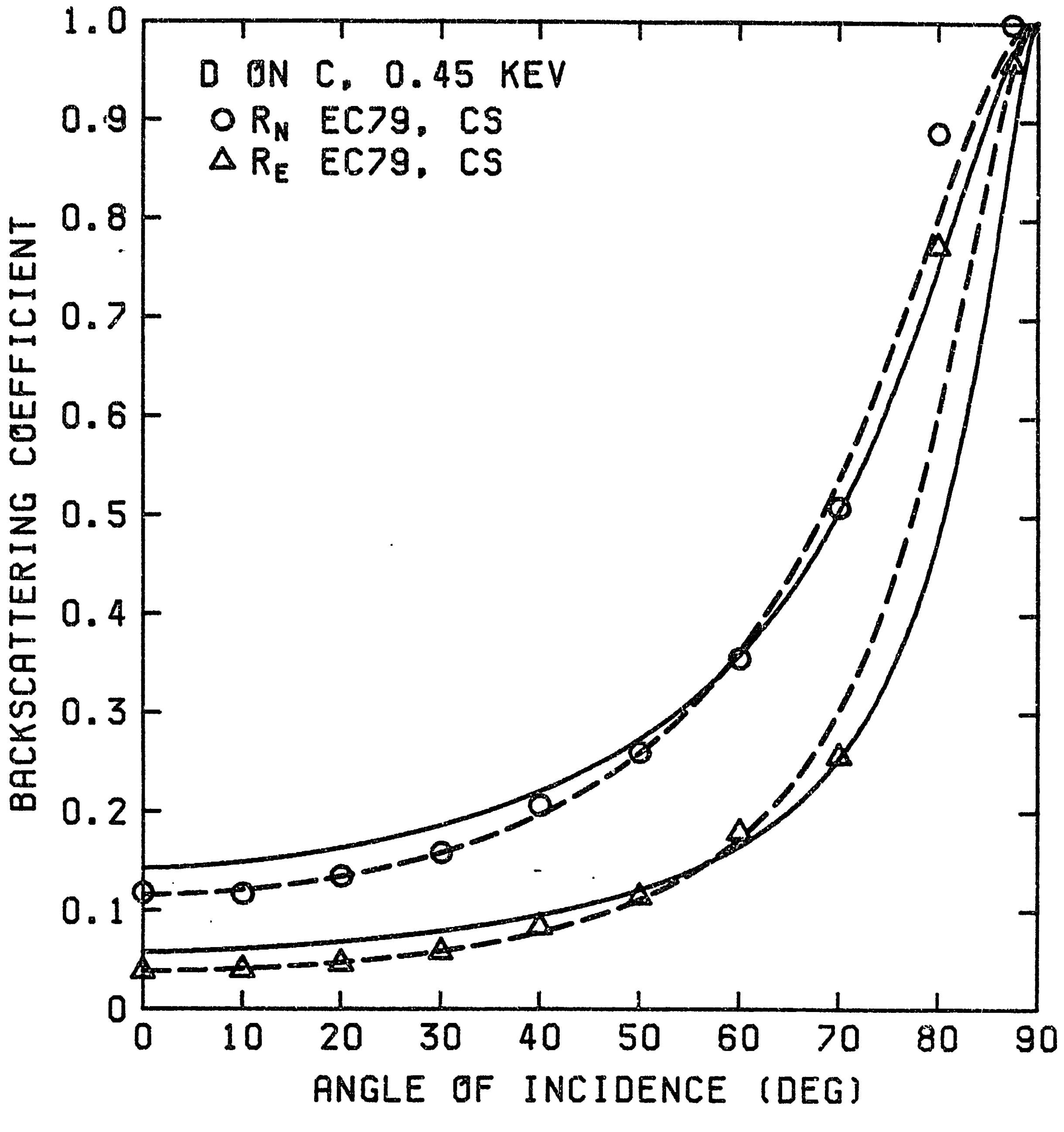
D ØN C, 0.45 KEV
○ R_N EC79, CS
△ R_E EC79, CS
BACKSCATTERING CØEFFICIENT
ANGLE ØF INCIDENCE (DEG)
0
0.1
0.2
0.3
0.4
0.5
0.6
0.7
0.8
0.9
1.0
10
20
30
40
50
60
70
80
90

FIG.22

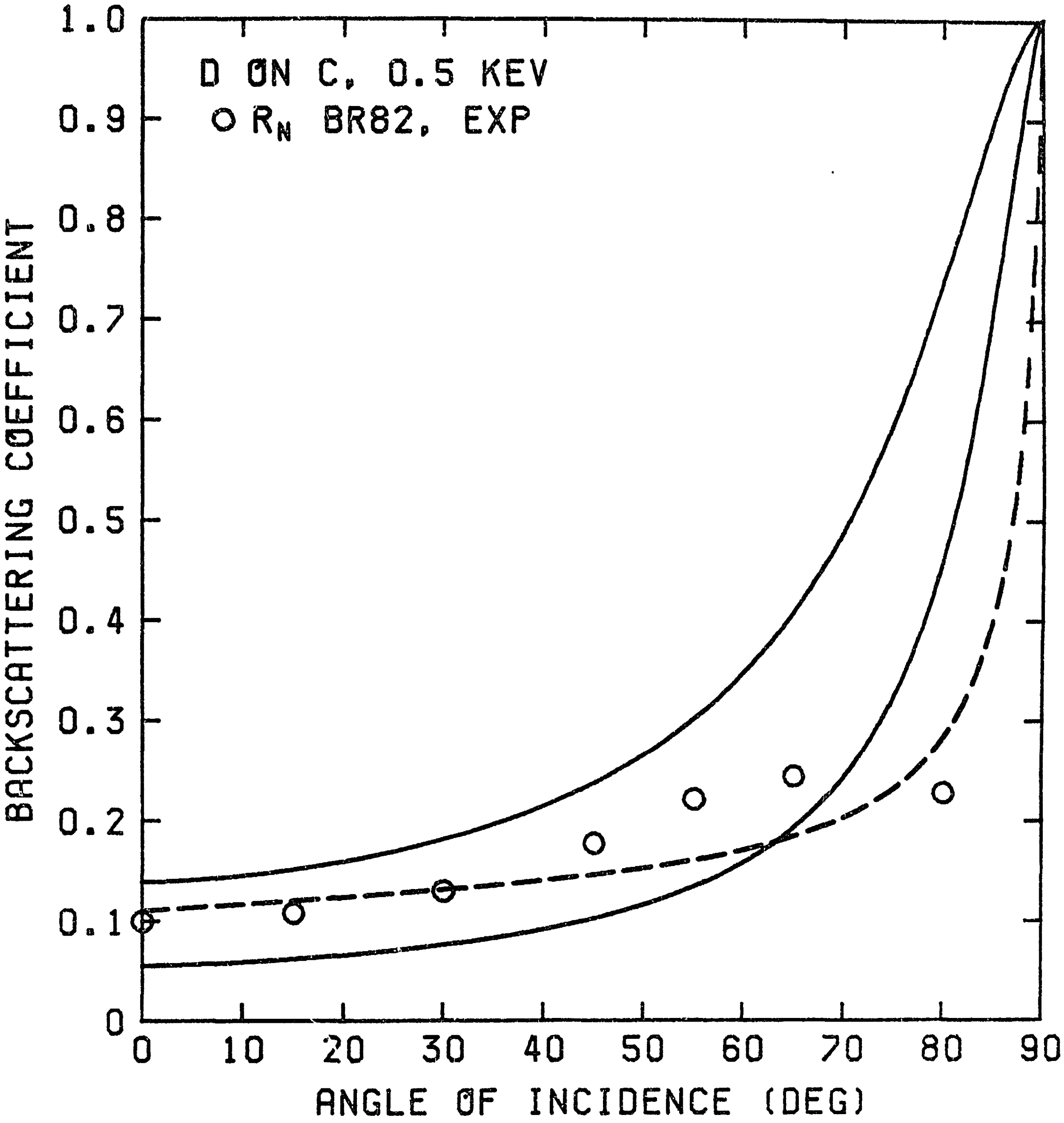
D ØN C, 0.5 KEV
O R_N BR82, EXP
BACKSCATTERING CØEFFICIENT
1.0
0.9
0.8
0.7
0.6
0.5
0.4
0.3
0.2
0.1
0
0
10
20
30
40
50
60
70
80
90
ANGLE ØF INCIDENCE (DEG)

FIG.23

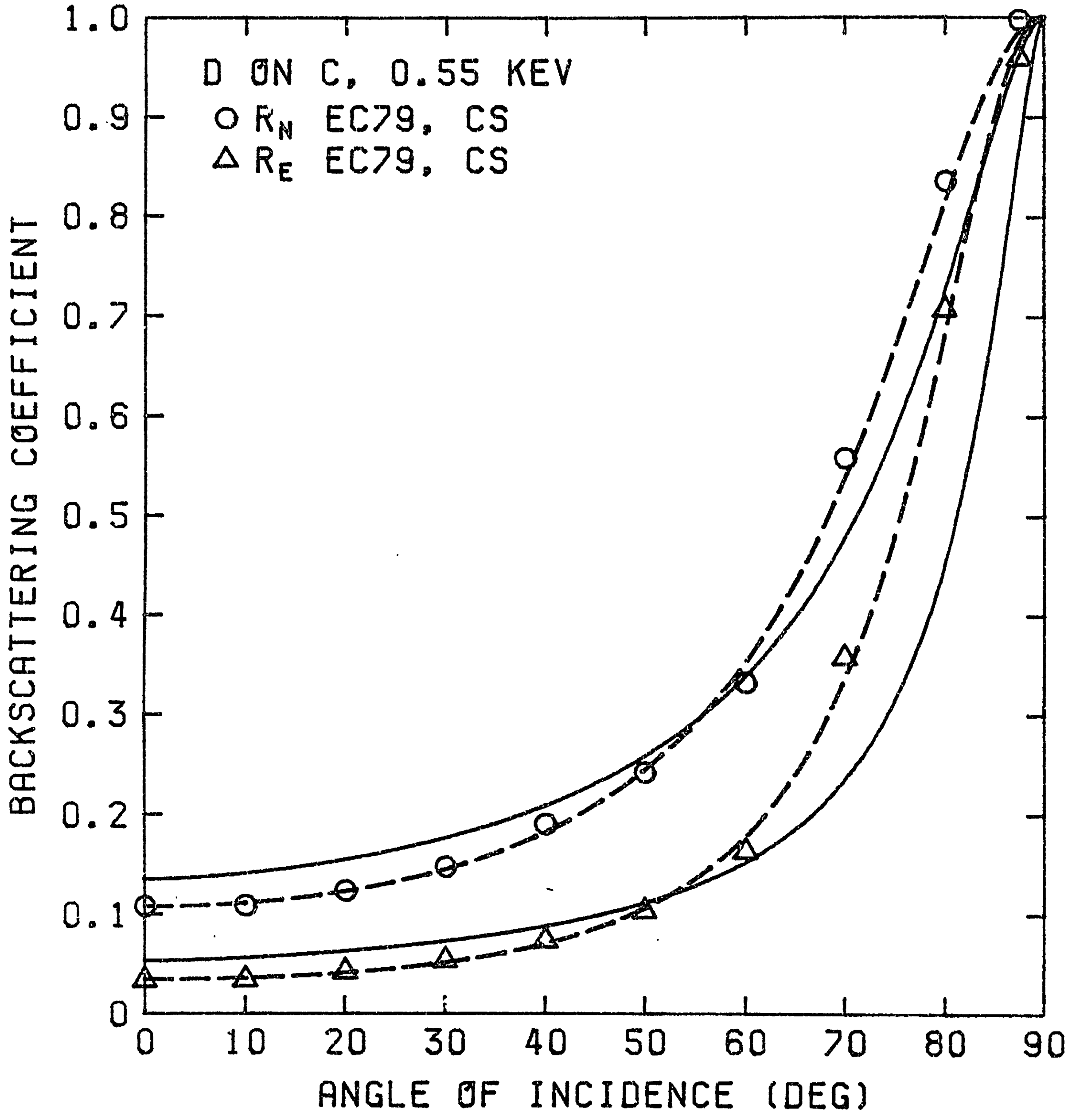
D ØN C, 0.55 KEV
O R_N EC79, CS
△ R_E EC79, CS
BACKSCATTERING CØEFFICIENT
ANGLE ØF INCIDENCE (DEG)
1.0
0.9
0.8
0.7
0.6
0.5
0.4
0.3
0.2
0.1
0
0
10
20
30
40
50
60
70
80
90

FIG.24

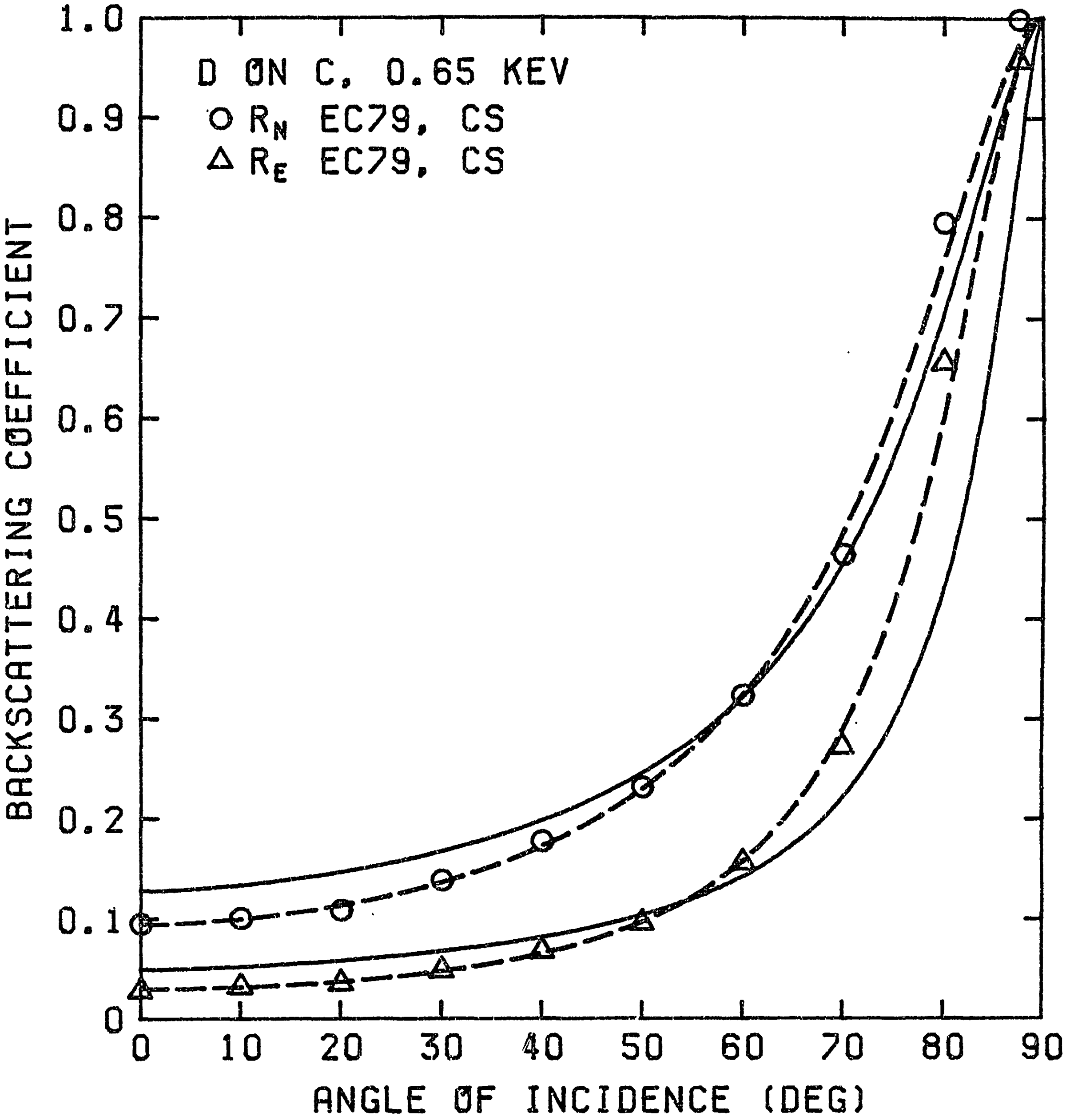
D ØN C, 0.65 KEV
○ R_N EC79, CS
△ R_E EC79, CS
BACKSCATTERING CØEFFICIENT
ANGLE ØF INCIDENCE (DEG)
1.0
0.9
0.8
0.7
0.6
0.5
0.4
0.3
0.2
0.1
0
0
10
20
30
40
50
60
70
80
90

FIG.25

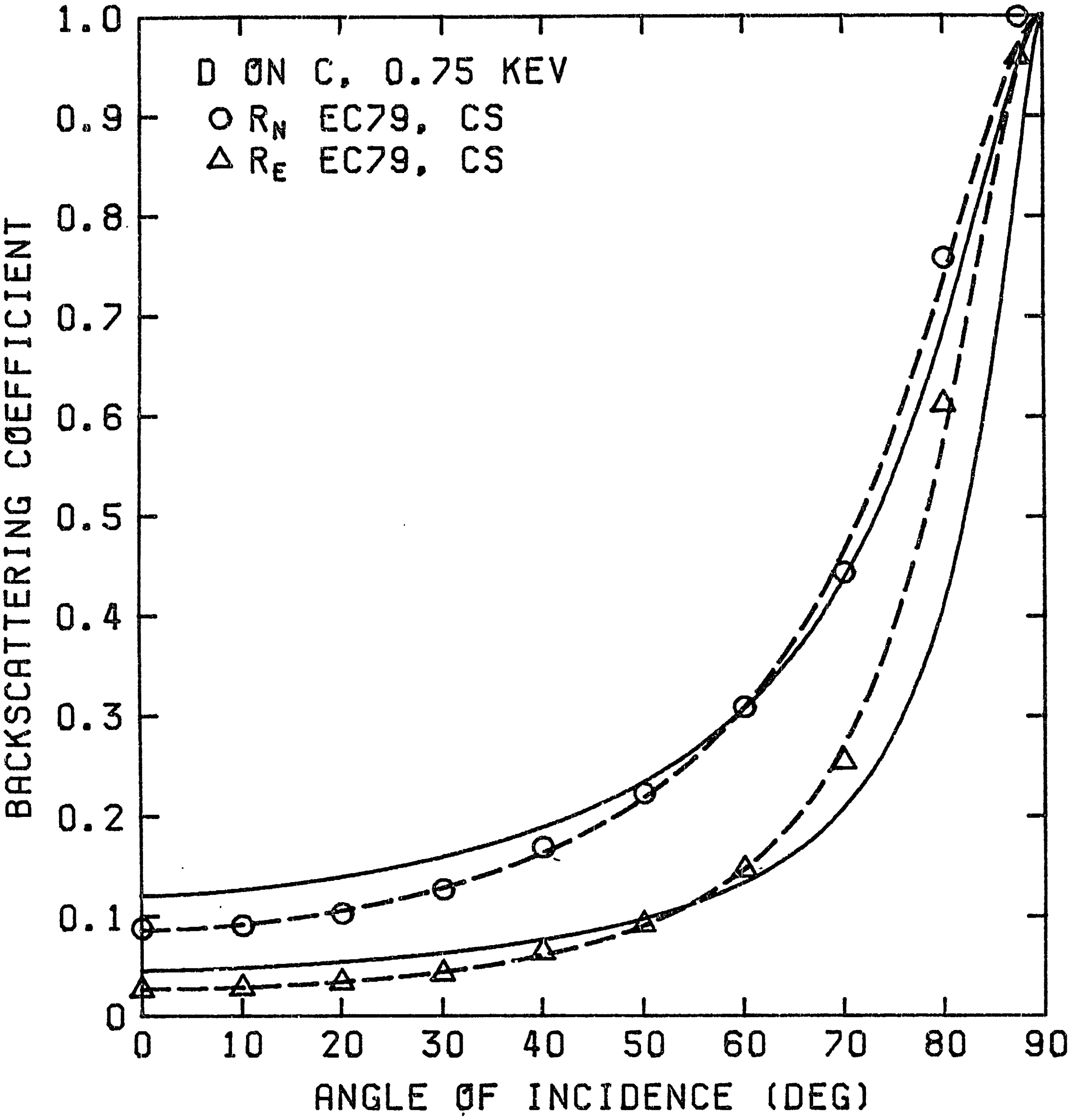

D ØN C, 0.75 KEV
○ R_N EC79, CS
△ R_E EC79, CS
BACKSCATTERING CØEFFICIENT
ANGLE ØF INCIDENCE (DEG)
1.0
0.9
0.8
0.7
0.6
0.5
0.4
0.3
0.2
0.1
0
0
10
20
30
40
50
60
70
80
90

FIG.26

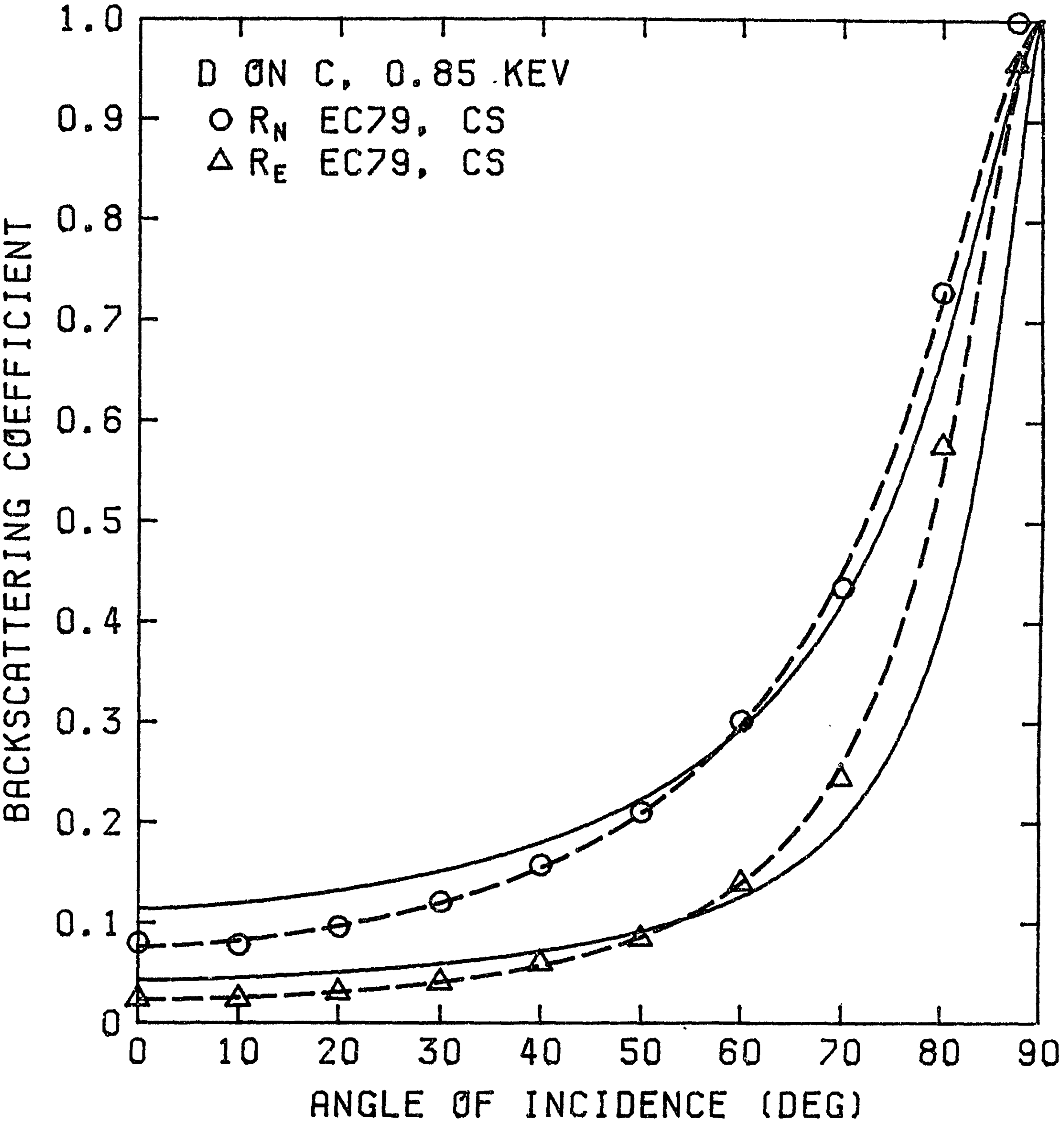
D ØN C, 0.85 KEV
○ R_N EC79, CS
△ R_E EC79, CS
BACKSCATTERING CØEFFICIENT
ANGLE ØF INCIDENCE (DEG)
1.0
0.9
0.8
0.7
0.6
0.5
0.4
0.3
0.2
0.1
0
0
10
20
30
40
50
60
70
80
90

FIG.27

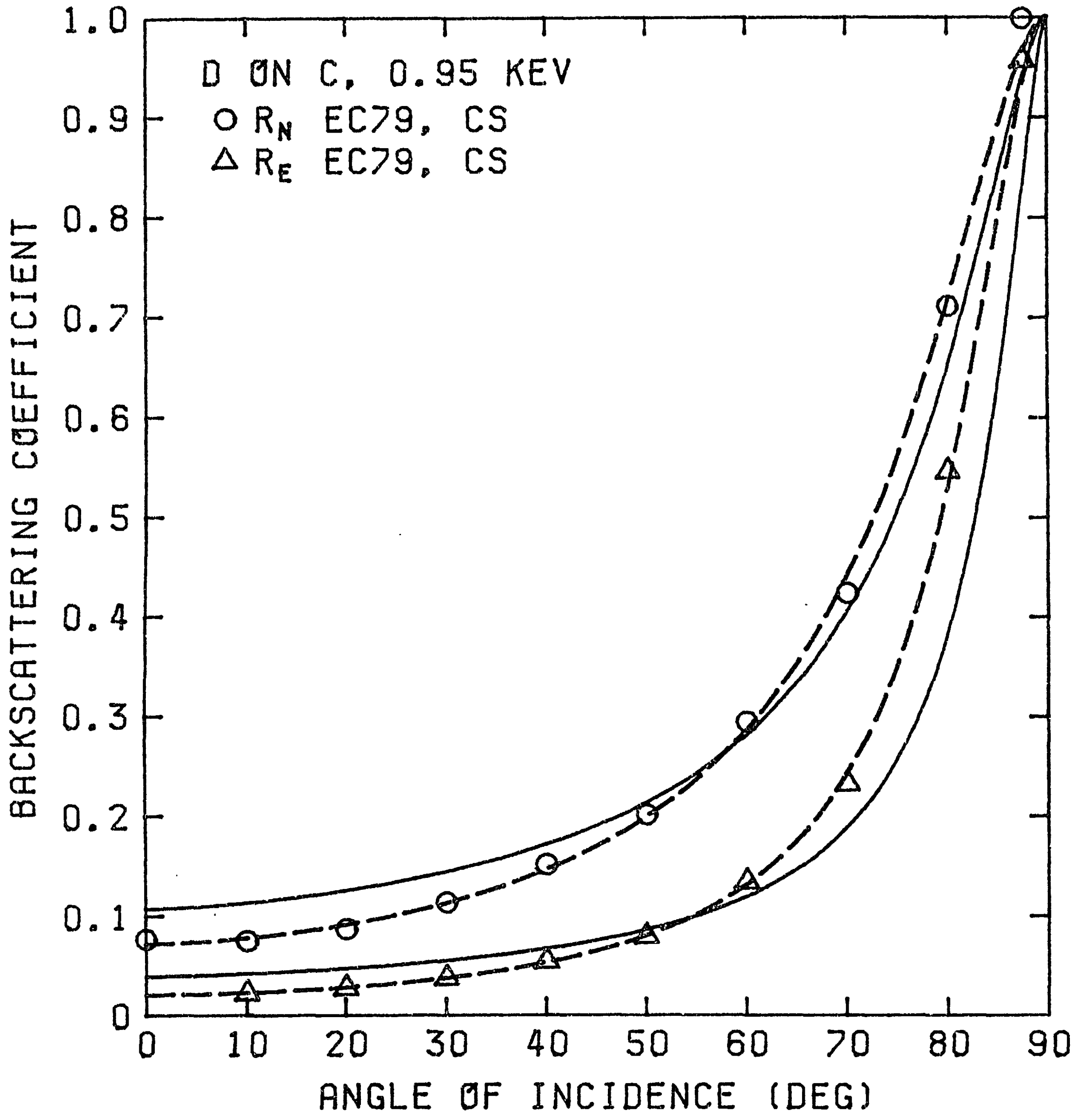

D ØN C, 0.95 KEV
○ R_N EC79, CS
△ R_E EC79, CS
BACKSCATTERING CØEFFICIENT
ANGLE ØF INCIDENCE (DEG)
1.0
0.9
0.8
0.7
0.6
0.5
0.4
0.3
0.2
0.1
0
0
10
20
30
40
50
60
70
80
90

FIG.28

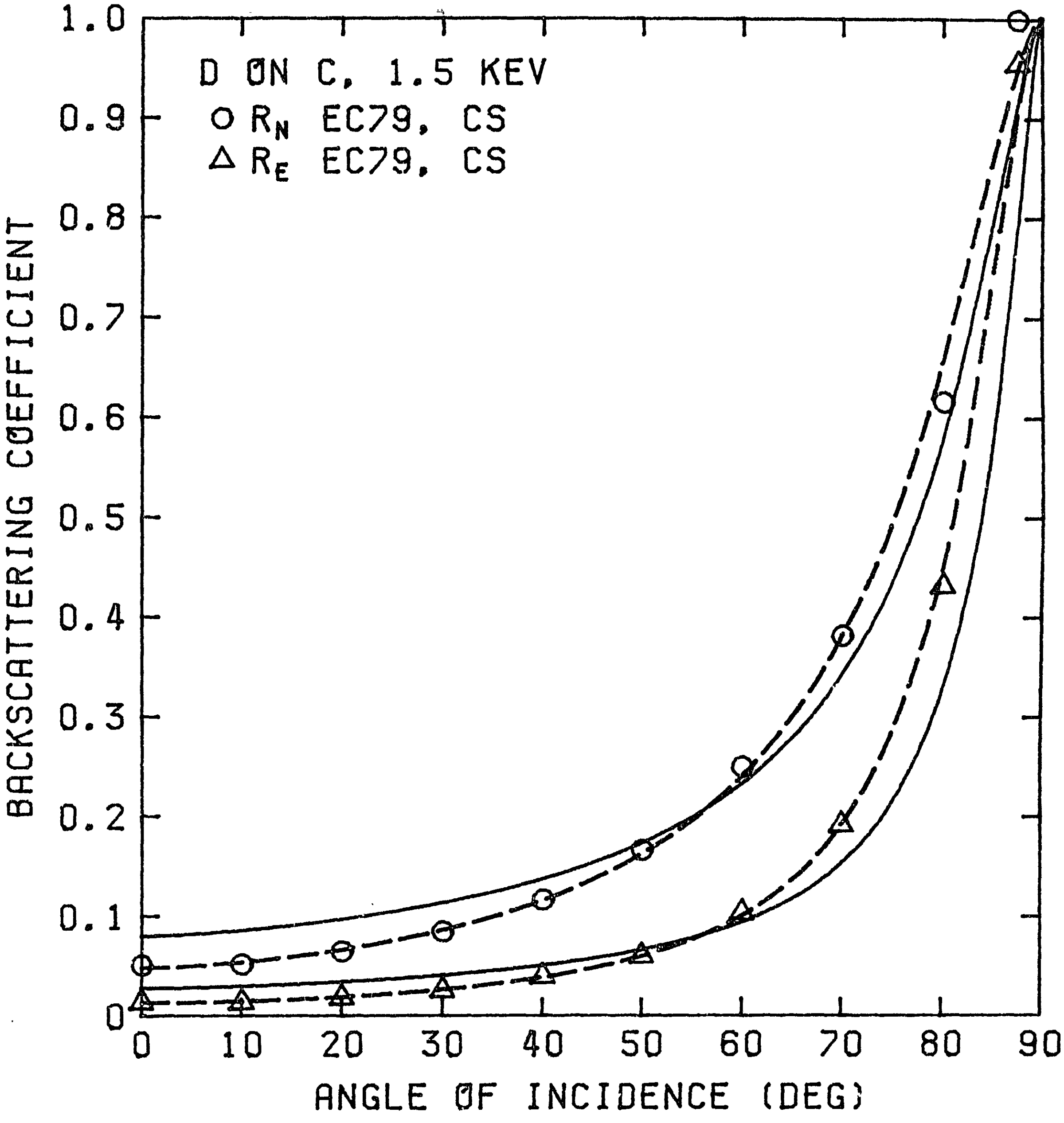
D ØN C, 1.5 KEV
○ R_N EC79, CS
△ R_E EC79, CS
BACKSCATTERING CØEFFICIENT
0
0.1
0.2
0.3
0.4
0.5
0.6
0.7
0.8
0.9
1.0
0
10
20
30
40
50
60
70
80
90
ANGLE ØF INCIDENCE (DEG)

FIG.29

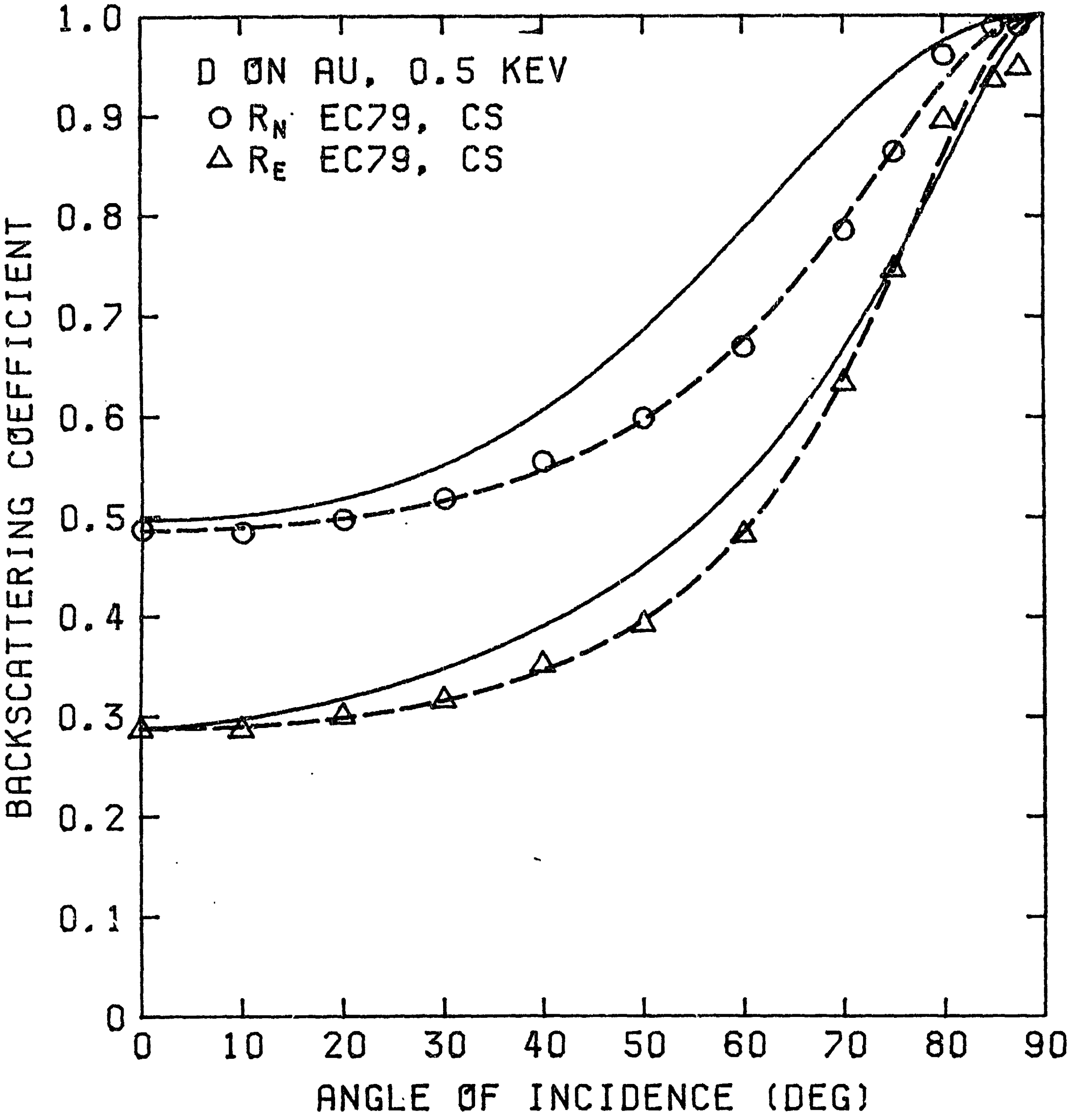
D ØN AU, 0.5 KEV
○ R_N EC79, CS
△ R_E EC79, CS
BACKSCATTERING CØEFFICIENT
ANGLE ØF INCIDENCE (DEG)
1.0
0.9
0.8
0.7
0.6
0.5
0.4
0.3
0.2
0.1
0
0
10
20
30
40
50
60
70
80
90

FIG.30

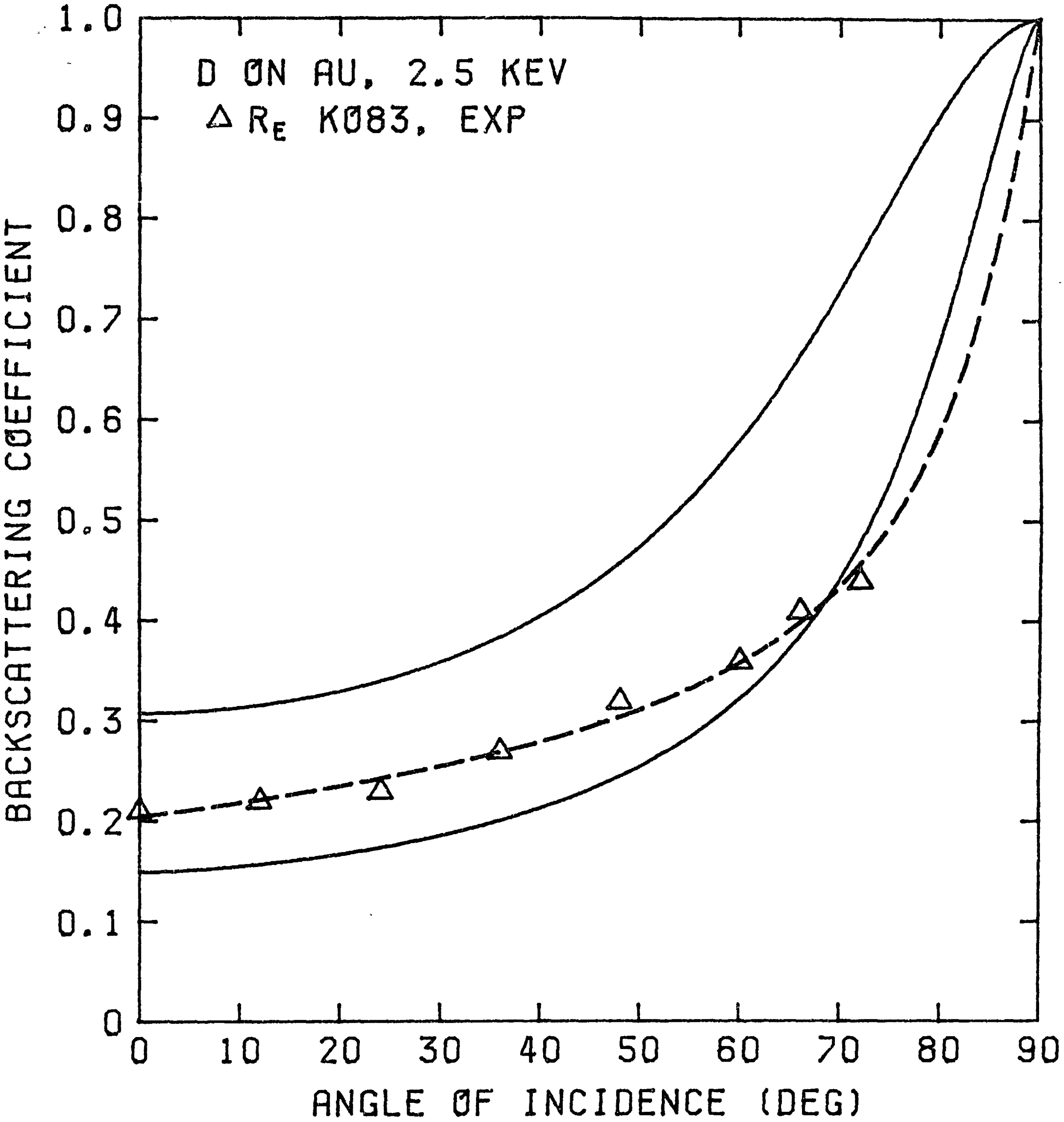
D ØN AU, 2.5 KEV
△ R_E KØ83, EXP
BACKSCATTERING CØEFFICIENT
ANGLE ØF INCIDENCE (DEG)
1.0
0.9
0.8
0.7
0.6
0.5
0.4
0.3
0.2
0.1
0
0
10
20
30
40
50
60
70
80
90

FIG.31

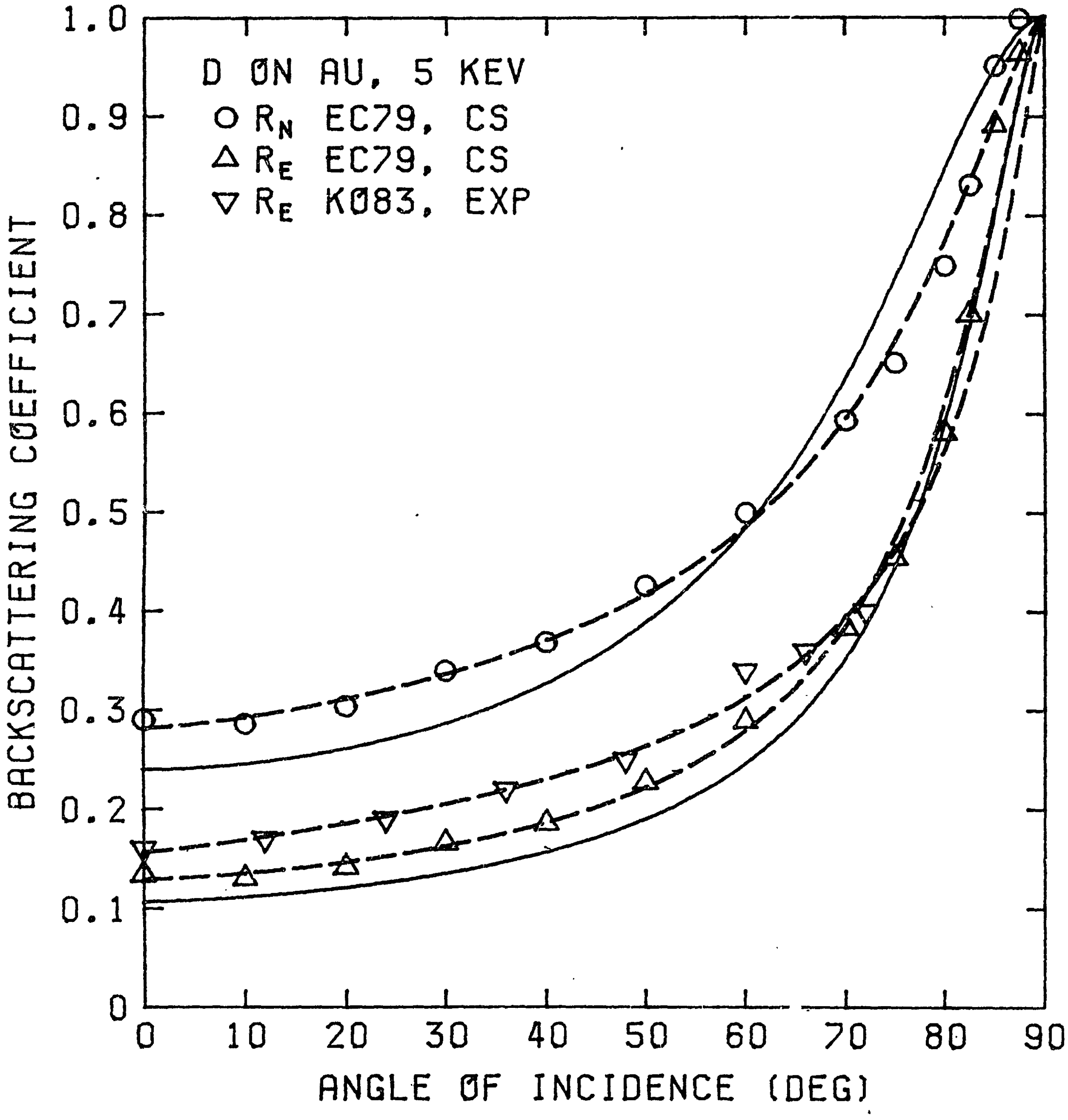
D ØN AU, 5 KEV
○ R_N EC79, CS
△ R_E EC79, CS
▽ R_E KØ83, EXP
BACKSCATTERING CØEFFICIENT
ANGLE ØF INCIDENCE (DEG)
1.0
0.9
0.8
0.7
0.6
0.5
0.4
0.3
0.2
0.1
0
0
10
20
30
40
50
60
70
80
90

FIG.32

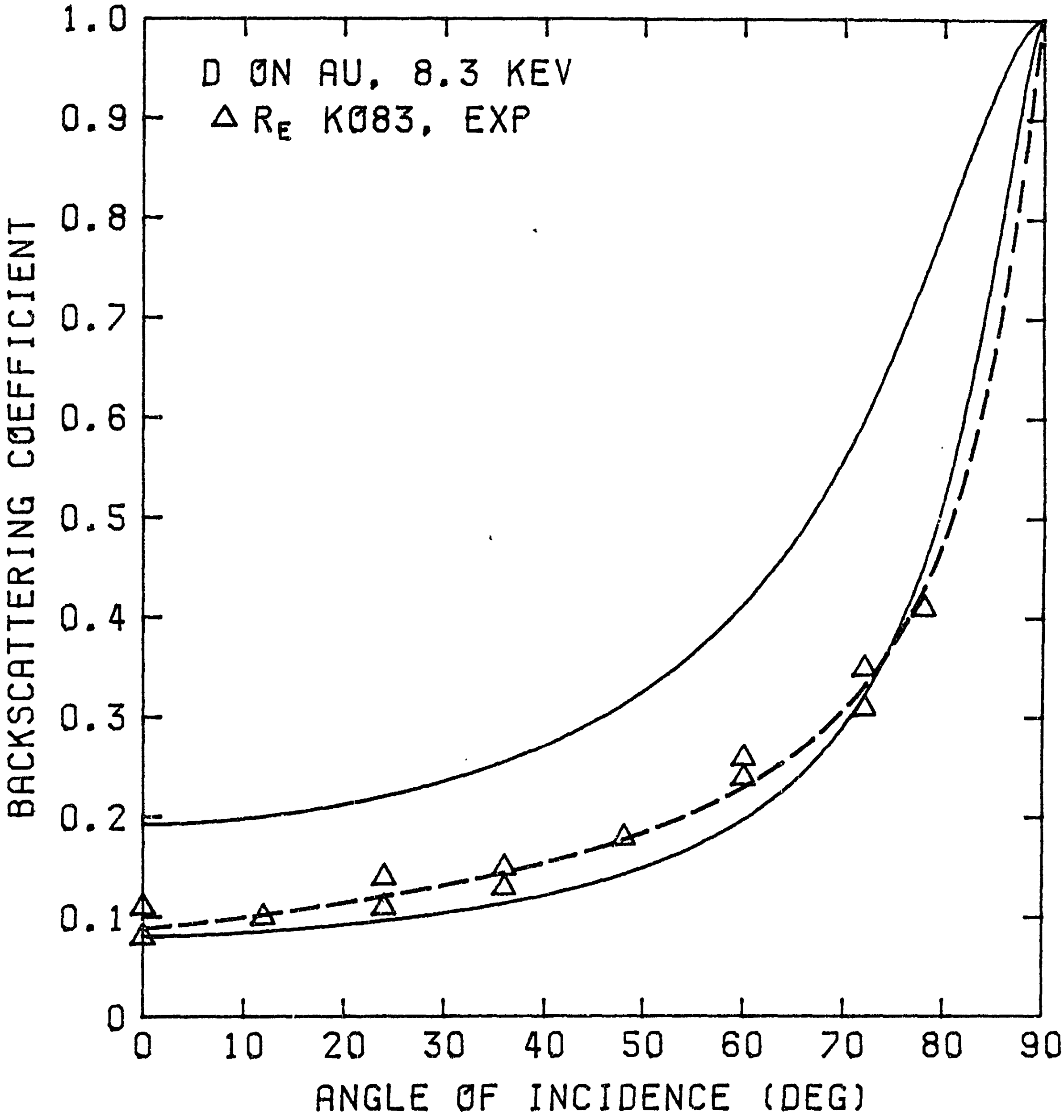
D ØN AU, 8.3 KEV
△ R_E KØ83, EXP
BACKSCATTERING CØEFFICIENT
ANGLE ØF INCIDENCE (DEG)
1.0
0.9
0.8
0.7
0.6
0.5
0.4
0.3
0.2
0.1
0
10
20
30
40
50
60
70
80
90

FIG.33

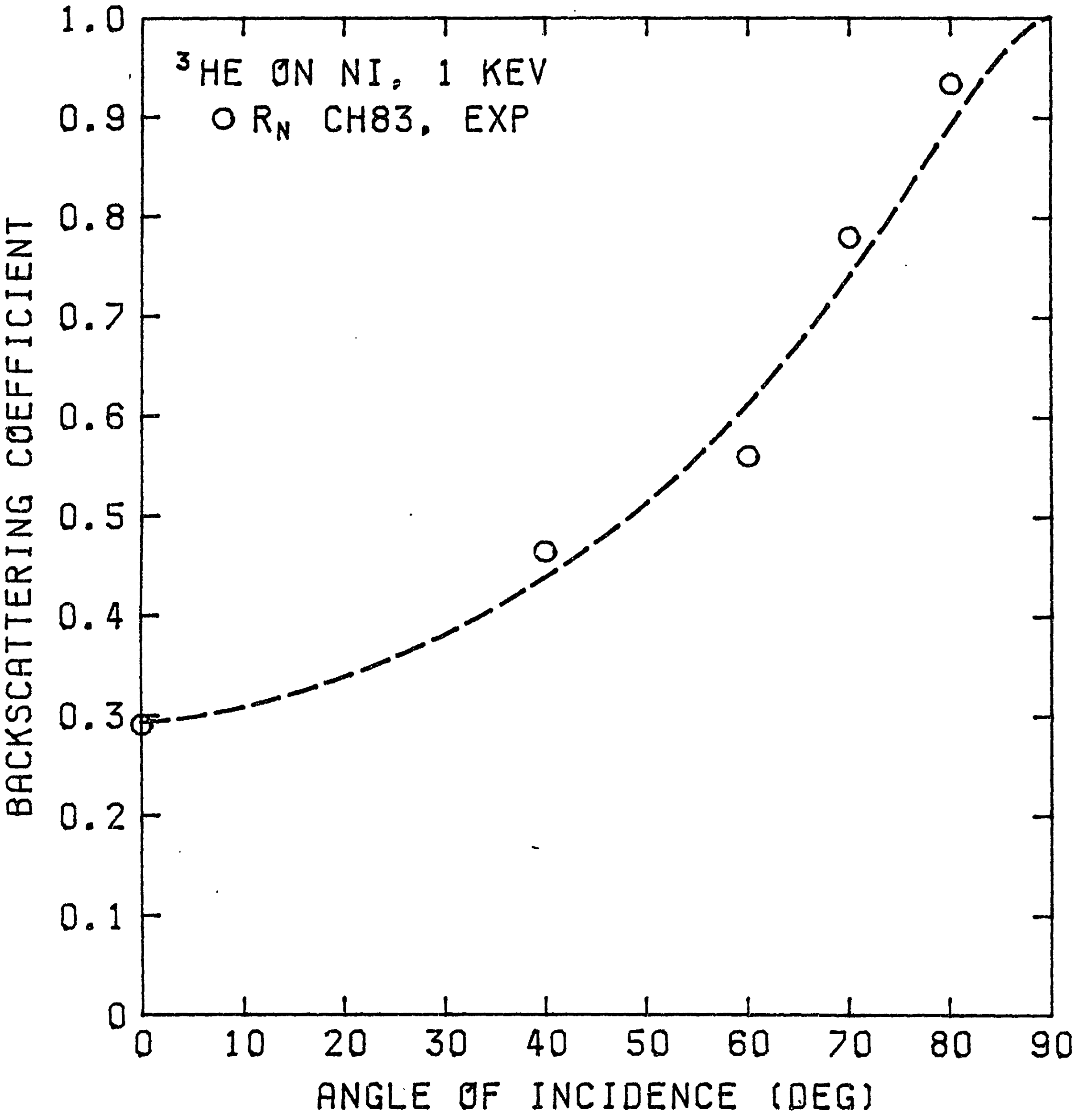

³HE ØN NI, 1 KEV
○ R_N CH83, EXP
BACKSCATTERING CØEFFICIENT
ANGLE ØF INCIDENCE (DEG)
1.0
0.9
0.8
0.7
0.6
0.5
0.4
0.3
0.2
0.1
0
0
10
20
30
40
50
60
70
80
90

FIG.34

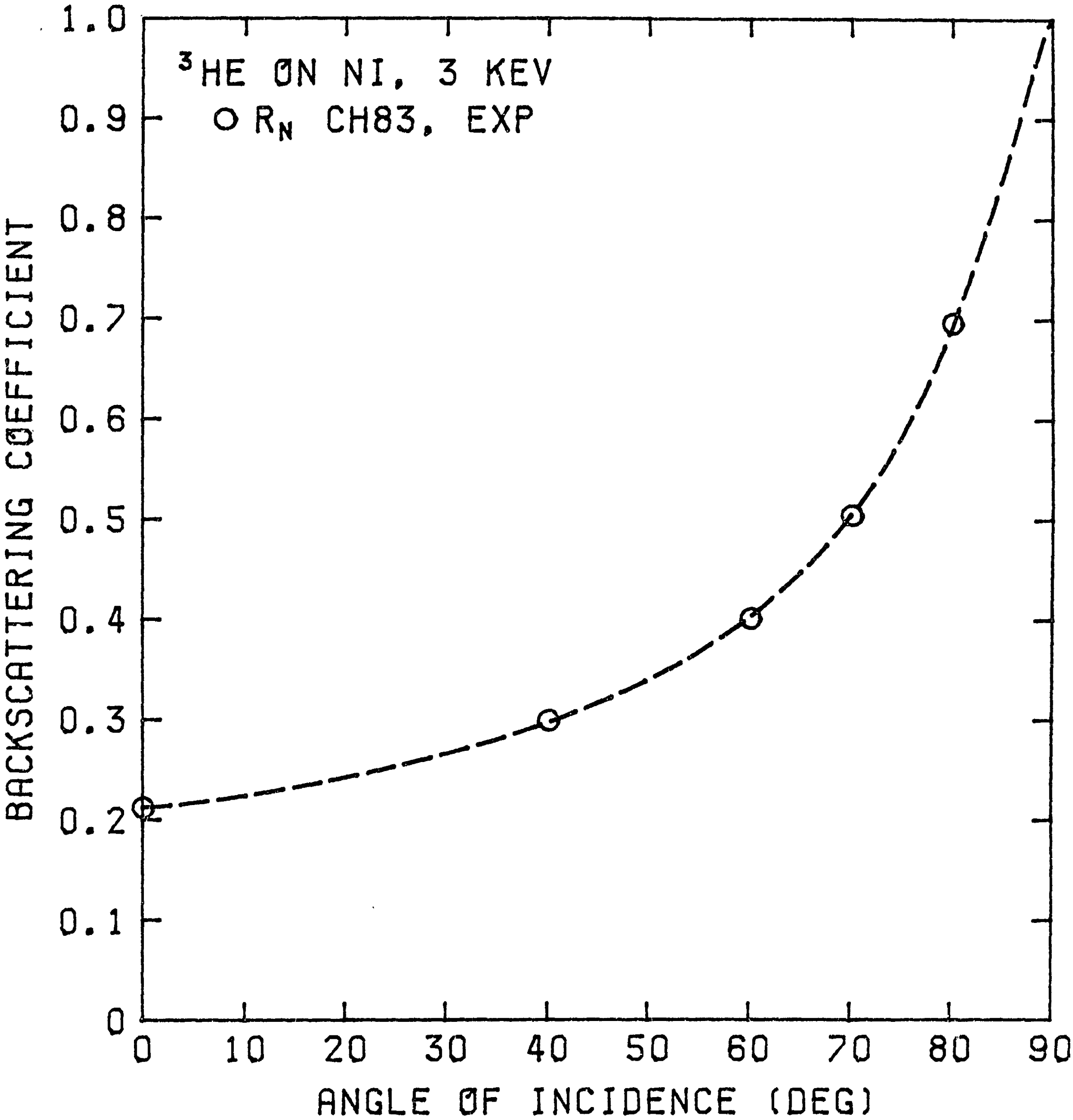

³HE ØN NI, 3 KEV
O R_N CH83, EXP
BACKSCATTERING CØEFFICIENT
ANGLE ØF INCIDENCE (DEG)
0
0.1
0.2
0.3
0.4
0.5
0.6
0.7
0.8
0.9
1.0
0
10
20
30
40
50
60
70
80
90

FIG.35

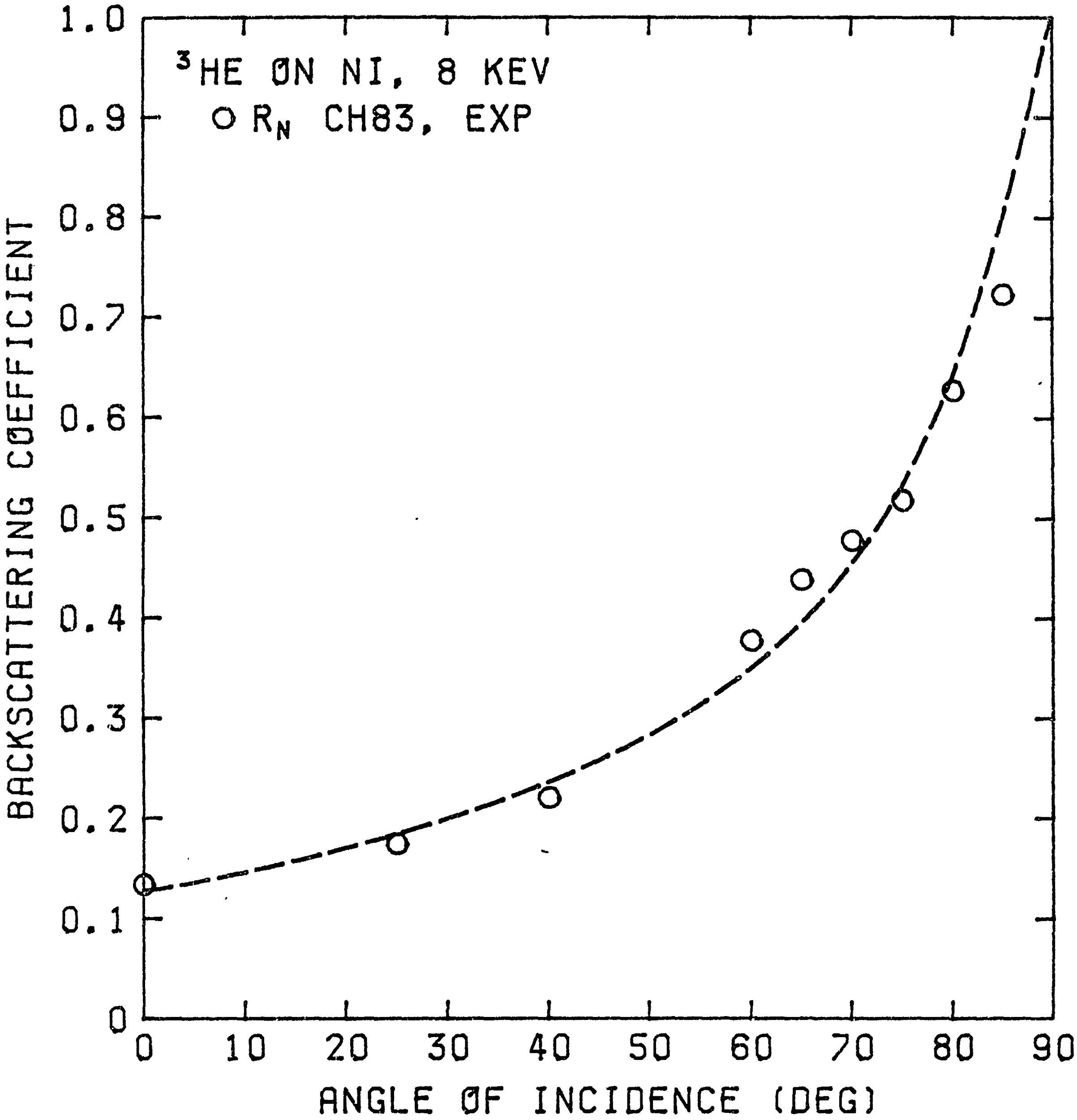

³HE ØN NI, 8 KEV
○ R_N CH83, EXP
BACKSCATTERING CØEFFICIENT
ANGLE ØF INCIDENCE (DEG)
1.0
0.9
0.8
0.7
0.6
0.5
0.4
0.3
0.2
0.1
0
0
10
20
30
40
50
60
70
80
90

FIG.36

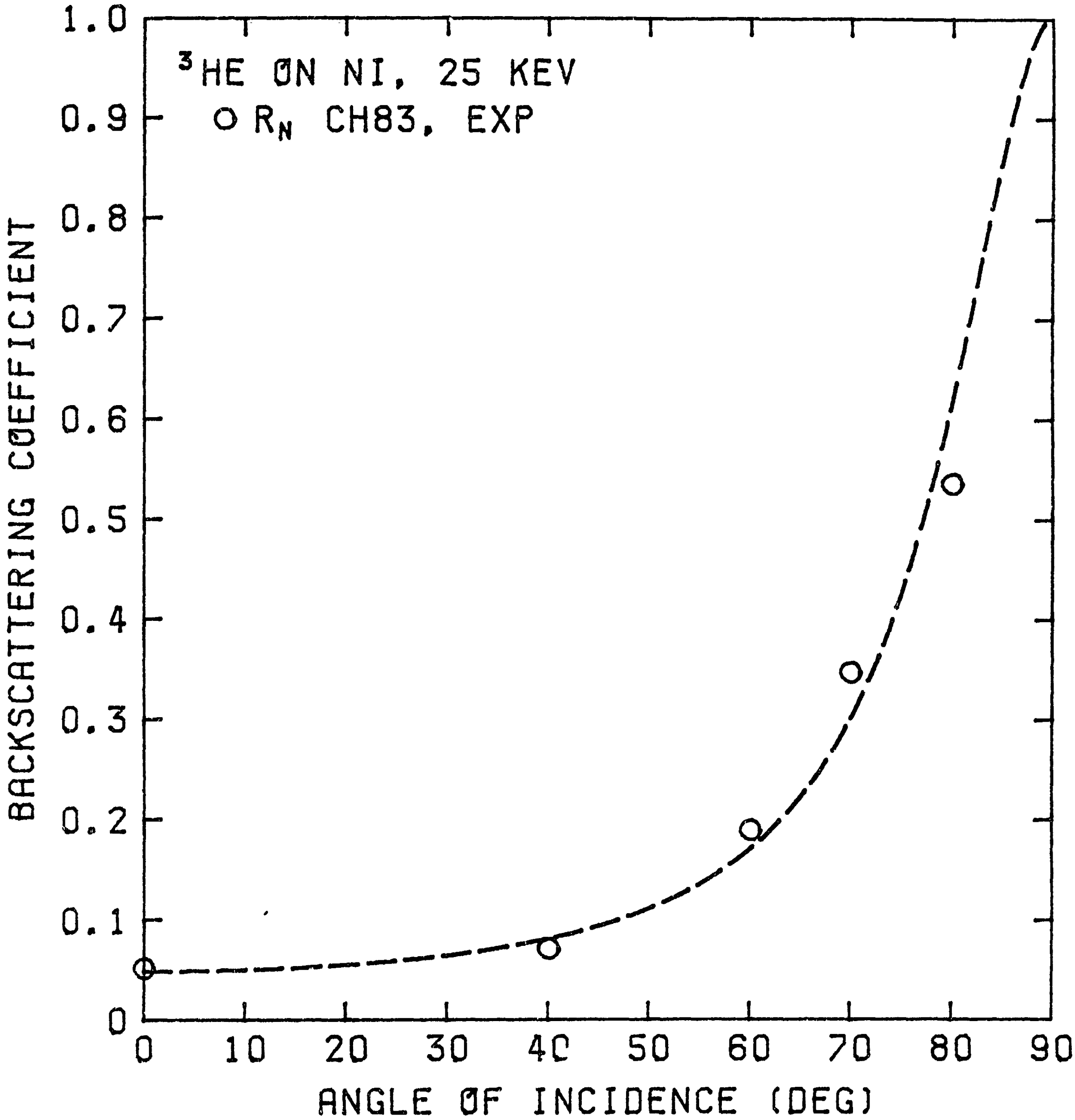

^{3}HE ØN NI, 25 KEV
○ R_N CH83, EXP
BACKSCATTERING CØEFFICIENT
ANGLE ØF INCIDENCE (DEG)
1.0
0.9
0.8
0.7
0.6
0.5
0.4
0.3
0.2
0.1
0
0
10
20
30
40
50
60
70
80
90

FIG.37

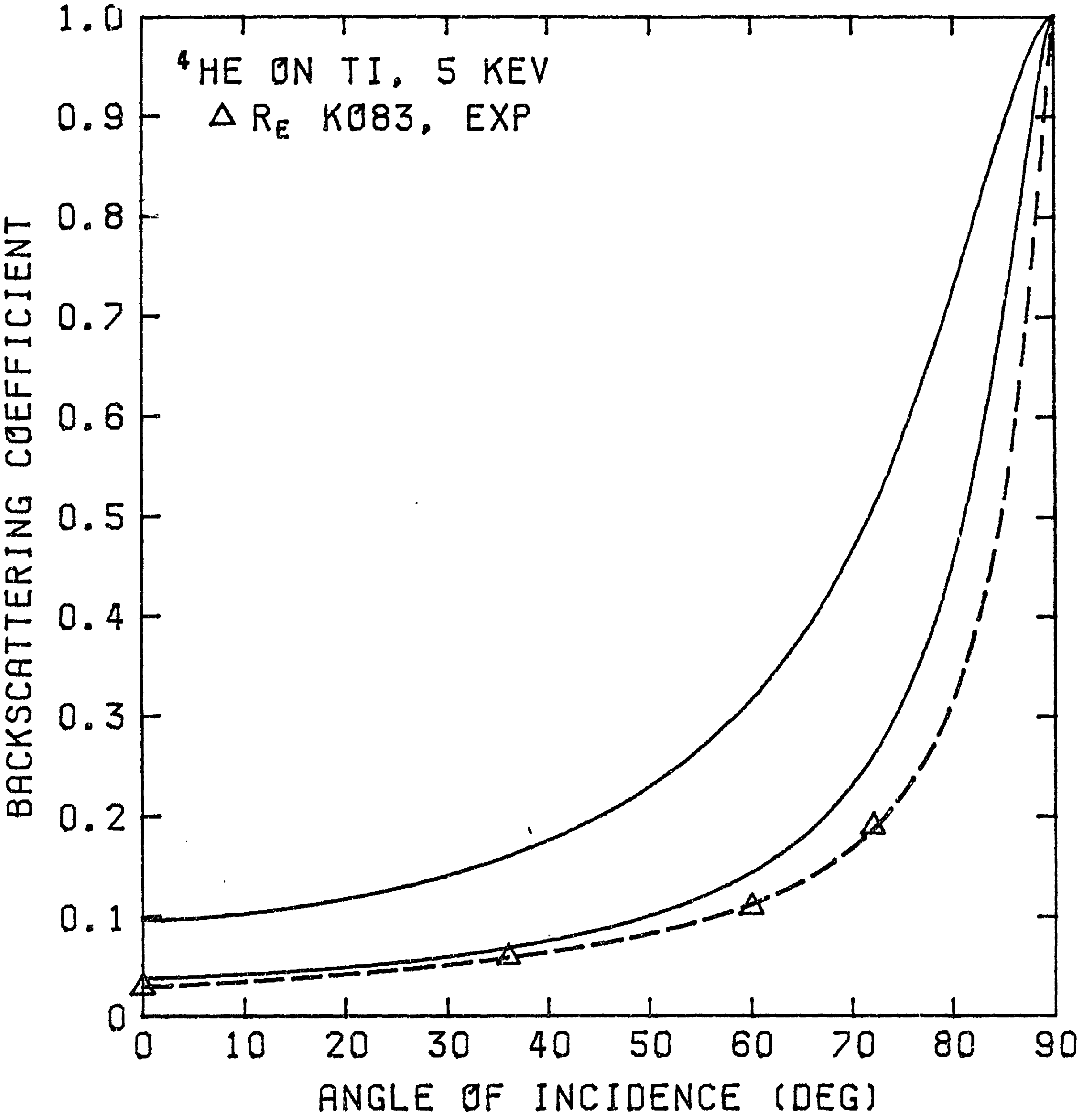

⁴HE ØN TI, 5 KEV
△ R_E KØ83, EXP
BACKSCATTERING CØEFFICIENT
ANGLE ØF INCIDENCE (DEG)
1.0
0.9
0.8
0.7
0.6
0.5
0.4
0.3
0.2
0.1
0
0
10
20
30
40
50
60
70
80
90

FIG.38

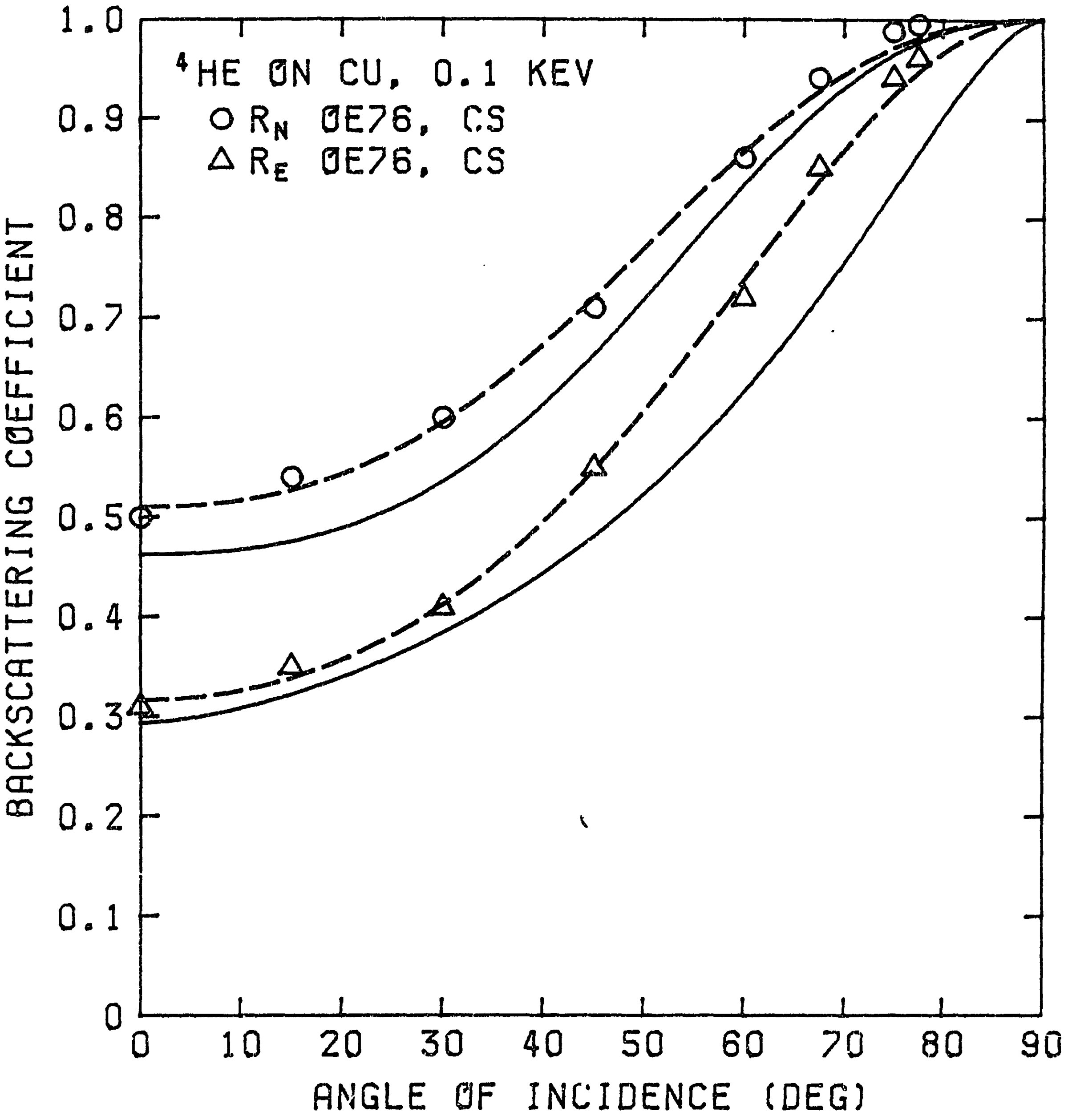

⁴HE ØN CU, 0.1 KEV
○ R_N ØE76, CS
△ R_E ØE76, CS
BACKSCATTERING CØEFFICIENT
ANGLE ØF INCIDENCE (DEG)
1.0
0.9
0.8
0.7
0.6
0.5
0.4
0.3
0.2
0.1
0
0
10
20
30
40
50
60
70
80
90

FIG.39

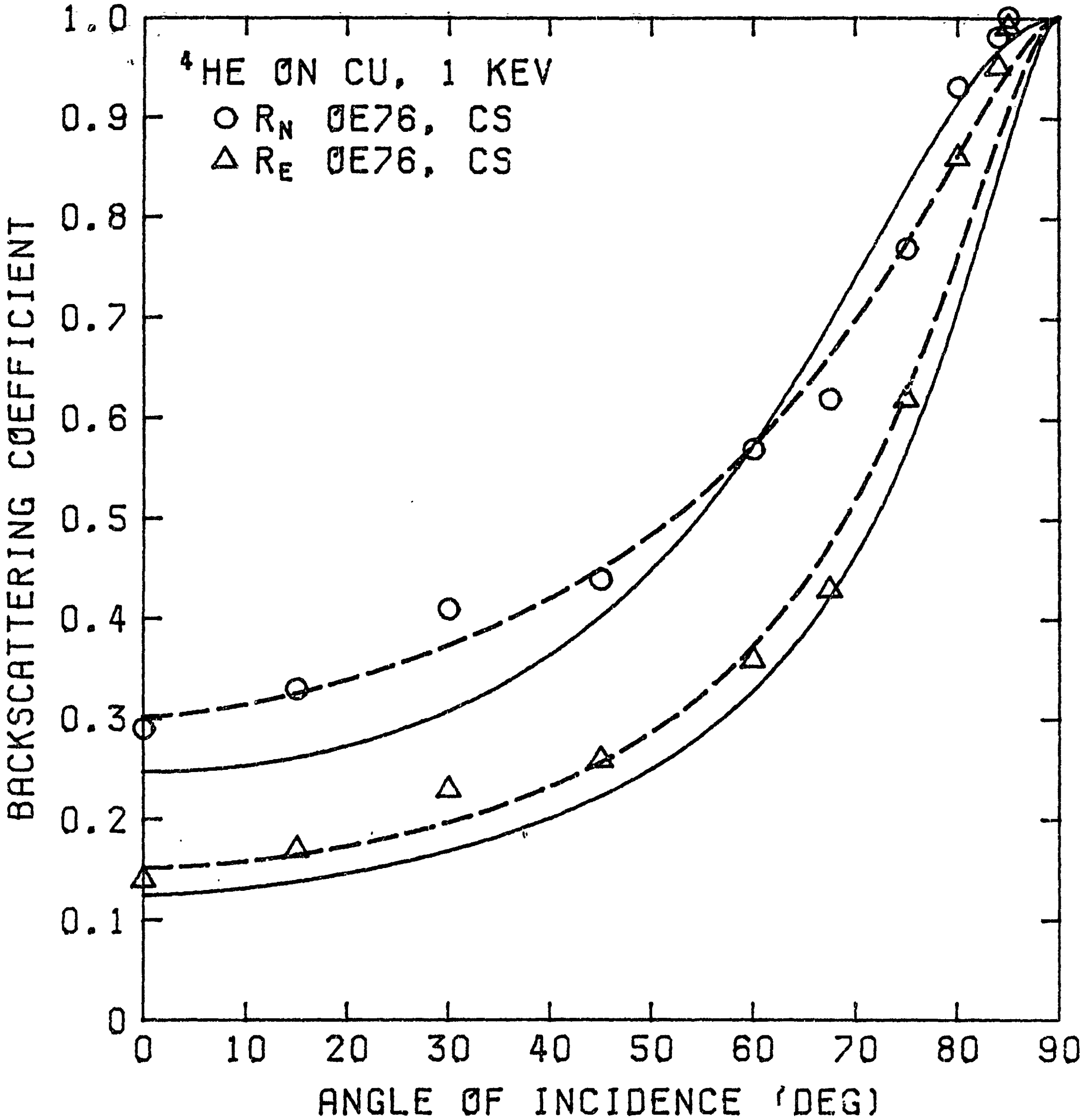
4HE ØN CU, 1 KEV
RN ØE76, CS
RE ØE76, CS
BACKSCATTERING CØEFFICIENT
ANGLE ØF INCIDENCE (DEG)
1.0
0.9
0.8
0.7
0.6
0.5
0.4
0.3
0.2
0.1
0
0
10
20
30
40
50
60
70
80
90

FIG.40

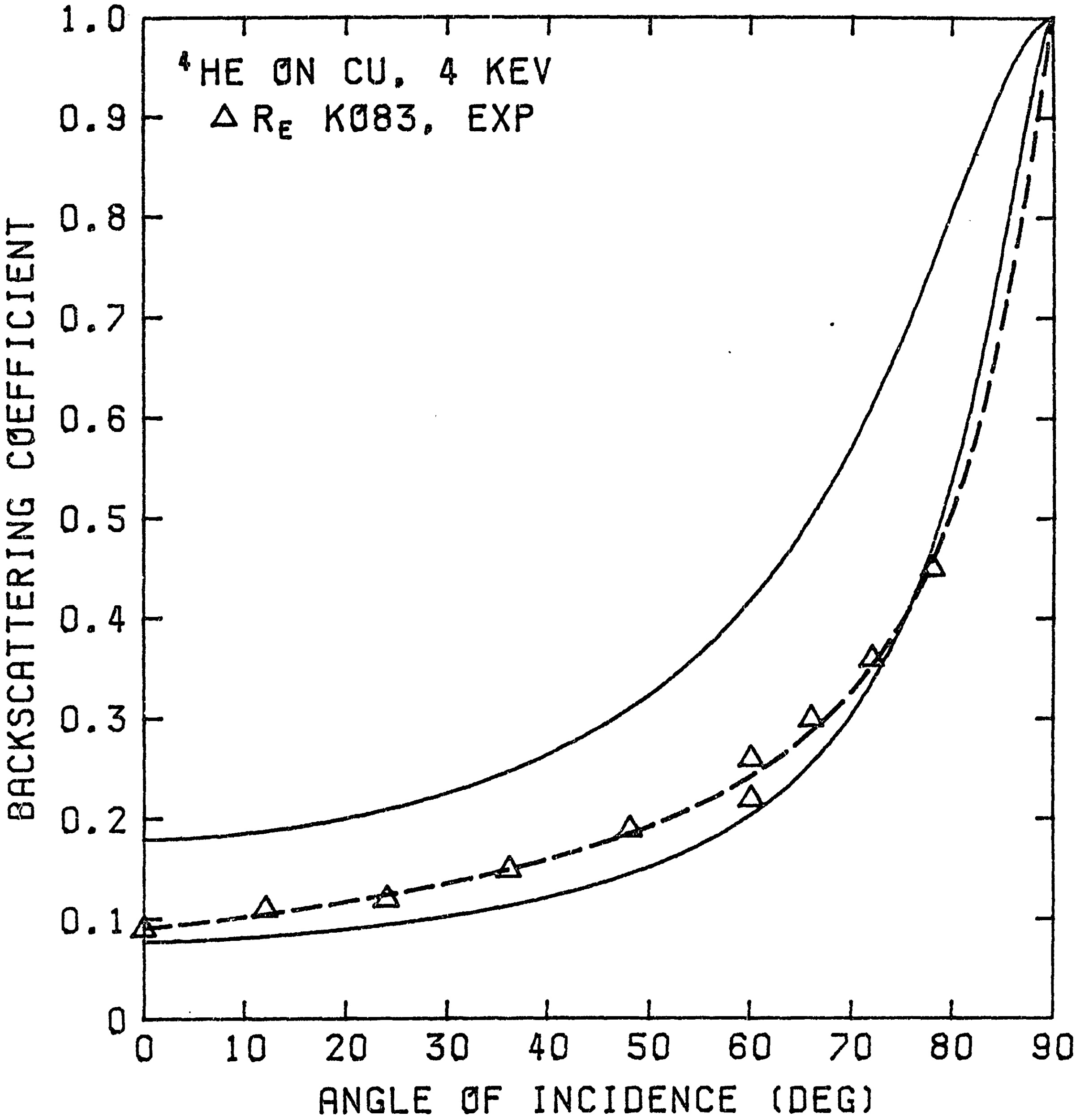

1.0
0.9
0.8
0.7
0.6
0.5
0.4
0.3
0.2
0.1
0
BACKSCATTERING CØEFFICIENT
⁴HE ØN CU, 4 KEV
△ R_E KØ83, EXP
0
10
20
30
40
50
60
70
80
90
ANGLE ØF INCIDENCE (DEG)

FIG. 41

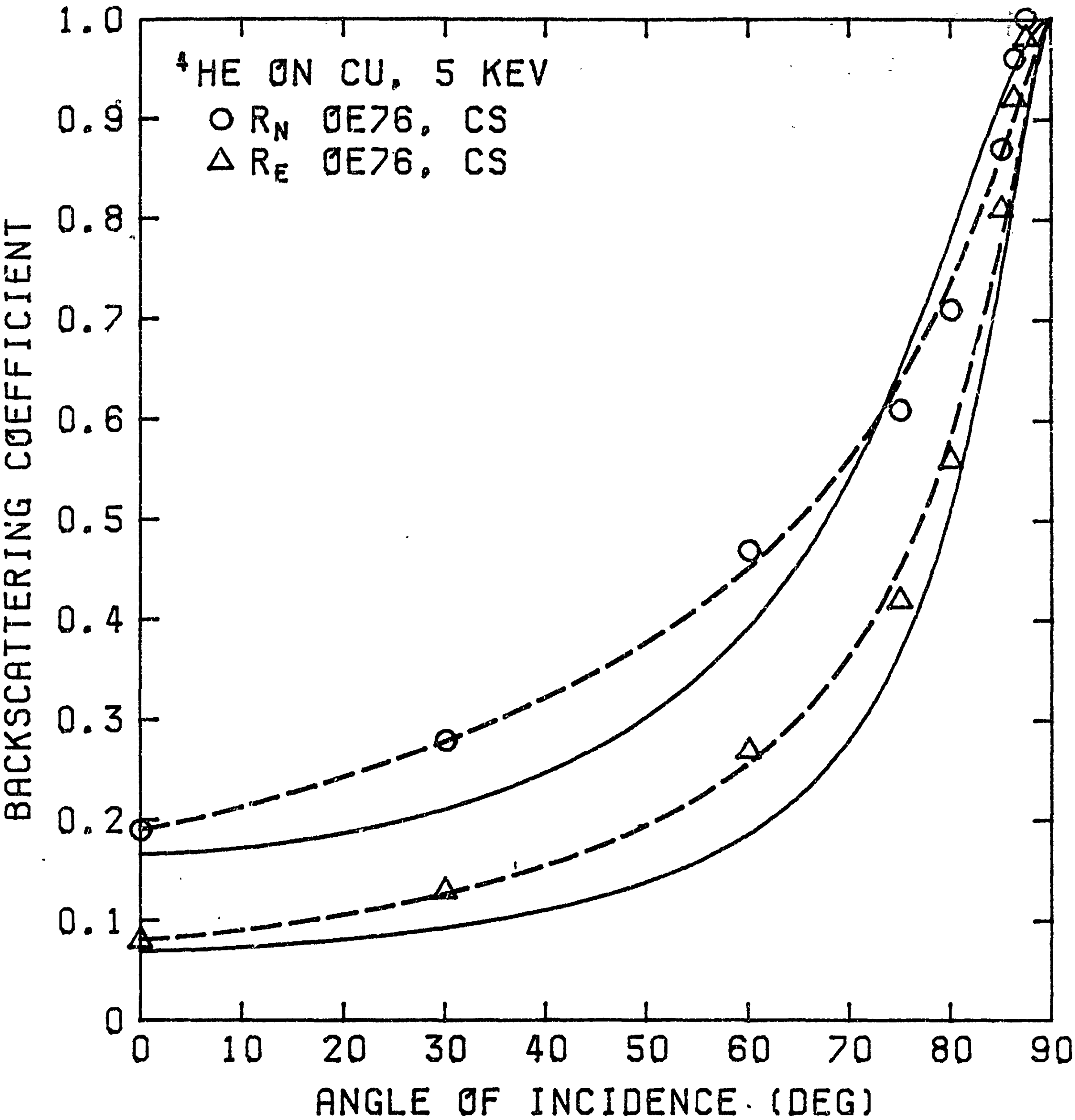

⁴HE ØN CU, 5 KEV
○ R_N ØE76, CS
△ R_E ØE76, CS
BACKSCATTERING CØEFFICIENT
ANGLE ØF INCIDENCE (DEG)
1.0
0.9
0.8
0.7
0.6
0.5
0.4
0.3
0.2
0.1
0
0
10
20
30
40
50
60
70
80
90

FIG.42

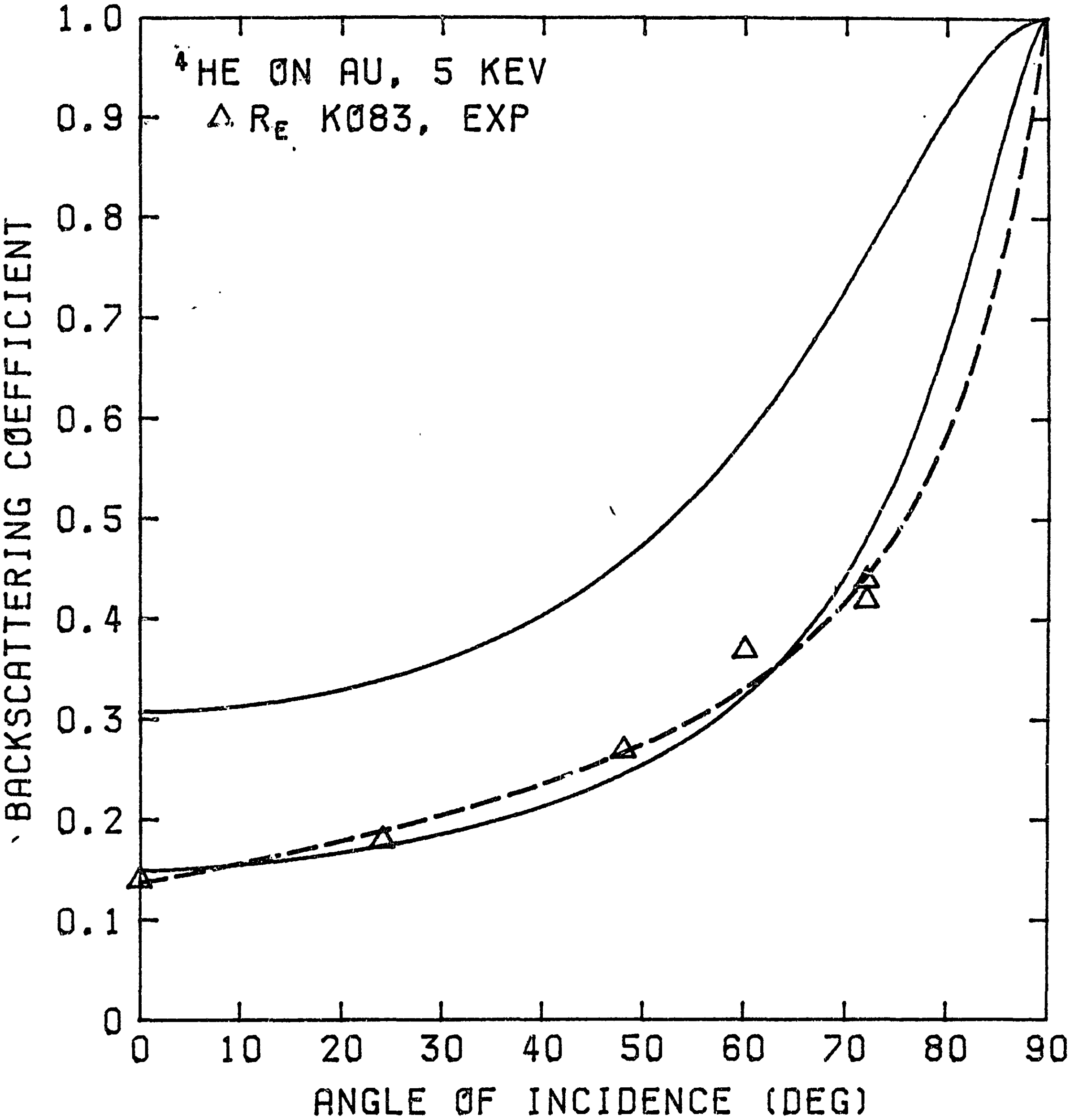
4HE ØN AU, 5 KEV
△ R_E KØ83, EXP
BACKSCATTERING CØEFFICIENT
0
0.1
0.2
0.3
0.4
0.5
0.6
0.7
0.8
0.9
1.0
0
10
20
30
40
50
60
70
80
90
ANGLE ØF INCIDENCE (DEG)

FIG. 43

SOURCES OF DATA

AK78 A. F. Akkerman: Phys. Status Solidi a 48 (1978) K47.

BR82 M. Braun and E. W. Thomas: J. Appl. Phys. 53 (1982) 6446.

CH83 C. K. Chen, W. Eckstein and B. M. U. Scherzer: Appl. Phys. A 31 (1983) 37.

EC79 W. Eckstein and H. Verbeek: Data on Light Ion Reflection, Max-Planck Inst. Plasma Phys. Rep. IPP 9/32 (1979).

KO83 N. N. Koborov, V. A. Kurnaev, V. G. Telkovsky and G. I. Zhabrev: Radiat. Eff. 69 (1983) 135.

OE76 O. S. Oen and M. T. Robinson: Nucl. Instrum. & Methods 132 (1976) 647.

RO74 J. E. Robinson: Radiat. Eff. 23 (1974) 29.

SO76 H. Sørensen: Appl. Phys. Lett. 29 (1976) 148.

LIST OF IPPJ-AM REPORTS

IPPJ-AM-1*	"Cross Sections for Charge Transfer of Hydrogen Beams in Gases and Vapors in the Energy Range 10 eV–10 keV" H. Tawara (1977) [Published in Atomic Data and Nuclear Data Tables 22, 491 (1978)]
IPPJ-AM-2*	"Ionization and Excitation of Ions by Electron Impact –Review of Empirical Formulae–" T. Kato (1977)
IPPJ-AM-3	"Grotrian Diagrams of Highly Ionized Iron FeVIII-FeXXVI" K. Mori, M. Otsuka and T. Kato (1977) [Published in Atomic Data and Nuclear Data Tables 23, 196 (1979)]
IPPJ-AM-4	"Atomic Processes in Hot Plasmas and X-Ray Emission" T. Kato (1978)
IPPJ-AM-5*	"Charge Transfer between a Proton and a Heavy Metal Atom" S.Hiraide, Y. Kigoshi and M. Matsuzawa (1978)
IPPJ-AM-6*	"Free-Free Transition in a Plasma –Review of Cross Sections and Spectra–" T. Kato and H. Narumi (1978)
IPPJ-AM-7*	"Bibliography on Electron Collisions with Atomic Positive Ions: 1940 Through 1977" K. Takayanagi and T. Iwai (1978)
IPPJ-AM-8	"Semi-Empirical Cross Sections and Rate Coefficients for Excitation and Ionization by Electron Collision and Photoionization of Helium" T. Fujimoto (1978)
IPPJ-AM-9	"Charge Changing Cross Sections for Heavy-Particle Collisions in the Energy Range from 0.1 eV to 10 MeV I. Incidence of He, Li, Be, B and Their Ions" Kazuhiko Okuno (1978)
IPPJ-AM-10	"Charge Changing Cross Sections for Heavy-Particle Collisions in the Energy Range from 0.1 eV to 10 MeV II. Incidence of C, N, O and Their Ions" Kazuhiko Okuno (1978)
IPPJ-AM-11	"Charge Changing Cross Sections for Heavy-Particle Collisions in the Energy Range from 0.1 eV to 10 Mev III. Incidence of F, Ne, Na and Their Ions" Kazuhiko Okuno (1978)
IPPJ-AM-12*	"Electron Impact Excitation of Positive Ions Calculated in the Coulomb-Born Approximation –A Data List and Comparative Survey–" S. Nakazaki and T. Hashino (1979)
IPPJ-AM-13	"Atomic Processes in Fusion Plasmas – Proceedings of the Nagoya Seminar on Atomic Processes in Fusion Plasmas Sept. 5-7, 1979" Ed. by Y. Itikawa and T. Kato (1979)
IPPJ-AM-14	"Energy Dependence of Sputtering Yields of Monatomic Solids" N. Matsunami, Y. Yamamura, Y. Itikawa, N. Itoh, Y. Kazumata, S. Miyagawa, K. Morita and R. Shimizu (1980)

IPPJ-AM-15 "Cross Sections for Charge Transfer Collisions Involving Hydrogen Atoms"
Y. Kaneko, T. Arikawa, Y. Itikawa, T. Iwai, T. Kato, M. Matsuzawa, Y. Nakai, K. Okuno, H. Ryufuku, H. Tawara and T. Watanabe (1980)

IPPJ-AM-16 "Two-Centre Coulomb Phaseshifts and Radial Functions"
H. Nakamura and H. Takagi (1980)

IPPJ-AM-17 "Empirical Formulas for Ionization Cross Section of Atomic Ions for Electron Collisions –Critical Review with Compilation of Experimental Data–"
Y. Itikawa and T. Kato (1981)

IPPJ-AM-18 "Data on the Backscattering Coefficients of Light Ions from Solids"
T. Tabata, R. Ito, Y. Itikawa, N. Itoh and K. Morita (1981)

IPPJ-AM-19 "Recommended Values of Transport Cross Sections for Elastic Collision and Total Collision Cross Section for Electrons in Atomic and Molecular Gases"
M. Hayashi (1981)

IPPJ-AM-20 "Electron Capture and Loss Cross Sections for Collisions between Heavy Ions and Hydrogen Molecules"
Y. Kaneko, Y. Itikawa, T. Iwai, T. Kato, Y. Nakai, K. Okuno and H. Tawara (1981)

IPPJ-AM-21 "Surface Data for Fusion Devices – Proceedings of the U.S–Japan Workshop on Surface Data Review Dec. 14-18, 1981"
Ed. by N. Itoh and E.W. Thomas (1982)

IPPJ-AM-22 "Desorption and Related Phenomena Relevant to Fusion Devices"
Ed. by A. Koma.(1982)

IPPJ-AM-23 "Dielectronic Recombination of Hydrogenic Ions"
T. Fujimoto, T. Kato and Y. Nakamura (1982)

IPPJ-AM-24 "Bibliography on Electron Collisions with Atomic Positive Ions: 1978 Through 1982 (Supplement to IPPJ-AM-7)"
Y. Itikawa (1982)

IPPJ-AM-25 "Bibliography on Ionization and Charge Transfer Processes in Ion-Ion Collision"
H. Tawara (1983)

IPPJ-AM-26 "Angular Dependence of Sputtering Yields of Monatomic Solids"
Y. Yamamura, Y. Itikawa and N. Itoh (1983)

IPPJ-AM-27 "Recommended Data on Excitation of Carbon and Oxygen Ions by Electron Collisions"
Y. Itikawa, S. Hara, T. Kato, S. Nakazaki, M.S. Pindzola and D.H. Crandall (1983)

IPPJ-AM-28 "Electron Capture and Loss Cross Sections for Collisions Between Heavy Ions and Hydrogen Molecules (Up-dated version of IPPJ-AM-20)
H. Tawara, T. Kato and Y. Nakai (1983)

IPPJ-AM-29 "Bibliography on Atomic Processes in Hot Dense Plasmas"
T. Kato, J. Hama, T. Kagawa, S. Karashima, N. Miyanaga, H. Tawara, N. Yamaguchi, K. Yamamoto and K. Yonei (1983)

IPPJ-AM-30 "Cross Sections for Charge Transfers of Highly Ionized Ions in Hydrogen Atoms (Up-dated version of IPPJ-AM-15)"
H. Tawara, T. Kato and Y. Nakai (1983)

IPPJ-AM-31 "Atomic Processes in Hot Dense Plasmas"
T. Kagawa, T. Kato, T. Watanabe and S. Karashima (1983)

IPPJ-AM-32 "Energy Dependence of the Yields of Ion-Induced Sputtering of Monatomic Solids"
N. Matsunami, Y. Yamamura, Y. Itikawa, N. Itoh, Y. Kazumata, S. Miyagawa, K. Morita, R. Shimizu and H. Tawara (1983)

IPPJ-AM-33 "Proceedings on Symposium on Atomic Collision Data for Diagnostics and Modelling of Fusion Plasmas, Aug. 29 – 30, 1983"
Ed. by H. Tawara (1983)

IPPJ-AM-34 "Dependence of the Backscattering Coefficients of Light Ions upon Angle of Incidence"
T. Tabata, R. Ito , Y. Itikawa, N. Itoh, K. Morita and H. Tawara (1984)

Available upon request to Research Information Center, Institute of Plasma Physics, Nagoya University, Nagoya 464, Japan, except for the reports noted with*.